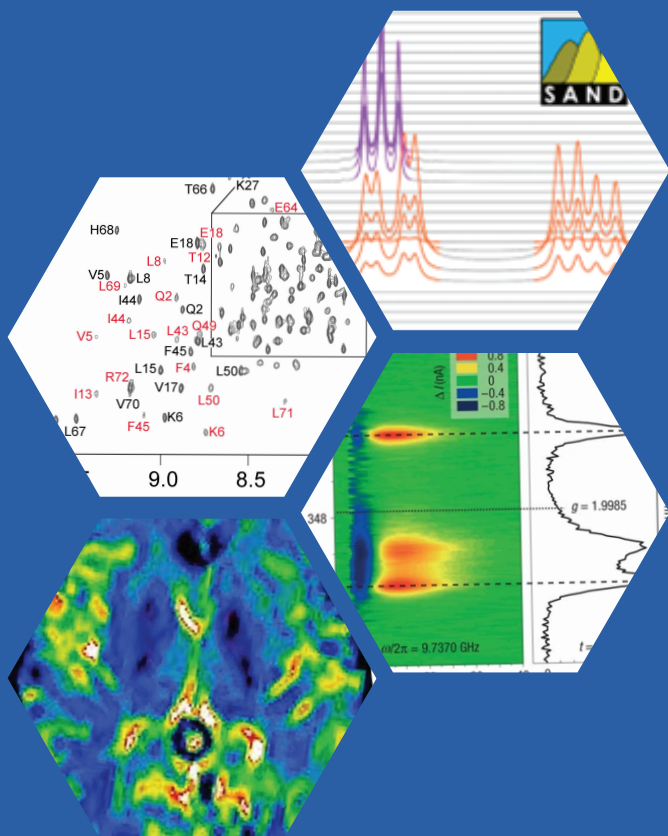




53rd Southeastern Magnetic Resonance Conference

Hosted by the National MagLab & UF • November 14-16 • Gainesville, FL



Harrell Medical Education Building
University of Florida College of Medicine

November 14-16, 2025

NATIONAL HIGH
MMAGNETIC
FIELD LABORATORY

UF UNIVERSITY of
FLORIDA



53th Southeastern Magnetic Resonance Conference

Hosted by the National MagLab & UF • November 14-16 • Gainesville, FL

CONFERENCE SCHEDULE

Friday, November 14, 2025

5:00 PM Registration, Poster Setup & Viewing

Session 1 – Welcome & Opening Session

6:30 PM	Welcome Remarks	Charlie Khemtong, Ph.D. University of Florida
6:35 PM	Keynote 1: Non-equilibrium Processes Studied by Pressure-jump NMR	Adriaan Bax, Ph.D. NIDDK/NIH
7:15 PM	<i>Flow Synthesis of Hyperpolarized Metabolites from Parahydrogen</i>	C. Russell Bowers, Ph.D. University of Florida
7:35 PM	<i>Unlocking Early Pancreatic Cancer Detection through Zinc-sensitive Metabolic MRI</i>	Veronica Clavijo Jordan, Ph.D. MGH/Harvard Medical School
8:00 PM	Poster Presentations and Reception	
10:00 PM	<i>End day</i>	

Saturday, November 15, 2025

Session 2 – MRI and Neurological Applications: Dedicated to Prof. Thomas Mareci

Chair: Jens Rosenberg, Ph.D.
University of Florida

8:25 AM	Opening Remarks	William Brey, Ph.D. NHMFL/Florida State University
8:30 AM	Keynote 2: 35 Years of (N)MR Spectroscopy in the Human Brain	Peter Barker, D.Phil. Johns Hopkins University
9:10 AM	<i>Longitudinal Changes in Microstructure Are Related to Changes in Gut Microbiome Following Morphine Use</i>	Luis Colon-Perez, Ph.D. U North Texas Health Sci Ctr
9:30 AM	<i>Remote Palpation of Live Human Brain Using MR Elastography</i>	Magdoom Kulam, Ph.D. NICHD/NIH
9:50 AM	<i>Gradient Coil Design Considerations for Neuroimaging</i>	Garrett Astary, Ph.D. GE Healthcare MR
10:10 AM	<i>Is the Brain a Hyperbolic Network</i>	Daniel DeYoung, Ph.D. Albion College
10:25 AM	Coffee Break	



53th Southeastern Magnetic Resonance Conference

Hosted by the National MagLab & UF • November 14-16 • Gainesville, FL

Session 3 – Solution NMR and Applications

Chair: Joanna Long, Ph.D.
University of Florida

- 10:50 AM *Cold-water Chemistry* Bill Baker, Ph.D.
University of South Florida
- 11:10 AM *Noncanonical RNA binding in LARP6* Robert Silvers, Ph.D.
Florida State University
- 11:25 AM *Molecular Dynamics Simulations to Predict NMR Relaxation of Mixtures in Strongly Inhomogeneous Fields* Tyler Meldrum, Ph.D.
William & Mary
- 11:40 AM *High-Resolution ¹³C NMR Reveals Enhanced Hepatic Fatty Acid Oxidation in AATD Mouse Model* Qingyang Shen
University of Florida
- 11:55 AM *Metabolite Fraction Libraries for Quantitative NMR Metabolomics* Art Edison, Ph.D.
University of Georgia
- 12:10 PM **Lunch**

Session 4 – EPR and Applications I

Chair: Stephen Hill, D.Phil.
NHMFL/Florida State University

- 1:30 PM **Keynote 3: Floquet Spin-Pair States in a π -Conjugated Polymer Thin Film** Christoph Boehme, Ph.D.
University of Utah
- 2:10 PM *Multiphoton State Transitions in the Multilevel Spin System Gd³⁺:YVO₄* Sebastian Atwood, Ph.D.
NHMFL & Florida State University
- 2:25PM *Frequency and Bandwidth Tunable Photonic Band Gap Resonators for Pulse EPR with at least Tenfold Greater Concentration Sensitivity* Alex Smirnov, Ph.D.
North Carolina State University
- 2:40 PM *Multi-Functional Role of Oxalate Decarboxylase Revealed by EPR Studies* Zain Becerra, Ph.D.
University of Florida
- 2:55 PM **Coffee Break**

Session 5 – Solid-State NMR

Chair: Leah Casabianca, Ph.D.
Clemson University

- 3:20 PM *Solid-State NMR of Insect Wing Membranes and a Refined Structure of Chitin* Terry Gullion, Ph.D.
West Virginia University
- 3:40 PM *Structure Determination of Membrane Proteins in Magnetically Aligned Discoidal Lipid Mimetics by Solid-State NMR* Alexander Nevzorov, Ph.D.
North Carolina State University



53th Southeastern Magnetic Resonance Conference

Hosted by the National MagLab & UF • November 14-16 • Gainesville, FL

4:00 PM	<i>Mechanochemical Routes to Conventional and Integrative Pharmaceutical Solid Forms: Insights from PXRD and Multinuclear Solid-State NMR Spectroscopy</i>	Peyton Osborn NHMFL/Florida State University
4:15 PM	<i>Structural Characterization of Surface Immobilized Platinum Hydrides by Indirect Detection Solid State NMR Spectroscopy</i>	Benjamin Atterberry, Ph.D. University of Florida
4:30 PM	<i>Structural Insight into Inhibitor-Mediated Modulation of Huntingtin Exon 1 Aggregation</i>	Greeshma Jain, Ph.D. University of Florida
4:45 PM	<i>Gangliosides Promote Structural Heterogeneity in Aβ42 Aggregates</i>	Jhinuk Saha, Ph.D. NHMFL/Florida State University
5:00 PM	Break	
<u>Session 6 – Lightning Presentations by Graduate Students & Postdocs</u>		Chair: Luiza Nogueira, Ph.D. University of Florida
5:20 PM	<i>Evaluating novel bTurea-based biradicals for MAS-DNP</i>	Shubha Gunaga, Ph.D. NHMFL/Florida State University
	<i>Elucidating Electronic Structure and Relaxation Pathways of Transition Metal Complexes via High Power EPR Spectroscopy</i>	Kavipriya Thangavel, Ph.D. NHMFL/Florida State University
	<i>Probing the Structures and Dynamics of Cobaltocenium Compounds via Ultra-Wideline ⁵⁹Co Solid-State NMR</i>	Dominic Chantra NHMFL/Florida State University
	<i>Design and Optimization of Highly Aligned Peptoid Macrodiscs for Solid-State NMR Studies of Membrane Proteins</i>	Adit Shah North Carolina State University
	<i>Measuring Slow Cerebrospinal Fluid Velocities in Preclinical Models Using Optimized Phase Contrast MRI at 21.1 T</i>	Dayna Richter NHMFL/Florida State University
	<i>Engineered Iron Oxide Interfaces Enable Reliable MRI Tracking of Therapeutic Extracellular Vesicles</i>	Arshia Arbabian NHMFL/Florida State University
6:20 PM	Dinner	
8:00 PM	Poster Viewing	
9:30 PM	End day	



53th Southeastern Magnetic Resonance Conference

Hosted by the National MagLab & UF • November 14-16 • Gainesville, FL

Sunday, November 16, 2025

Session 7 – MRI: Emerging Technologies and Innovations

8:30 AM	<i>DMRI is a Flexible Platform for Assessing Aberrant Metabolism</i>	Chair: Bradley Wilkes, Ph.D. University of Florida
8:50 AM	<i>A Multi-nuclear Volume Coil for H/X Pre-clinical MR at Ultra High Magnetic Fields</i>	Matthew Merritt, Ph.D. University of Florida
9:05 AM	<i>BOLD Functional Connectivity Correlates of PTSD Severity and Chronicity during Image Viewing</i>	David Doty, Ph.D. Doty Scientific, Inc.
9:20 AM	<i>Calibrated MR-ARFI with a Non-Magnetic Micropositioner</i>	Robert Claar University of Florida
9:35 AM	<i>Imaging Neuronal Transmission using Novel Genetic Encodable MRI Reporters</i>	Ryan Willoughby, Ph.D. University of Alabama at Birmingham
9:55 AM	Coffee Break	Nan Li, Ph.D. UT Southwestern Medical Center

Session 8 – EPR and Applications II

10:30 AM	<i>Optimization Methods and Instrumental Advances in Dissolution Dynamic Nuclear Polarization</i>	Chair: Alexander Angerhofer, Ph.D. University of Florida
10:50 AM	<i>Achieving Liquid-State ¹H DNP through Particle-Mediated ¹H–¹H Cross Relaxation.</i>	Lloyd Lumata, Ph.D. University of Texas at Dallas
11:05 AM	<i>Optical Control of Molecular Qubits</i>	Sungsool Wi, Ph.D. NHMFL/Florida State University
11:20 AM	<i>Beyond The First Coordination Sphere: Pulsed EPR Spectroscopy Sheds Light on Outer-Sphere Interactions Driving Enzyme Catalysis</i>	Haochuan Mao, Ph.D. Florida State University
11:40 AM	<i>From light to friction: how metal oxides drive radical formation in lubricants</i>	Brad Pierce, Ph.D. University of Alabama
11:55 AM	<i>Intrinsic and Cooperative Dynamics of α-Synuclein Terminal Domains under Controlled Confinement</i>	Tatyana I. Smirnova, Ph.D. North Carolina State University
12:10 AM	Conference Highlights & Closing Remarks	Kurt Warncke, Ph.D. Emory University
		Charlie Khemtong, Ph.D. University of Florida

Adjourn or AMRIS Facility Tour (optional)



53th Southeastern Magnetic Resonance Conference

Hosted by the National MagLab & UF • November 14-16 • Gainesville, FL

SPECIAL THANKS TO OUR SPONSORS



UF Department of Biochemistry and Molecular Biology
UNIVERSITY of FLORIDA



Cambridge Isotope Laboratories, Inc.
isotope.com



Abstract No.		Presenting Author	Institution	Abstract Title
Keynotes				
K01	NMR	Adriaan Bax	NIDDK/NIH	Non-equilibrium Processes Studied by Pressure-jump NMR
K02	MRI	Peter Barker	Johns Hopkins University	35 Years of (N)MR Spectroscopy in the Human Brain
K03	EPR	Christoph Boehme	University of Utah	Floquet Spin-Pair States in a π -Conjugated Polymer Thin Film
Invited Talks				
IT01	NMR/MRI	C. Russell Bowers	University of Florida	Flow Synthesis of Hyperpolarized Metabolites from Parahydrogen
IT02	MRI	Veronica Clavijo Jordan	MGH/Harvard Medical School	Unlocking Early Pancreatic Cancer Detection through Zinc-sensitive Metabolic MRI
IT03	MRI	Luis Colon-Perez	U North Texas Health Sci Ctr	Longitudinal Changes in Microstructure Are Related to Changes in Gut Microbiome Following Morphine Use
IT04	MRI	Magdoom Kulam	NICHHD/NIH	Remote Palpation of Live Human Brain Using MR Elastography
IT05	MRI	Garrett Astarý	GE Healthcare MR	Gradient Coil Design Considerations for Neuroimaging
IT06	NMR	Bill Baker	University of South Florida	Remote Palpation of Live Human Brain Using MR Elastography
IT07	NMR	Terry Gullion	West Virginia University	Solid-State NMR of Insect Wing Membranes and a Refined Structure of Chitin
IT08	NMR	Alexander Nevzorov	North Carolina State University	Solid-State NMR of Insect Wing Membranes and a Refined Structure of Chitin
IT09	MRI	Matthew Merritt	University of Florida	DMRI is a Flexible Platform for Assessing Aberrant Metabolism
IT10	EPR/DNP	Lloyd Lumata	University of Texas at Dallas	Optimization Methods and Instrumental Advances in Dissolution Dynamic Nuclear Polarization
IT11	EPR	Brad Pierce	University of Alabama	Beyond The First Coordination Sphere: Pulsed EPR Spectroscopy Sheds Light on Outer-Sphere Interactions Driving Enzyme Catalysis

Contributed Talks

CT01	MRI	Daniel DeYoung	Albion College	Is the Brain a Hyperbolic Network
CT02	NMR	Robert Silvers	Florida State University	Noncanonical RNA binding in LARP6
CT03	NMR	Tyler Meldrum	William and Mary	Molecular Dynamics Simulations to Predict NMR Relaxation of Mixtures in Strongly Inhomogeneous Fields
CT04	NMR	Qingyang Shen	University of Florida	High-Resolution ¹³ C NMR Reveals Enhanced Hepatic Fatty Acid Oxidation in AATD Mouse Model
CT05	NMR	Art Edison	University of Georgia	Metabolite Fraction Libraries for Quantitative NMR Metabolomics
CT06	EPR	Sabastian Atwood	FSU- NHMFL	Multiphoton State Transitions in the Multilevel Spin System Gd ³⁺ :YVO ₄
CT07	EPR	Alex Smirnov	North Carolina State University	Frequency and Bandwidth Tunable Photonic Band Gap Resonators for Pulse EPR with at least Tenfold Greater Concentration Sensitivity
CT08	EPR	Zain Becerra	University of Florida	Multi-Functional Role of Oxalate Decarboxylase Revealed by EPR Studies
CT09	NMR	Peyton Osborn	FSU- NHMFL	Mechanochemical Routes to Conventional and Integrative Pharmaceutical Solid Forms: Insights from PXRD and Multinuclear Solid-State NMR Spectroscopy
CT10	NMR	Benjamin Atterberry	University of Florida	Structural Characterization of Surface Immobilized Platinum Hydrides by Indirect Detection Solid State NMR Spectroscopy
CT11	NMR	Greeshma Jain	University of Florida	Structural insight into inhibitor-mediated modulation of Huntingtin Exon 1 aggregation
CT12	NMR	Jhinuk Saha	FSU- NHMFL	Gangliosides Promote Structural Heterogeneity in Aβ ₄₂ Aggregates

CT13	MRI	David Doty	Doty Scientific, Inc.	A Multi-nuclear Volume Coil for H/X Pre-clinical MR at Ultra High Magnetic Fields
CT14	MRI	Robert Claar	University of Florida	BOLD Functional Connectivity Correlates of PTSD Severity and Chronicity during Image Viewing
CT15	MRI	Ryan Willoughby	University of Alabama at Birmingham	Calibrated MR-ARFI with a Non-Magnetic Micropositioner
CT16	MRI	Nan Li	UT Southwestern Medical Center	Imaging Neuronal Transmission using Novel Genetic Encodable MRI Reporters
CT17	EPR/DNP	Sungsool Wi	FSU- NHMFL	Achieving Liquid-State ^1H DNP through Particle-Mediated ^1H - ^1H Cross Relaxation
CT18	EPR	Haochuan Mao	Florida State University	Optical Control of Molecular Qubits
CT19	EPR	Tatyana I. Smirnova	North Carolina State University	From light to friction: how metal oxides drive radical formation in lubricants
CT20	EPR	Kurt Warncke	Emory University	Intrinsic and Cooperative Dynamics of α -Synuclein Terminal Domains under Controlled Confinement
Lightning Talks				
LT01	EPR/DNP	Shubha S. Gunaga	FSU- NHMFL	Evaluating novel bTurea-based biradicals for MAS-DNP
LT02	EPR	Kavipriya Thangavel	FSU- NHMFL	Elucidating Electronic Structure and Relaxation Pathways of Transition Metal Complexes via High Power EPR Spectroscopy
LT03	NMR	Dominic Chantra	FSU- NHMFL	Probing the Structures and Dynamics of Cobaltocenium Compounds via Ultra-Wideline ^{59}Co Solid-State NMR
LT04	NMR	Adit Shah	North Carolina State University	Design and Optimization of Highly Aligned Peptoid Macrodiscs for Solid-State NMR Studies of Membrane Proteins

LT05	MRI	Dayna Richter	FSU- NHMFL	Measuring Slow Cerebrospinal Fluid Velocities in Preclinical Models Using Optimized Phase Contrast MRI at 21.1 T
LT06	MRI	Arshia Arbabian	FSU- NHMFL	Engineered Iron Oxide Interfaces Enable Reliable MRI Tracking of Therapeutic Extracellular Vesicles
Posters - EPR				
P001	EPR/DNP	Ishani Marasinghage	University of Florida	Local Charge Distribution Modulates Hydration Dynamics in the Intrinsically Disordered Protein IA3
P002	NMR/DNP	Sungsool Wi	FSU – NHMFL	Advancing Liquid-State ¹⁹ F DNP: High-Field, Large-Volume Overhauser Polarization at Ambient Temperature
P003	EPR	Tianyan Li	University of Florida	Investigating the Impact of Charge Distributions on the Unfolded and Folded Conformations of IA3s
P004	EPR/DNP	Tomas Orlando	FSU – NHMFL	Liquid State ¹³ C and ¹⁹ F DNP-Enhanced NMR Spectroscopy in One and Two Dimensions
P005	EPR	Mahsa Moshari	University of Florida	Phase & Dynamic Behavior in Lyotropic Liquid Crystals for MRI Agent Design and Drug Delivery by Magnetic Resonance Spectroscopy
P006	EPR	Kiera Powers	FSU – NHMFL	Functionalized Materials as Polarizing Agents for Dynamic Nuclear Polarization in Liquids
P007	EPR	Brittany Grimm	FSU – NHMFL	EPR Characterization of a Photo-Responsive Fe ³⁺ Spin-Crossover Complex
P008	EPR	Shayak Biswas	University of Florida	Effects of Anomeric Linkage of α- and β-Cerebrosides on Biophysical Properties of the Lipid Membrane
P009	EPR	Korrigan Amadi	FSU – NHMFL	Field homogeneity Improvement and Dead-Time Reduction for an Integrated EPR and DNP Spectrometer
P010	EPR	Hana Alsheikh	University of Florida	Effects of Anomeric Linkage of α- and β-Cerebrosides on Biophysical Properties of the Lipid Membrane

P011	EPR	Johan van Tol	FSU – NHMFL	A 263 GHz Pulsed EPR Spectrometer with AWG Capabilities
P012	EPR	Shamiul Islam	University of Florida	Biophysical Characterization of GPI Anchor Conformation Using a Synthetic Bifunctional Probe
P013	EPR	Shady Fouad	Emory University	Coupling of protein backbone and solvent dynamics in α -synuclein revealed by using controlled confinement and multi-probe EPR spectroscopy
P014	EPR	Kavipriya Thangavel	FSU – NHMFL	Elucidating Electronic Structure and Relaxation Pathways of Transition Metal Complexes via High Power EPR Spectroscopy
P015	EPR	Ritu Kaushik	University of Florida	Engineering Surface Lysines and Hydrophobic Clusters to Modulate Hydration, Stability, and Bioconjugation in <i>Bacillus subtilis</i> Lipase A
P016	EPR	Ivan Weaver	FSU – NHMFL	CW and Pulsed EPR Investigation of HoW ₁₀ Crystals as Potential Spin Qubit Materials
Posters - MRI				
P017	MRI	Barbara Balsamo	University of Florida	Region-specific GNAL Knockout Reveals Differential Network Dysfunction in a Mouse model of Dystonia
P018	MRI	Nesmine Maptue	University of Florida	In vivo Hyperpolarized ¹³ C MRI Detects Abnormal Mitochondrial Metabolism in CDAA-induced Hepatic Steatosis
P019	MRI	Dayna Richter	FSU- NHMFL	Measuring Slow Cerebrospinal Fluid Velocities in Preclinical Models Using Optimized Phase Contrast MRI at 21.1 T
P021	MRI	Gaurav Sharma	University of Florida	Accelerating jHSQC Acquisition through Non-Uniform sampling: Achieving Uniform-quality Spectra in Half the time
P020	MRI	Arshia Arbabian	FSU- NHMFL	Engineered Iron Oxide Interfaces Enable Reliable MRI Tracking of Therapeutic Extracellular Vesicles
P022	MRI	Diba Allameh Zadeh	University of Florida	Characterization of lipid based Lyotropic Liquid Crystals Phase Behavior and Their Potential as MRI Contrast Agents and therapeutic Applications

P023	MRI	Warren Boschen	Vanderbilt university	Phase Dispersion in Multiband Imaging
P024	MRI	Emily G. Cushman	Clemson University	An Educational Approach to Connecting Chemistry and Healthcare Using Magnetic Resonance Imaging
P025	MRI	Julia Martin	FSU- NHMFL	Methodologies for analyzing RF shield efficiency at 21.1T MRI
P026	MRI	Kate Payen	FSU- NHMFL	Sustainability: Assessing ways to reduce energy consumption in NMR/MRI systems
Posters - NMR				
P027	NMR	Greeshma Jain	University of Florida	Structural insight into inhibitor-mediated modulation of Huntingtin Exon 1 aggregation
P028	NMR	Beining Jin	University of Florida	The Conformational Equilibria of a Human GPCR Compared between Lipid Vesicles and Aqueous Solutions by Integrative ¹⁹ F-NMR
P029	NMR	Nessa Pesaran Afsharian	University of Florida	¹⁹ F-NMR quantification of drug efficacy exemplified with the human A _{2A} adenosine receptor
P030	NMR	Viraj Wijesekara	University of Florida	Investigating lipid organization and GPCR-lipid interactions in membrane mimetics with NMR spectroscopy and molecular dynamic simulations
P031	NMR	Rongfu Zhang	FSU- NHMFL	A ¹⁷ O Solid-State NMR Relaxation Approach for Probing Water on Membrane Surfaces
P032	NMR	Nazifa Tasnim Ahmad	FSU-FAMU-NHMFL	Gangliosides GM3 And GD3 Modulate Insulin Aggregation Pathways and Reduce Cytotoxicity Through Structural Remodeling
P033	NMR	Cletus Obi	FSU-FAMU-NHMFL	Magnetic Alignment of Saponin-based Lipid Nanodiscs
P034	NMR	Sara Termos	FSU- NHMFL	Nutation-Induced Distortions in Solid-State NMR Spectra of High-Spin Quadrupolar Nuclei

P035	NMR	Rajan Rai	FSU- NHMFL	Understanding Self-Association of Fluorinated Phenylalanine through NMR Spectroscopy and Quantum Chemistry
P036	NMR	Alexander Perez	FSU- NHMFL	Mechanochemical Synthesis and Multinuclear Solid-State NMR Characterization of Amoxicillin Hydrochloride Salts
P037	NMR	Jiaxing Fan	FSU- NHMFL	Structurally characterizing FtsL101-146 in lipid bilayers
P038	NMR	Shashwata Moitra	Cryogenic Ltd	An experimental proof of the applicability of cryogen-free technology for high resolution solid state and liquid state NMR
P039	NMR	Sean Holmes	FSU- NHMFL	Pushing the Limits of NMR Crystallography: A Study on Three Forms of Glycylglycine
P040	NMR	Sekinah Dauda	Clemson University	Understanding Interactions between Micro and Nano Plastics with Metabolites at the Molecular Level
P041	NMR	Jordan Sanders	Clemson University	Developing a Tool to Understand the Structure of Hydrogens on Nanoplastics Surface
P042	NMR	Makaylab Grandal	Rowan University	Investigating the Relationship Between Carbon Quantum Dots and Nuclear Spin Relaxation
P043	NMR	Kattayani Sarkar	University of Florida	Design and NMR Investigation of Ni ²⁺ -Chelated Monoolein Nanoparticles: A Path to Stabilizer-Free Lipid Carriers
P044	NMR	Tzu-Ying Chiu	Georgia Institute of Technology	Peptide nanostructures can be pathological or therapeutic: how solid-state NMR guides control assembly pathways to produce desired molecular structures
P045	NMR	Rasaq Ayinde Adams	University of Florida	Unveiling Catalytic Intermediates on Metal Nanoparticle Surfaces via Parahydrogen-Enhanced NMR
P046	NMR	Neel Shah	University of Florida	Microwave Fixation Prevents Post-Mortem Metabolism for NMR Spectroscopy Metabolomics

Non-equilibrium processes studied by pressure-jump NMR

Ad Bax

Laboratory of Chemical Physics, National Institute of Diabetes and Digestive and Kidney Diseases,
National Institutes of Health, Bethesda, Maryland 20892, USA

The equilibrium between a protein's folded and unfolded state is strongly impacted by hydrostatic pressure. Many proteins can be unfolded by applying a modest amount (≤ 2.5 kbar) of hydrostatic pressure, applicable to measurements by NMR.

Rapidly and repeatedly dropping the pressure from denaturing conditions (i.e. 2.5 kbar) to 1 bar, synchronized with detection of the NMR spectrum, allows study of the actual folding process under native conditions. A device that allows such rapid (ms) and repeated ($>100,000$ times) switching, enables direct monitoring of the folding process by two- and three-dimensional NMR.

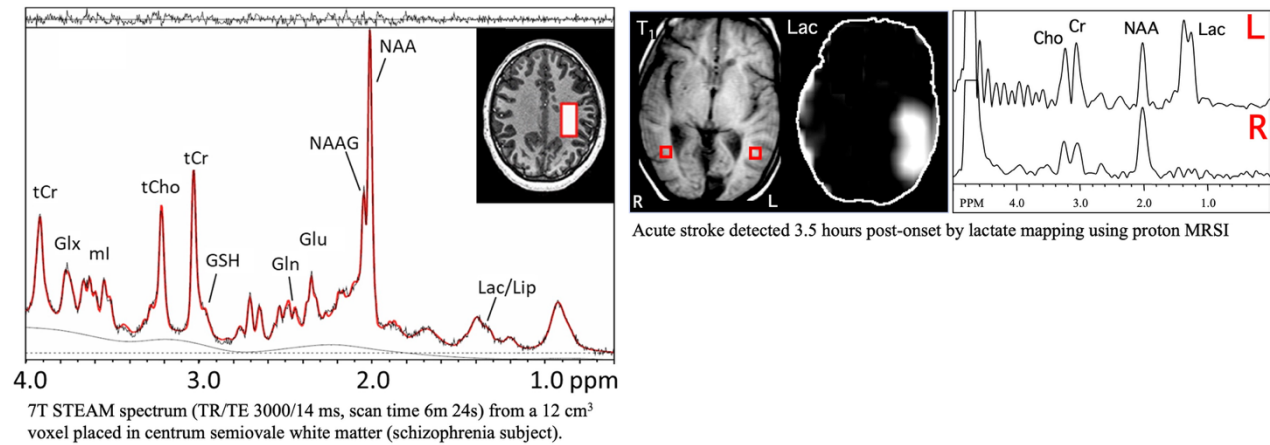
Hydrostatic pressure also can be used to resolubilize oligomerized or otherwise aggregated peptides and proteins. Such experiments hold promise for revealing structural information on the Alzheimer's related A β peptide in the oligomerized state, which differs substantially from the monomeric and the fibrillar states.

35 years of (N)MR spectroscopy in the human brain

Peter B Barker

Russell H Morgan Department of Radiology and Radiological Science, The Johns Hopkins University School of Medicine, Baltimore, MD 21287

The development of whole-body MRI scanners in the late 1980s at field strengths of 1.5T, together with other fundamental technological advances such shielded field gradients and single-shot spatial localization techniques, enabled the non-invasive collection of spectra from the human in just a few minutes of scan time. Since that time, there have been many technical advances and clinical studies performed, and it remains an active area of research and development. This presentation will review key technical developments including spatial localization techniques for both single voxel spectroscopy and spectroscopic imaging, spectral analysis, spectral editing, and the effects of increasing magnetic field strength. In addition, the metabolic information from *in vivo* MRS will be discussed, including metabolic changes that can be detected in various pathological states, and applications in the clinic. Finally, some of the challenges facing the clinical use of MRS and sustainability will be discussed.



References

1. Bruhn H, Frahm J, Gyngell ML, et al. Noninvasive differentiation of tumors with use of localized H-1 MR spectroscopy in vivo: initial experience in patients with cerebral tumors. *Radiology* 1989;172:541–548.
2. Frahm J, Bruhn H, Gyngell ML, Merboldt KD, Hanicke W, Sauter R. Localized proton NMR spectroscopy in different regions of the human brain in vivo. Relaxation times and concentrations of cerebral metabolites. *Magn Reson Med* 1989;11:47–63.
3. Barker PB, Soher BJ, Blackband SJ, Chatham JC, Mathews VP, Bryan RN. Quantitation of proton NMR spectra of the human brain using tissue water as an internal concentration reference. *NMR in Biomedicine* 1993;6:89–94.
4. Duyn JH, Gillen J, Sobering G, van Zijl PC, Moonen CT. Multisection proton MR spectroscopic imaging of the brain. *Radiology* 1993;188:277–282.
5. Provencher SW. Estimation of metabolite concentrations from localized in vivo proton NMR spectra. *Magn Reson Med* 1993;30:672–679.
6. Barker PB, Gillard JH, van Zijl PC, et al. Acute stroke: evaluation with serial proton MR spectroscopic imaging. *Radiology* 1994;192:723–732.
7. Mescher M, Merkle H, Kirsch J, Garwood M, Gruetter R. Simultaneous in vivo spectral editing and water suppression. *NMR Biomed* 1998;11:266–272.
8. Barker PB, Hearshen DO, Boska MD. Single-voxel proton MRS of the human brain at 1.5T and 3.0T. *Magn Reson Med* 2001;45:765–769.
9. Tkac I, Andersen P, Adriani G, Merkle H, Ugurbil K, Gruetter R. In vivo 1H NMR spectroscopy of the human brain at 7 T. *Magn Reson Med* 2001;46:451–456.
10. Maudsley AA, Darkazanli A, Alger JR, et al. Comprehensive processing, display and analysis for in vivo MR spectroscopic imaging. *NMR Biomed* 2006;19:492–503.
11. Choi C, Ganji SK, DeBerardinis RJ, et al. 2-hydroxyglutarate detection by magnetic resonance spectroscopy in IDH-mutated patients with gliomas. *Nat Med* 2012;18:624–629.
12. Cordova JS, Shu HK, Liang Z, et al. Whole-brain spectroscopic MRI biomarkers identify infiltrating margins in glioblastoma patients. *Neuro Oncol* 2016;18:1180–1189.
13. Huang V, Rejimon A, Reddy K, et al. Spectroscopic MRI-Guided Proton Therapy in Non-Enhancing Pediatric High-Grade Glioma. *Tomography* 2023;9:633–646.

Floquet Spin-Pair States in a π -Conjugated Polymer Thin Film

Christoph Boehme

Department of Physics and Astronomy, University of Utah, Salt Lake City, Utah 84112

boehme@physics.utah.edu

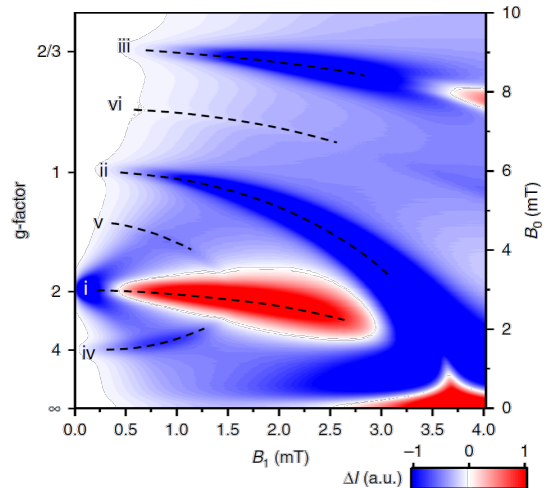
Organic semiconductors—particularly π -conjugated polymer thin films—provide a unique environment where charge carriers form weakly coupled spin pairs, or polaron pairs, with small spin–spin and spin–orbit interactions [1]. When these systems are subjected to strong magnetic resonance drive—where the oscillating drive field B_1 becomes comparable to or exceeds the static Zeeman field B_0 —the conventional spin eigenstates are profoundly altered. In this regime, spins hybridize with the oscillating drive field to form Floquet spin-light states [2], whose properties go beyond the familiar linear-response picture of magnetic resonance.

Recent theoretical and experimental work [2-4] has revealed the rich phenomenology of these Floquet states under strong EPR drive, including nonlinear magnetic resonance effects such as multi-photon transitions, fractional g-factor resonances, and spin–photon collectivity, reminiscent of the Dicke effect in non-linear optics. The color plot in the figure displays Floquet theory-based simulations of the room temperature recombination current in a perdeuterated Poly[2-methoxy-5-(2-ethylhexyloxy)-1,4 phenylene-vinylene] (MEH-PPV) thin film under bipolar charge carrier injection conditions, as a function of B_0 and B_1 . Experimentally, these effects can be directly observed through electrically detected magnetic resonance (EDMR) spectroscopy, which provides a highly sensitive probe for EPR at the small B_0 .

This presentation will highlight recent advances in the study of these phenomena, including experimental observations of non-Bloch–Siegert type drive induced resonance shifts, multi-photon resonances [4,5] and coherent control under strong-drive with pulsed EDMR [6].

Our results establish electrically readable Floquet states in organic semiconductors as a promising new platform for exploring strong-drive spin dynamics and coherent control. Their unique combination of tunability, initializability, long-lived coherence, and electrical readout suggests potential applications for quantum sensing.

References: [1] E. L. Frankevich et al. *Phys. Rev. B* **46**, 9320 (1992); T. Grünbaum et al., *Faraday Discuss* **221**, 92 (2020); McCamey, D. R., et al. *Phys. Rev. Lett.* **104**.1 017601 (2010); [2] R. C. Roundy and M. E. Raikh, *Phys. Rev. B* **88**, 125206 (2013); R. K. Malla, and M. E. Raikh, *Phys. Rev. B* **96** (8), 085311 (2017); [3] S. Jamali et al., *Nat. Commun.* **12**, 465, 1 (2021); [4] D. P. Waters et al., *Nat. Phys.* **11**, 910 (2015); S. Jamali et al. *Nano Lett.* **17**, 4648 (2017). J. P. Ashton et al., *Phys. Rev. B* **102**, 020101 (2020); S. I. Atwood et al., *Phys. Rev. B* **110**, 195304 (2024); [5] S. I. Atwood et al., *Phys. Rev. B* **110**, L060103 (2024); [6] T. H. Tannahewa et al., *Phys. Rev. B* **109** 075303 (2024).



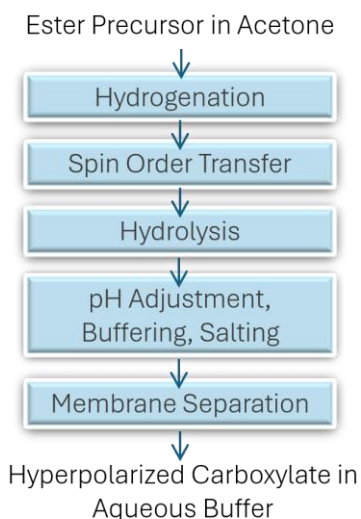
Simulation of spin-dependent recombination current change in a perdeuterated MEH-PPV film as a function of static field B_0 and oscillating field B_1 for a frequency of 85 MHz. Figure has been adapted from Ref. [3]:

Flow Synthesis of Hyperpolarized Metabolites from Parahydrogen

Yiheng Yan and Russ Bowers*,
University of Florida, Department of Chemistry

Chalermchai Khemtong
University of Florida, Department of Medicine

Parahydrogen (pH_2), the metastable proton singlet spin isomer of dihydrogen, is a plentiful source of nuclear spin order that can be used to amplify NMR signals by up to five orders of magnitude, enabling carbon-13 metabolic MRI. Currently, parahydrogen-induced hyperpolarization is restricted to the preparation of discrete batches with substantial losses in polarization during the time-consuming extraction of solvents from the aqueous metabolite solution. Here, we present solutions to the key steps in the continuous flow synthesis of hyperpolarized metabolites in purified aqueous solution: hydrogenation, spin order transfer, and extraction into aqueous buffer. The continuous generation of hyperpolarized metabolites will enable long-duration metabolic imaging beyond fast imaging pulse sequences after injection of a single bolus at non-physiological concentrations.



Abstract title: Unlocking early pancreatic cancer detection through zinc sensitive metabolic MRI

Authors: Farzad Moloudi^{1,5}, Mozhdeh Sojoodi^{2,5}, Ethan French¹, Patricia Gonzalez Pagan¹, Pamela Pantazopoulos¹, Nabeel Bardeesy^{4,5,6}, Kenneth K Tanabe^{2,4}, Motaz Qadan^{2,4}, Peter Caravan^{1,3,5}, and Veronica Clavijo Jordan^{1,3,5}

¹ Martinos Center for Biomedical Imaging, Department of Radiology. ² Division of Gastrointestinal and Oncologic Surgery. ³ The Institute for Innovation in Imaging, Massachusetts General Hospital, Boston, MA, USA. ⁴ Krantz Family Center for Cancer Research. ⁵ Harvard Medical School, Boston, MA, USA. ⁶ The Cancer Program, Broad Institute, Cambridge, MA, USA.

Introduction

Pancreatic ductal adenocarcinoma (PDAC) is frequently diagnosed late and is difficult to distinguish from inflammatory pancreatic disease or to monitor during therapy. Secretagogue-stimulated zinc-secretion MRI (SSZS-MRI) leverages dysregulated zinc handling in the tumor-bearing pancreas to enable noninvasive detection, discrimination from benign states, and therapy surveillance.

Methods

Animal models: 10⁴ KPC cells were injected directly into the pancreas tail to generate an orthotopic PDAC model, chronic or acute pancreatitis was obtained by repeated caerulein, or pancreatic duct ligation. *MR Imaging:* SSZS-MRI consisted of T1-weighted imaging before/after i.p. secretin+caerulein and i.v. GdL (0.07 mmol/kg); contrast-to-noise ratio (CNR) was quantified in pancreas/tumor ROIs. A KRAS^{G12D} inhibitor (MRTX1133, 30 mg/kg i.p. BID) was used for longitudinal response and post-withdrawal surveillance. *Ex vivo measures:* ZIP3, ZIP4, ZnT1 expression was measured by IHC.

Results

SSZS-MRI showed zinc hypersecretion in the tumor-bearing pancreas, yielding increased T1 signal relative to controls. In models of chronic and acute pancreatitis, zinc hypersecretion was absent, allowing discrimination of PDAC from non-malignant inflammatory disease. During MRTX1133 therapy, pancreatic SSZS-MRI signal decreased within 3–5 days, concordant with tumor control/regression. Following drug withdrawal, pancreatic signal rose within 1–3 days and tracked tumor regrowth, providing an early readout of recurrence. IHC supported imaging readouts, with altered zinc-transporter expression patterns between tumor and adjacent pancreas that normalized with effective therapy.

Conclusions

SSZS-MRI detects PDAC via zinc dysregulation, differentiates it from chronic and acute pancreatitis, and sensitively reports response to KRAS^{G12D} inhibition and early recurrence after treatment withdrawal. By imaging the tumor-bearing pancreas rather than the often-occult primary mass, SSZS-MRI addresses key diagnostic and surveillance gaps and may enable earlier, more precise clinical decision-making.

Longitudinal changes in microstructure are related to changes in gut microbiome following morphine use.

Luis M. Colon-Perez*

Department of Pharmacology and Neuroscience, University of North Texas Health Science Center, Fort Worth, TX, 76107

Opioids are potent analgesics via its strong activation of μ -opioid receptors known to affect the opioid and dopaminergic systems, which ultimately mediates changes in pathological use behavior; however, new research lines are looking at complementary changes in the gut that may be an essential signaling mechanism mediating maladaptive behavior. The gut-brain axis (GBA) is a bidirectional signaling process that permits feedback between the brain and the gut. The GBA is altered in subjects with opioid use disorder (OUD), suggesting a complementary mechanism modulating the brain's function/structure and gut that may play an essential role in developing the pathological symptoms of OUD. In this presentation we will share initial results of a longitudinal and noninvasive study consisting of small animal MR imaging, and gut microbiome analysis. Our hypothesis is that the chronic consumption of morphine will lead to progressive complementary changes in brain and gut microbiome markers, and these will be associated with morphine self-administration. We employed DTI and NODDI metrics to identify changes in brain microstructure and 16s rDNA analysis of fecal matter to identify changes in gut microbiome. Our analysis finds early changes in gut microbiota and specific that continued into the later stages of morphine use. In MRI, we identified alterations in diffusion indices both within subjects and between groups, showing a main effect in the striatum and thalamus. We conclude that gut changes precede the effects observed in MRI, with the striatum and thalamus emerging as crucial links mediating communication between the gut and the brain.

Remote Palpation of Live Human Brain Using MR Elastography

Magdoom Kulam^{1,2,3*}, Alexandru V. Avram¹, Joelle E. Sarlls⁴, Peter J. Basser¹

¹Eunice Kennedy Shriver National Institute of Child Health and Human Development, National Institutes of Health, Bethesda, MD, United States, ²The Military Traumatic Brain Injury Initiative (MTBI²), Uniformed Services University of the Health Sciences, Bethesda, MD, United States, ³The Henry M Jackson Foundation for the Advancement of Military Medicine (HJF) Inc., Bethesda, MD, United States, ⁴National Institute of Neurological Disorders and Stroke, National Institutes of Health, Bethesda, MD, United States

Background

Palpation is a time-honored means of diagnosing diseases but is usually limited to superficial organs such as the liver. MR elastography (MRE) [1] allows interrogating deeper organs by imaging the propagation of mechanical waves introduced into the tissue typically using a tamper. MRE of the brain is challenging due to the presence of the skull that attenuates the external vibrations introduced into the brain and the anisotropic nature of brain mechanical properties, which require a 4th-order elasticity tensor for accurate representation. In this study, we use the intrinsic pulsations of the brain with every heartbeat along with diffusion tensor imaging (DTI) [2] to remotely palpate the tissue.

Methods

MRI data was acquired in three healthy young adults on a 3T Siemens Prisma scanner. The diffusion tensor and 3D displacement vector fields in the brain were simultaneously measured in each segment of the cardiac cycle based on the magnitude and phase of the pulsed gradient spin echo (PGSE) MRI signal, respectively. The displacement amplitude at the cardiac frequency (i.e., ~1 Hz) is used to estimate the elasticity tensor in each voxel by inverting the mass and momentum conservation equations along with *a priori* knowledge of the fiber orientation provided by DTI. Novel scalar invariants and glyphs are derived from the measured elasticity tensor to feature tissue mechanical properties which were then mapped onto fiber tracts derived from DTI.

Results

Despite a near uniform mean diffusivity (MD) in the brain parenchyma, the average stiffness is highly heterogeneous, as shown in the figure above. Domains with discontinuous stiffness, such as at tissue interfaces [3], result in impedance mismatches, which may explain the injury pattern observed in traumatic brain injury (TBI). The extent of mechanical anisotropy is also not correlated with diffusion anisotropy indicating these are distinct physical properties of the material.

Conclusion

We have introduced a new method to map the elasticity tensor of the human brain *in vivo* with the potential to diagnose subtle neurological diseases and disorders so far invisible in radiology.

References

1. Muthupillai, R., et al. "Magnetic resonance elastography by direct visualization of propagating acoustic strain waves." *Science* 269.5232 (1995): 1854-1857.
2. Basser, Peter J., James Mattiello, and Denis LeBihan. "MR diffusion tensor spectroscopy and imaging." *Biophysical journal* 66.1 (1994): 259-267.
3. Shively, Sharon Baughman, et al. "Characterisation of interface astroglial scarring in the human brain after blast exposure: a post-mortem case series." *The Lancet Neurology* 15.9 (2016): 944-953.

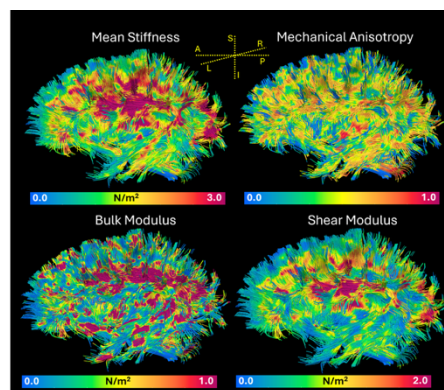


FIG: Mechanical properties mapped onto the fiber tracts

Abstract title: Gradient Coil Design Considerations for Neuroimaging

Authors: Garrett Astary, Ph.D..

Affiliation: GE HealthCare

Magnetic resonance imaging has become an invaluable tool for studying the brain due to its ability to provide anatomical information as well as quantitative metrics related to biological function and underlying tissue structure. A critical component of the MR imaging system, the gradient coil is tasked with spatially encoding the image and may be used to apply additional encoding such that the acquired signal is sensitive to molecular motion (e.g., diffusion, flow) providing supplemental biological information. The aim of this talk is to provide an overview of the gradient coil design process for a neuroimaging system. A brief review of gradient coil function and system performance design goals is provided. Key gradient coil performance characteristics, design tradeoffs, and the design optimization process will be described. Finally, a head-only gradient coil design capable of high gradient strength and slew rate, relative to whole-body designs, will be discussed.

Cold-water Chemistry

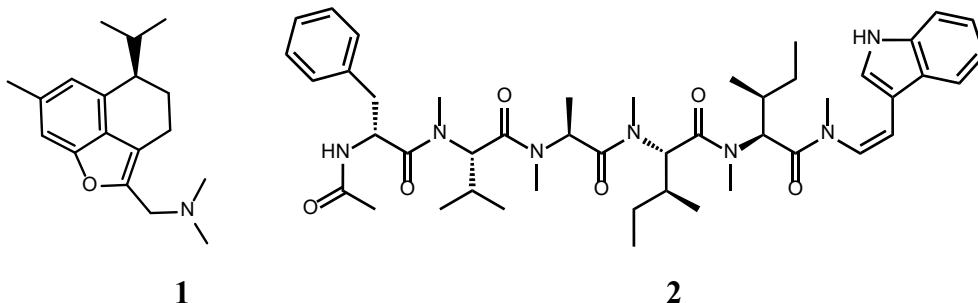
Bill J. Baker

Department of Chemistry, University of South Florida

Introduction: Shallow-water communities of temperate and tropical marine environments harbor significant biodiversity, including metabolite-rich sponges, tunicates and corals. These organisms have been explored for decades as sources of natural product derived bioactive metabolites to drive drug discovery programs. Less attention has been focused on cold-water habitats that include polar marine environments and the deep-sea. While cold-water regions are often difficult to access, the limited data available suggests biodiversity there is similarly rich in biologically active metabolites.

Methods: Field-collected specimens are prepared for analysis by lyophilization followed by solvent extraction. Concentrated extracts are screened for biomedical applications. Active extracts are purified to obtain bioactive metabolites. Extensive mass spectrometry and nuclear magnetic resonance spectroscopy are applied to purified metabolites to establish their structure.

Results: Work from our lab includes sampling cold-water environments in Antarctica and the deep-sea offshore of Ireland. For example, A coral specimen from the Irish deep-sea yielded a family of aminated terpenes, the anthotheibinenes (**1**)¹ with activity against the respiratory syncytial virus (RSV), and from the deep-sea of Antarctica we found a sponge that produces the friomaramides (**2**), which have activity against the liver stage of malaria.²



Conclusion: These and other examples to be discussed have established the veracity of cold-water marine organisms as source of biomedically important metabolites.

1. Olsen, SH; Afoullouss, S; Young, RM; Johnson, M; Allcock, LA; Baker, BJ Amino- and halogen-bearing sesquiterpenes from the Irish deep-sea octocoral *Anthothela grandiflora*. *Org Lett* **2024**, 9419.

2. Bracegirdle, J; Casandra, D; Rocca, JR; Adams, JH; Baker, BJ Highly *N*-methylated peptides from the Antarctic sponge *Inflatella coelosphaeroides* are active against *Plasmodium falciparum*. *J Nat Prod* **2022**, 2454.

Solid-State NMR of Insect Wing Membranes and a Refined Structure of Chitin

Samuel Eddy¹, Bill Nese¹, Julianna Burnside¹, Tyler Seifert¹, Terry Gullion^{1*}, Faith J. Scott²,
Frederic Mentink-Vigier²

¹Department of Chemistry, West Virginia University, Morgantown, WV

²National High Magnetic Field Laboratory, Tallahassee, FL

Insects are the most diverse group of animals with approximately 80% of all species, and their success is attributed to their exoskeleton and the ability of many insect species to fly. The exoskeleton has been extensively studied by solid-state NMR, and past experiments have shown the exoskeleton to be made mostly of chitin and protein. NMR experiments with ¹³C and ¹⁵N labeling showed the presence of catechol crosslinking between chitin and protein.¹ The insect wing is considered an extension of the exoskeleton. However, structural details of the thin wing membrane at the molecular level are lacking. We examined the wing membranes of cicada, ladybug, honeybee, and butterfly with solid-state NMR. The similarities and differences between the wing membrane compositions will be discussed.

The general structure of chitin has been determined by room-temperature x-ray crystallography.^{2,3} The x-ray determined structures showed disorder of the hydroxymethyl groups but presupposes the remaining structure to be ordered. We isolated chitin from cicada and examined its structure with CPMAS and MAS-DNP from 100 K to room temperature. Our results show that the hydrogen bonding network of chitin is richer and more dynamic than suggested by crystallography. We discuss the nature of hydrogen bonding and its impact on the structure of chitin.

References

1. J. Schaefer, K. J. Kramer, J. R. Garbow, G. S. Jacob, E. O. Stejskal, T. L. Hopkins, R. D. Speirs, Aromatic Cross-Links in Insect Cuticle: Detection by Solid-State ¹³C and ¹⁵N NMR, *Science*, **235**, 1200-1204.
2. R. Minke and J. Blackwell, The Structure of α -chitin, *J. Mol. Biol.*, 1978, **120**, 167–181.
3. P. Sikorski, R. Hori and M. Wada, Revisit of α -Chitin Crystal Structure Using High Resolution X-ray Diffraction Data, *Biomacromolecules*, 2009, **10**, 1100–1105.



Structure Determination of Membrane Proteins in Magnetically Aligned Discoidal Lipid Mimetics by Solid-State NMR

Alexander A. Nevzorov*, Adit Shah, Azamat R. Galiakhmetov

Department of Chemistry, North Carolina State University, 2620 Yarbrough Drive, Raleigh, NC, 27695-8204

Solid-state NMR has emerged as a powerful tool for structure determination of membrane proteins. While Magic-Angle Spinning (MAS) NMR remains the most widely used tool for this purpose, proteoliposomes are often densely packed inside the rotor at a reduced water content and low lipid-to-protein ratios. We have been developing magnetically aligned membrane mimetics, which preserve basic features of a native-like environment for membrane proteins such as high (>50:1) lipid-to-protein ratios, planar surface, high hydration (at 10-15% w/v), and physiological temperature (37 °C). Of particular interest is the development of detergent-free, magnetically aligned macrodiscs of ca. 20-30 nm in diameter, which in contrast to static bicelles facilitate averaging out uniaxial orientations of protein molecules by means of rotational diffusion [1]. Amphipathic synthetic constructs made of peptoid chains wrap around the discs and make them water-soluble. In the absence of MAS, however, the dipolar couplings need to be suppressed by application of specialized NMR pulse sequences to improve spectral resolution. For this purpose, we have developed a computer-assisted algorithm termed ROULETTE (Random Optimization Using the Liouville Equation Tailored to The Experiment) [2] in order to generate pulse sequences for averaging out proton-proton dipolar couplings while simultaneously evolving nearest-neighbor heteronuclear dipolar couplings. Examples include the orientationally dependent ^1H - ^{15}N and $^1\text{H}_\alpha$ - $^{13}\text{C}_\alpha$ dipolar couplings, which directly contain structural information. We show that, together with ^{15}N CSA anisotropy, these measurements provide sufficient angular restraints to determine the structure of a small coat protein from Pfl bacteriophage without assuming an α -helical conformation *a priori* [3]. Structures of the Pfl protein have been determined in lipids of different hydrophobic thickness, including DMPC- and DPPC-based macrodiscs [4]. Contrary to our expectations, the tilt of the transmembrane helix has not changed, which may indicate that the helical conformation is governed by the flanking Lysine and Arginine residues, which may cause a local thickening of the DMPC membrane while preserving the overall helix orientation. Moreover, we will discuss the development of assignment protocols in oriented lipid bilayers including ^{15}N - ^{15}N , ^1H - ^{15}N - ^{15}N and ^{15}N - ^{13}C spin correlation experiments. In addition, preliminary spectra of a much larger membrane protein, proteorhodopsin, will be demonstrated in magnetically aligned macrodiscs. These recent developments greatly extend the utility of oriented-sample NMR for structure determination of membrane proteins in near-native lipid environments. Supported by NSF CHE 2404331.

References

- [1]. Galiakhmetov, A. R.; Davern, C. M.; Esteves, R. J. A.; Awosanya, E. O.; Guthrie, Q. A. E.; Proulx, C.; Nevzorov, A. A., *Biophysical Journal* **121** 3263-3270 (2022)
- [2]. Lapin, Nevzorov, A. A., *Journal of Magnetic Resonance* **317**, 106794 (2020)
- [3]. Awosanya, E. O., Lapin, J. A. and Nevzorov, A. A., *Angewandte Chemie International Edition* **59** (9) 3554-3557 (2020)
- [4]. Galiakhmetov, A. R.; Shah, A. A.; Lane, A.; Davern, C. M.; Proulx, C.; Nevzorov, A. A., *Journal of Structural Biology-X* **9** 100095 (2024)

DMRI is a Flexible Platform for Assessing Aberrant Metabolism

Matthew E. Merritt, Department of Biochemistry and Molecular Biology, University of Florida

Deuterium magnetic resonance imaging (DMRI) offers a powerful, non-radioactive approach for visualizing metabolic activity in vivo. This emerging modality leverages stable isotope tracers such as [6,6-²H₂]glucose, [²H₇]glucose, and [D₁₅]octanoate to quantify substrate turnover and energy flux in tissues with spatial and temporal resolution comparable to proton MRI. Using custom-built ²H coils and high-field MRI systems (up to 11 T), DMRI enables direct observation of labeled metabolites, including glucose, lactate, and glutamate/glutamine (Glx), without the need for hyperpolarization or ionizing radiation.

In the rat brain, ²H MRS and 2-point Dixon imaging following [²H₇]glucose administration revealed persistent Glx labeling and metabolic water production, capturing dynamic glucose utilization. In the appropriate time window following administration, we show that HDO production correlates nearly perfectly with lactate and glx appearance, suggesting the high signal-to-noise ratio HDO peak is a good metric of cerebral glucose consumption.

Extending this approach to hepatic metabolism, DMRI following [D₁₅]octanoate administration distinguishes normal from diet-induced steatotic liver in mice. High-fat diet (HFD) models exhibit elevated total HDO production but reduced octanoate oxidation per gram of liver protein, consistent with impaired β-oxidation. These findings provide new insight into the metabolic dysfunction underlying Metabolic Dysfunction-Associated Steatotic Liver Disease (MASLD) and its progression to steatohepatitis (MASH).

In a model of skin cancer, orthotopic implantation of BRAF^{V600E} Yumm1.7 melanomas demonstrates that treatment with combined BRAF (dabrafenib) and MEK (trametinib) inhibition markedly reduces glucose uptake, lactate formation, and metabolic water generation—findings that parallel FDG-PET responses while avoiding radioisotopes. These results support DMRI as a sensitive indicator of glycolytic modulation in cancer therapy.

Together, these studies demonstrate that DMRI constitutes a flexible and quantitative imaging platform for mapping central carbon and lipid metabolism across multiple organ systems and in cancer.

Acknowledgments:

Supported by NIH R01-EB032376, R01-DK132254, and the NSF Cooperative Agreement DMR-2128556 to the National High Magnetic Field Laboratory.

Optimization Methods and Instrumental Advances in Dissolution Dynamic Nuclear Polarization

Lloyd Lumata*, Department of Physics, University of Texas at Dallas, Richardson, TX 75080

Dissolution dynamic nuclear polarization (DNP) enhances NMR sensitivity by transferring the high polarization of electron spins to nuclear spins in a frozen sample via microwave irradiation under cryogenic and high-field conditions, then rapidly dissolving the polarized solid to produce a hyperpolarized liquid at room temperature [1,2]. The versatility of dissolution DNP lies in its ability to hyperpolarize virtually any NMR-active nucleus, providing enormous signal enhancements for nuclei such as ^{13}C , ^{15}N , and others that are inherently insensitive under thermal equilibrium.

A typical dissolution DNP sample consists of three primary components: (i) a *polarizing agent*, (ii) the *target nuclei or sample*, and (iii) a *glassing solvent*. Central to the NMR signal amplification process of DNP are the polarizing agents or the sources of free electrons, typically provided by organic free radicals [1]. The vitreous glassing matrix such as glycerol/water ensures that the molecules containing the target nuclei as well as the polarizing agents are homogeneously dispersed throughout the entire DNP sample. Additionally, trace amounts of paramagnetic complexes or other chemical additives are sometimes incorporated to further boost hyperpolarized NMR signal intensity. Because the DNP process relies on interactions between electron and nuclear spins within the frozen glassy matrix at cryogenic conditions, the specific composition and formulation of the DNP sample critically influence the maximum attainable signal enhancement of the target nuclei. Moreover, certain instrumental advances in dissolution DNP were also developed to further boost the hyperpolarized NMR signals [1,2]. Employment of high B/T conditions, modulation of microwave frequencies, use of magnetic tunnel, utilization of ^1H -X nuclei cross polarization, and other instrumental tinkering have also led to further increases in DNP signals. Other instrumental developments include the use of cryogen-free magnet systems to mitigate the cost of using liquid helium in dissolution DNP operations (see Fig. 1) and experimental developments to make the hyperpolarized injectable liquids from dissolution DNP transportable [1].



Figure 1: Photo of a homebuilt cryogen-free dissolution DNP system at UT Dallas.

In this talk, these optimization methods and instrumental advances in dissolution DNP technology will be discussed in light of attaining the highest hyperpolarized NMR signal enhancements for in vitro and in vivo hyperpolarized NMR and MRI experiments.

References:

- 1) A. Asaadzade, F. Khashami, W. Feizi, D. Anable, C. Larsen, Q. Wang, L. Lumata, *Optimization of hyperpolarized NMR signals in dissolution dynamic nuclear polarization*, *Advances in Magnetic Resonance Technology and Applications* 12, 157-173 (2024).
- 2) P. Niedbalski, A. Kiswandhi, C. Parish, Q. Wang, F. Khashami, L. Lumata, *NMR Spectroscopy Unchained: Attaining the Highest Signal Enhancements in Dissolution Dynamic Nuclear Polarization*, *The Journal of Physical Chemistry Letters* 9, 5481–5489 (2018).

Beyond the first coordination sphere: pulsed EPR spectroscopy sheds light on outer-sphere interactions driving enzyme catalysis

Authors: Brad S. Pierce^{1}, Nicholas J. York¹, Ryan P. Madigan³, Paula F. Nino³, Frank W. Foss, Jr³, Molly M. Lockart^{2*}*

- 1 Department of Chemistry & Biochemistry, University of Alabama, 250 Hackberry Lane, Tuscaloosa, Alabama 35487, United States
- 2 Department of Chemistry and Biochemistry, Samford University, 800 Lakeshore Drive, Homewood, AL 35229, United States
- 3 Department of Chemistry & Biochemistry, The University of Texas at Arlington, 700 Planetarium Place, Arlington, TX 76019 United States

ABSTRACT

3-mercaptopropionate (**3MPA**) dioxygenase (MDO) is a mononuclear non-heme iron enzyme that catalyzes the O₂-dependent oxidation of thiol-bearing substrates to yield the corresponding sulfinic acid. MDO is a member of the CDO family of small molecule thiol dioxygenases and thus shares a conserved sequence of active site residues (Serine-155, Histidine-157, and Tyrosine-159), collectively referred to as the SHY-motif. It has been demonstrated that these amino acids interact with the mononuclear Fe-site, influencing steady-state catalysis, catalytic efficiency, O₂-binding, and substrate coordination. However, the underlying mechanism by which this is accomplished is poorly understood. Here, pulsed EPR spectroscopy (¹H HYSCORE and Mims ENDOR) are applied to validate DFT computational models for the MDO Fe-site simultaneously coordinated by substrate and nitric oxide, (**3MPA/NO**)-MDO. The enhanced resolution provided by ENDOR spectroscopy allows for direct observation of Fe-bound substrate conformations and H-bond donation from Tyr159 to the Fe-bound NO ligand. Further inclusion of SHY-motif residues within the validated model reveals a distinct channel restricting movement of the Fe-bound NO-ligand. It has been argued that the iron-nitrosyl emulates the structure of potential Fe(III)-superoxide intermediates within the MDO catalytic cycle. While the merit of this assumption remains unclear, the model reported here offers a framework to evaluate oxygen binding at the substrate-bound Fe-site and possible reaction mechanisms. It also underscores the significance of hydrogen bonding interactions within the enzymatic active site.

Abstract title: Is the Brain a Hyperbolic Network

Authors: Daniel DeYoung* Albion College

Many real world networks are modelled as hyperbolic networks[5][4], and there are claims the brain is such a network[8][12]. There is even a claim that a disturbance of the brains hyperbolic nature is responsible for Alzheimer's[11]. This work will investigate how hyperbolic the brains network is on the macro-scale. Using denitions of hyperbolicity dened in graph-theory as an analog to geometry[7][6]. An algorithm is developed to measure the hyperbolicity of binary graphs of brain connectivity derived using MRTrix on the 100 unrelated subjects set of the Human Connectome Project[10][9][1][2][3].

References

- [1] Andersson, J. L., Skare, S., and Ashburner, J. (2003). How to correct susceptibility distortions in spin-echo echo-planar images: application to diusion tensor imaging. *NeuroImage*, 20(2):870888.
- [2] Andersson, J. L. and Sotiropoulos, S. N. (2015). Non-parametric representation and prediction of single-and multi-shell diusion-weighted mri data using gaussian processes. *NeuroImage*, 122:166176.
- [3] Andersson, J. L. and Sotiropoulos, S. N. (2016). An integrated approach to correction for o-resonance effects and subject movement in diusion mr imaging. *NeuroImage*, 125:10631078.
- [4] Borassi, M., Chessa, A., and Caldarelli, G. (2015a). Hyperbolicity measures democracy in real-world networks. *Physical Review E*, 92(3).
- [5] Borassi, M., Coudert, D., Crescenzi, P., and Marino, A. (2015b). On Computing the Hyperbolicity of Real-World Graphs, pages 215-226. Springer Berlin Heidelberg.
- [6] Carballosa, W., Portilla, A., Rodríguez, J. M., and Sagarreta, J. M. (2014). Planarity and hyperbolicity in graphs. *Graphs and Combinatorics*, 31(5):13111324.
- [7] Gromov, M. (1987). *Essays in Group Theory*, volume 8. Springer New York.
- [8] Sharpee, T. O. (2019). An argument for hyperbolic geometry in neural circuits. *Current Opinion in Neurobiology*, 58:101104.
- [9] Sotiropoulos, S. N., Moeller, S., Jbabdi, S., Xu, J., Andersson, J. L., Auerbach, E. J., Yacoub, E., Feinberg, D., Setsompop, K., Wald, L. L., Behrens, T. E. J., Ugurbil, K., and Lenglet, C. (2013). Effects of image reconstruction on ber orientation mapping from multichannel diusion mri: Reducing the noise floor using sense. *Magnetic Resonance in Medicine*, 70(6):16821689.
- [10] Van Essen, D., Ugurbil, K., Auerbach, E., Barch, D., Behrens, T., Bucholz, R., Chang, A., Chen, L., Corbetta, M., Curtiss, S., Della Penna, S., Feinberg, D., Glasser, M., Harel, N., Heath, A., Larson-Prior, L., Marcus, D., Michalareas, G., Moeller, S., Oostenveld, R., Petersen, S., Prior, F., Schlaggar, B., Smith, S., Snyder, A., Xu, J., and Yacoub, E. (2012). The human connectome project: A data acquisition perspective. *NeuroImage*, 62(4):22222231.
- [11] Wright, K. (2025). A potential tool for diagnosing alzheimer's disease. *Physics*, 18.
- [12] Zhang, H., Rich, P. D., Lee, A. K., and Sharpee, T. O. (2023). Hippocampal spatial representations exhibit a hyperbolic geometry that expands with experience. *Nature Neuroscience*, 26(1):131139.

Noncanonical RNA binding in LARP6

Blaine H. Gordon, Victoria S. Ogunkunle, and Robert Silvers*

Department of Chemistry & Biochemistry, Florida State University, Tallahassee, FL 32306, USA

La-related proteins (LARPs) are RNA-binding proteins that are involved in a variety of disease-related processes. Most LARPs recognize short single-stranded poly(U/A) motifs via a conserved hydrophobic pocket. Human LARP6 (HsLARP6) is an exception, binding a structured 5' stem-loop (5'SL) that controls type I collagen translation and fibroproliferative disease progression. We recently presented the *de novo* solution NMR structure of the La domain of HsLARP6 in the bound state (Figure 1).^[1] Chemical shift perturbation, solvent paramagnetic relaxation enhancement, intermolecular NOEs, and targeted mutagenesis converge on a previously unknown binding interface that integrates electrostatic and hydrophobic contacts with shape complementarity in 5'SL binding. This noncanonical interface enables the La domain to discriminate 5'SL RNA from homopolymeric or purely helical hairpin RNAs with low-nanomolar affinity, overturning earlier views that the adjacent RRM is required for recognition. The structure provides the first molecular model for 5'SL recognition and expands the paradigm of La-mediated RNA binding beyond 3' terminal oligo-U/A motifs. These insights provide the biophysical framework for molecular recognition of 5'SL by LARP6 that is related to collagen biosynthesis in fibrosis and associated pathologies.

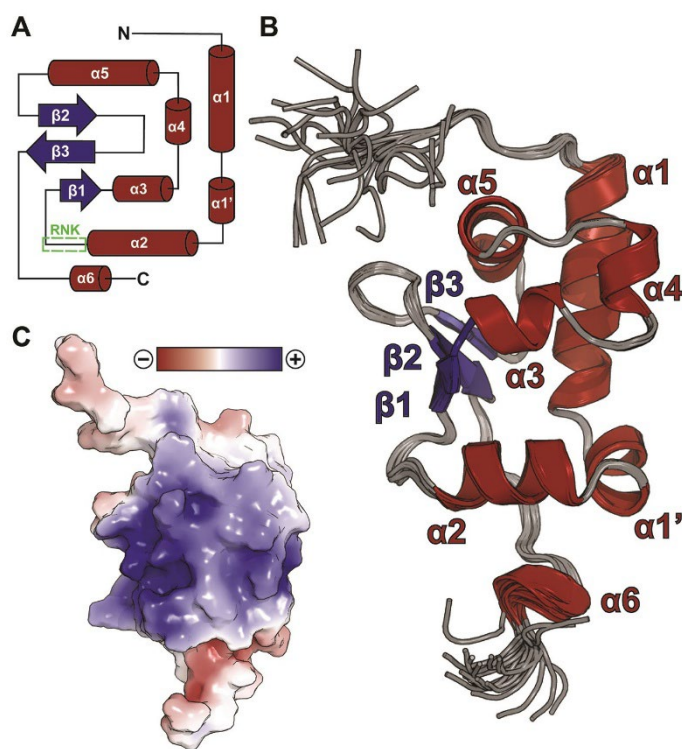


Figure 1. Structure and topology of the A2M5-bound La domain of HsLARP6. (A) Secondary structure topology of the La domain of HsLARP6. (B) Bundle of 20 structures of the A2M5-bound La domain as determined by the solution NMR spectroscopy (PDB: 9NGX). The structures are displayed in cartoon representation with α -helices, β -strands, and loops are shown in red, blue, and gray, respectively. (C) The surface charge of the La domain as determined by APBS shows a continuous basic patch (blue). The structure is oriented identically to the structure shown in panel (B). Figure modified after Gordon et al.^[1]

References:

- [1] Blaine H Gordon, Victoria S Ogunkunle, Robert Silvers, Noncanonical RNA binding of human La-related protein 6, *Nucleic Acids Research* 2025, 53 (14), gkaf682, <https://doi.org/10.1093/nar/gkaf682>

Molecular dynamics simulations to predict NMR relaxation of mixtures in strongly inhomogeneous fields

Tyler Meldrum*, Thomas Felton, Eliza Evans

*William & Mary, Department of Chemistry**Williamsburg, Virginia*

NMR relaxation is intimately connected to molecular motion and molecular motion can be atomistically probed using molecular dynamics (MD) simulations. Previous work has shown that spin-spin (T_2) and spin-lattice (T_1) relaxation times can be calculated for single-component systems using MD simulations and show good agreement with experiments.¹

We have expanded upon previous work (1) to predict spin-spin relaxation for binary systems using MD simulations, (2) determine molecular self-diffusion coefficients from MD simulations, and (3) convert T_2 values to $T_{2,\text{eff}}$ values, compatible with CPMG sequences in inhomogeneous fields, using this diffusion information. We show good agreement between simulations and experiment, both in the CPMG decay data and in the inverse-Laplace-transformed T_2 spectrum, as shown in Figure 1.

Simulations were run using the computing cluster at William & Mary running open source MD software. Experimental data were collected using single-sided NMR instrumentation (PM5 NMR-MOUSE) with a strong ($\sim 24 \text{ T m}^{-1}$) field gradient. We postulate that these results could help inform analysis of more complex mixtures using NMR relaxometry. In addition, examination of the MD results in context of NMR data may help draw connections between molecular motion, intermolecular forces, and NMR relaxation.

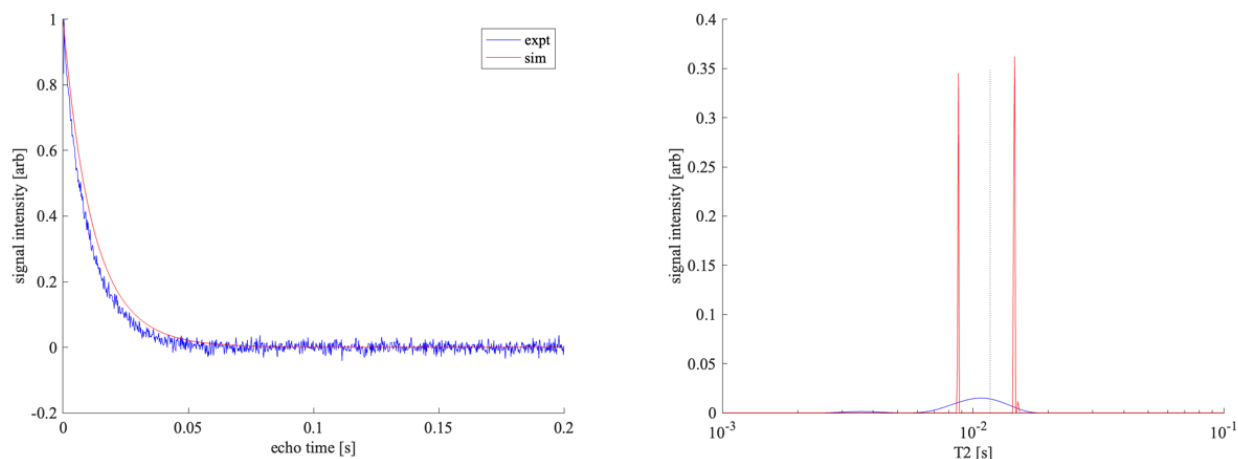


Figure 1. Comparison of simulated (red) and experimental (blue) data for the 1:1 v/v mixture of toluene and $\text{C}_{16}\text{H}_{34}$. Left panel: CPMG decay data using a $200 \mu\text{s}$ echo time. Right panel: T_2 spectrum, obtained from the inverse Laplace transformation of the CPMG data.

Reference

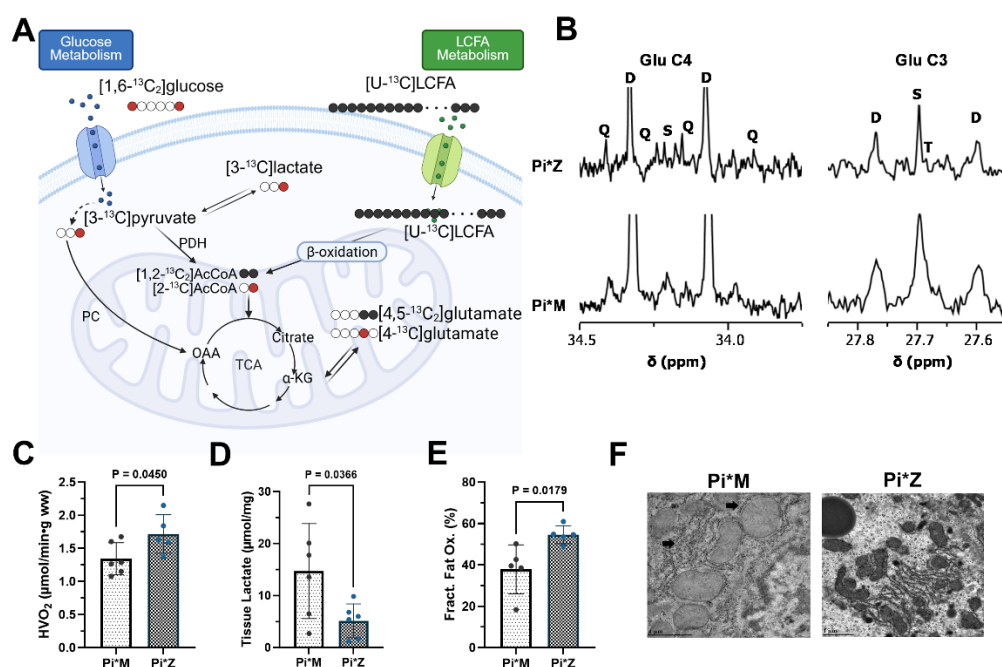
1. Singer, Philip M., Dilip Asthagiri, Walter G. Chapman, and George J. Hirasaki. "Molecular Dynamics Simulations of NMR Relaxation and Diffusion of Bulk Hydrocarbons and Water." *Journal of Magnetic Resonance* 277 (April 2017): 15–24.

High-resolution ¹³C NMR reveals enhanced hepatic fatty acid oxidation in AATD mouse model

Qingyang Shen^{1,2}, Regina Oshins³, Nesmine Maptue¹, Nazli Khodayari³, Chalermchai Khemtong^{1,2}

¹Department of Medicine, Division of Endocrinology, Diabetes & Metabolism, ²Department of Biochemistry and Molecular Biology, ³Department of Medicine, Division of Pulmonary, Critical Care and Sleep Medicine, University of Florida, Gainesville, FL, USA

Background: Alpha-1 antitrypsin deficiency (AATD) is associated with hepatic accumulation of misfolded ZAAT proteins, endoplasmic-reticulum stress, and progressive injury, but its impact on liver energy metabolism remains poorly defined. Here, we combine ¹³C NMR and isotopomer analysis to analyze energy metabolism and estimate metabolic fluxes in the livers of mice with AATD. **Methods:** Livers isolated from humanized Pi*M (control) and Pi*Z (AATD) mice were perfused with a Krebs–Henseleit buffer containing 5.5 mM [1,6-¹³C]glucose, 0.4 mM [U-¹³C]long-chain fatty acids (LCFA, **Fig. 1A**). Following perfusion, livers were extracted with perchloric acid and analyzed by ¹³C NMR to estimate fractional substrate oxidation and metabolic fluxes. **Results:** ¹³C NMR spectra of liver tissue extracts confirm oxidation of both ¹³C-glucose and ¹³C-LCFA into the Krebs cycle as evidenced by C4 and C3 multiplets of glutamate resonances (**Fig. 1B**). Oxygen measurements recorded during the perfusion reveal that Pi*Z livers consumed much higher oxygen for energy production than the Pi*M group (**Fig. 1C**). However, ¹H NMR analyses of tissue extracts show that Pi*Z livers produced much lower lactate despite the elevated oxygen consumption (**Fig. 1D**). Substrate selection in Pi*Z livers was reprogrammed toward fats, with increased fractional oxidation of LCFA measured in Pi*Z livers (**Fig. 1E**). Histology of liver tissues clearly demonstrates abnormal structures of mitochondria in Pi*Z liver (**Fig. 1F**). **Conclusions:** High-resolution ¹³C NMR of liver extracts, integrated with flux analysis, shows that AATD (Pi*Z) livers adapted to enhanced reliance of long-chain fatty acids for energy production coupled with elevated oxygen consumption. These results confirm metabolic reprogramming in the liver of mice lacking circulating alpha-1 antitrypsin proteins.



Metabolite Fraction Libraries for Quantitative NMR Metabolomics

Christopher Esselman^{1,4}, Kara Garrison^{2,4}, Leandro Ponce^{3,4}, Ricardo M. Borges⁵, Frank Delaglio⁶, Arthur S. Edison^{1,2,4}

1. Institute of Bioinformatics, University of Georgia, Athens, Georgia, USA.
2. Department of Biochemistry and Molecular Biology, University of Georgia, Athens, Georgia, USA.
3. College of Engineering, University of Georgia, Athens, Georgia, USA.
4. Complex Carbohydrate Research Center, University of Georgia, Athens, Georgia, USA.
5. Instituto de Pesquisa de Produtos Naturais Walter Mors, Universidade Federal do Rio de Janeiro, Rio de Janeiro, Brazil
6. Institute for Bioscience and Biotechnology Research, National Institute of Standards and Technology and the University of Maryland, Rockville, Maryland, USA.

Abstract body

Nuclear Magnetic Resonance (NMR) has unique strengths in metabolomics studies, particularly in quantifying mixtures and elucidating the structures of unknown molecules. One-dimensional (1D) proton (¹H) NMR is the most common method, but spectral overlap is significant, making annotation and quantification challenging. We present a new approach that utilizes chromatographically separated fractions from a pooled sample, henceforth called a metabolite fraction library (mFL). We developed an algorithm to extract highly correlated peaks from the mFL, collectively forming a metabolite basis set (mBS). The mBS can be fit to NMR profiling data, enabling comprehensive quantification. Applied to mixtures of 53 known metabolites, our approach quantified 50 of them, identified an impurity, and quantified 91-96% of the spectra used for fitting. The method is demonstrated using the filamentous fungus *Neurospora crassa*, resulting in 45 metabolites identified with high confidence, 45 with medium confidence, and quantifying 94% of the spectrum.

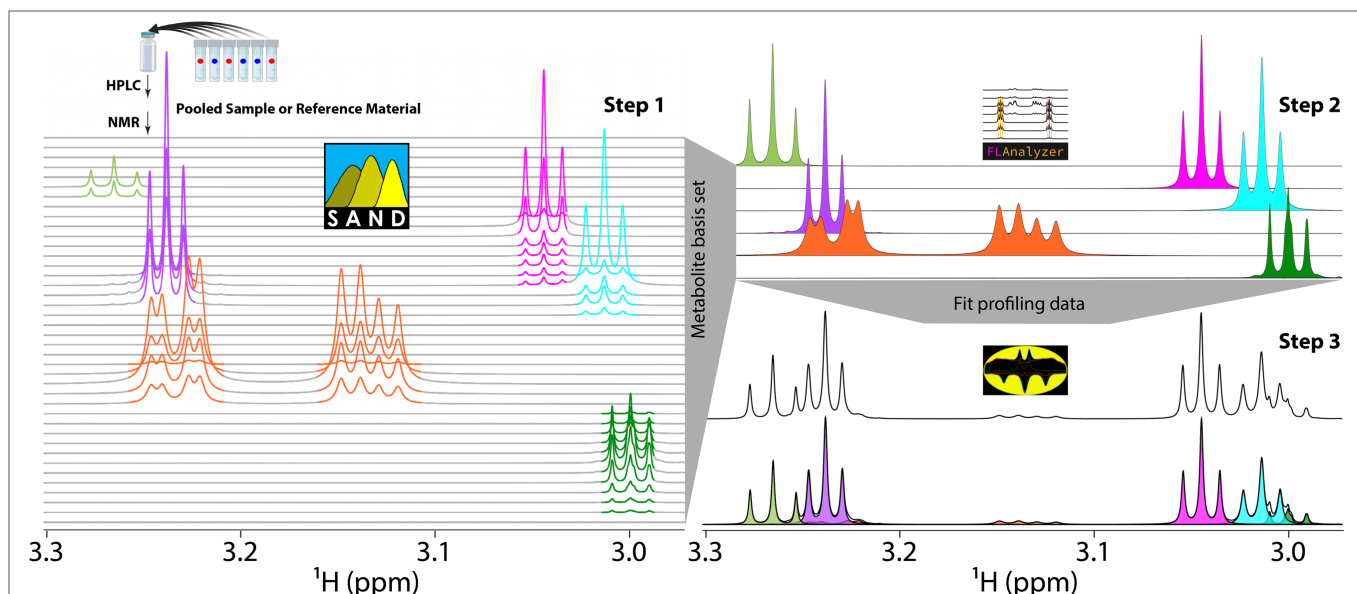


Fig. 1: Overview of the method. **Step 1** represents the construction of the metabolite fraction library (mFL), starting with a pooled sample or reference material, followed by HPLC chromatography with untargeted fraction collection, 1D ¹H NMR spectroscopy of all fractions, and tabular domain creation using SAND. **Step 2** creates the metabolite basis set (mBS) by correlating all peaks in the mFL across eluting fractions using a MATLAB application called FLAnalyzer. The mBS can be database-matched to derive known compound annotations. **Step 3** fits the known and unknown mBS elements into an unfractionated 1D ¹H NMR spectrum of a mixture from the study. We use BATMAN with the mBS as prior knowledge in a Bayesian fit to the data.

Multiphoton State Transitions in the Multilevel Spin System $\text{Gd}^{3+}:\text{YVO}_4$

Sabastian I. Atwood,¹ Manoj Subramanya,¹ Tomas Orlando,¹ and Stephen Hill^{1,2}

1. National High Magnetic Field Laboratory, Florida State University, Tallahassee, FL 32310, United States
2. Department of Physics, Florida State University, Tallahassee, FL 32306, United States;
Department of Chemistry and Biochemistry, Florida State University, Tallahassee, FL 32306, United States

A multilevel quantum system offers the possibility of running certain quantum algorithms entirely within the system, without the need to couple to other systems [1]. To that end, Leuenberger and Loss have proposed a scheme using multiphoton resonances to prepare and control an anharmonic multilevel spin system with single, multifrequency pulses [1]. High-spin paramagnetic systems such as rare earth metals or lanthanides embedded in solid state or molecular structures offer strong coupling with microwave excitation and tunable energy levels via an external static magnetic field. These properties make them promising test grounds for multilevel quantum state operations via electron paramagnetic resonance (EPR) spectroscopy. Previous studies have demonstrated coherent multiphoton transitions using monotone excitation of Mn^{2+} in a single crystal of MgO [2]. We report preliminary continuous wave and pulsed EPR studies of Gd^{3+} doped in crystalline YVO_4 demonstrating control of the level anharmonicity and identifying signatures of coherent two-photon transitions. At the same time, the data show consistent signs of coupling between Gd^{3+} and surrounding nuclei, coupling that might complicate coherent transitions into the desired superposition state. These initial results suggest that $\text{Gd}^{3+}:\text{YVO}_4$ is a candidate for demonstrating coherent multiphoton control with multifrequency excitation, but that host crystals with low-spin nuclei may also be desirable.

1. M. Leuenberger and D. Loss. *Nature* **410**, 789 (2001)
2. S. Bertaina, L. Chen, N. Groll, J. Van Tol, N. S. Dalal, and I. Chiorescu. *Phys. Rev. Lett.* **102**, 050501 (2009); S. Bertaina, N. Groll, L. Chen, and I. Chiorescu. *Phys. Rev. B* **84**, 134433 (2011); S. Bertaina, M. Martens, M. Engels, D. Barakel, and I. Chiorescu. *Phys. Rev. B* **92**, 024408 (2015)

Frequency and bandwidth tunable photonic band gap resonators for pulse EPR with at least tenfold greater concentration sensitivity

Sergey Milikisiyants, Alexander A. Nevzorov, Alex I. Smirnov*

North Carolina State University, Raleigh, NC, USA

Rapid growth in applications of pulse EPR spectroscopy in physics, chemistry, and biology over recent years is mainly owned by advances in EPR instrumentation and method development. Specifically, the progress in microwave technologies, such as high-power solid-state and compact traveling-wave tube (TWT) amplifiers and ns-scale pulse shaping enabled by AWGs (arbitrary wave form generators), significantly increased excitation bandwidth, improved selectivity of spin excitation, and, overall, increased pulse EPR sensitivity. Particularly remarkable progress has been achieved in pulse EPR at Q-band (35 GHz), which became the resonance frequency of choice for pulse dipolar spectroscopy (PDS). For example, today state-of-the-art 300 W TWT Q-band amplifier from Bruker Biospin provides ca. 100 MHz excitation bandwidth when used with a single mode Bruker Q-band EN5107D2 resonator. With such high microwave power available, one of the main remaining bottlenecks of further concentration sensitivity improvement is the inherently small accessible sample volume/resonator size of single mode microwave cavities that limits the number of spins for induction detection. Moreover, the increased excitation bandwidth dictates lowering the resonator Q-factor and this inevitably causes losses in EPR signal.

Here we introduce a new design of frequency and bandwidth tunable high Q-factor photonic band gap resonators for pulse Q-band EPR with accessible sample volume of up to two orders of magnitude larger than that of the existing single mode cavities. The resonator is tunable over a wide range of both frequency and the excitation bandwidth (resonator match – from critically coupled to fully overcoupled). The resonators were tested using commercial Bruker E580 pulse EPR spectrometer and demonstrated at least an order of magnitude gain in signal-to-noise ratio (SNR) for samples with the same spin concentration vs. commercial Bruker EN5107D2 resonator. Supported by NIH R01GM153951 to AIS and AAN.

Multi-Functional Role of Oxalate Decarboxylase Revealed by EPR Studies

Zain Becerra*, Alexander Angerhofer

Department of Chemistry, University of Florida, Box 117200, Gainesville, FL32611, USA

Oxalate decarboxylase (OxDC) is an essential Mn-dependent bicupin enzyme involved in the regulation of pH in the soil bacterium *Bacillus subtilis*. Intriguingly, recent studies have shown an additional catalase-like activity associated with this enzyme. Catalase activity in cells is essential to prevent cellular oxidative damage by dismutation of hydrogen peroxide into water and oxygen. This finding has expanded the understanding of the enzyme's biological significance and catalytic versatility. This contribution presents a mechanistic analysis of the multi-functionality of OxDC, supported by Electron Paramagnetic Resonance (EPR) cryogenic and spin-trap studies.

CW EPR at low temperatures shows that hydrogen peroxide oxidizes Mn(II) to Mn(III) in OxDC. We are able to observe Mn(III) via parallel-mode EPR. Interestingly, in the presence of hydroxylamine, a mild reducing agent, the EPR signal associated with Mn(III) is quenched. Moreover, both oxalate-degrading and catalase-like activity is significantly inhibited by hydroxylamine. The reduction in activity indicates the necessity of Mn(III) for both functions.

Additionally spin trapping by 5-tert-butoxycarbonyl-5-methyl-1-pyrroline-N-oxide (BMPO) was employed to detect, identify, and discriminate between different reactive oxygen species (ROS). The spectra indicate the presence of the hydroxyl radical (OH[•]) and superoxide radical anion (O₂^{•-}) were detected during the breakdown of hydrogen peroxide. These findings provide new insights into the mechanism of the catalase-like activity of OxDC and its potential role in the detoxification of ROS.

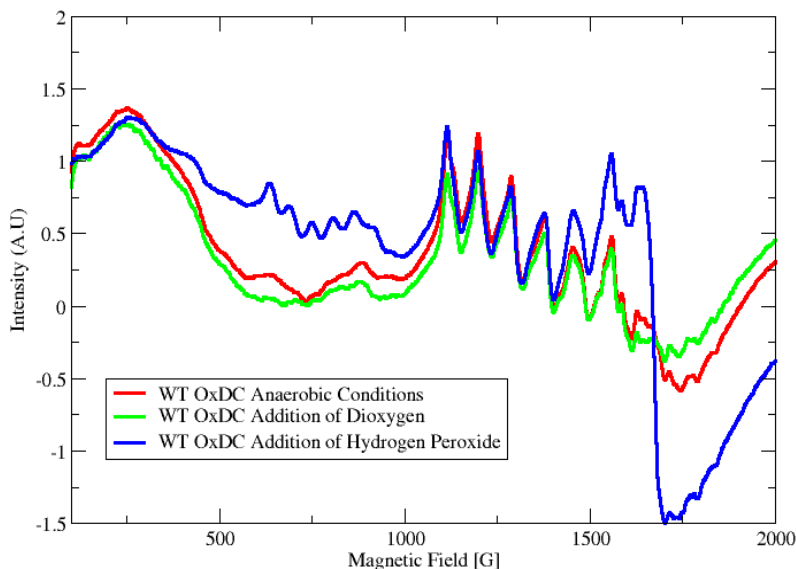
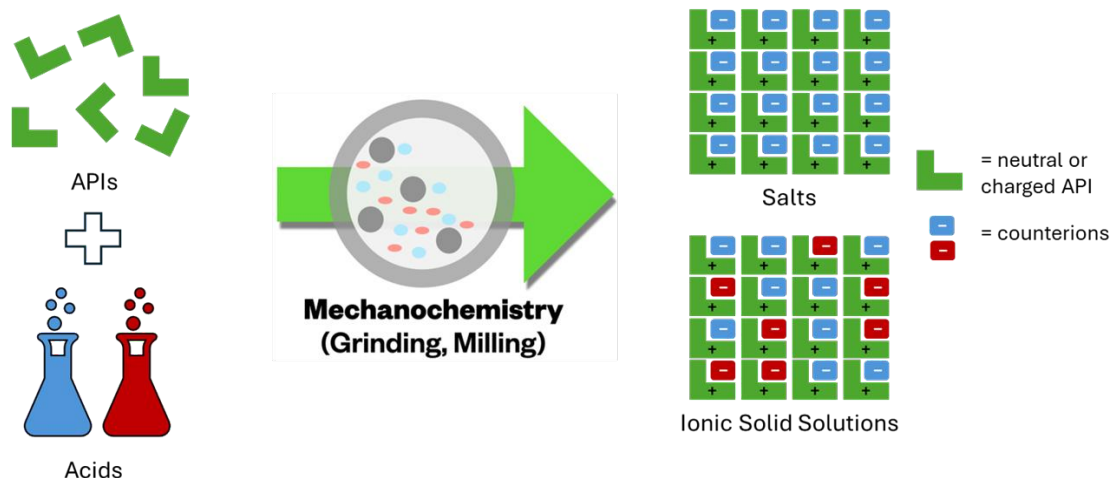


Figure 1.. X-Band EPR spectra of WT OxDC at pH 4.0 in parallel mode. The black trace is for Wt-OxDC in a poly-acetate buffer as prepared, the blue trace is for OxDC prepared in anaerobic conditions, the green trace after the addition of hydrogen peroxide, and the red trace after bubbling the solution with oxygen. All spectra were taken on the same sample at 5 K. EPR parameters of parallel-mode frequencies of 9.416 GHz, respectively, modulation frequency of 100 kHz, modulation amplitude of 10 G, and microwave power of 0.63 mW.

Mechanochemical Routes to Conventional and Integrative Pharmaceutical Solid Forms: Insights from PXRD and Multinuclear Solid-State NMR SpectroscopyPeyton Osborn^{1,2*}, Sean Holmes^{1,2}, Zach Dowdell^{1,2}, Robert W. Schurko^{1,2}.¹*Department of Chemistry and Biochemistry, Florida State University, Tallahassee, FL, 32306*²*National High Magnetic Field Laboratory, Tallahassee, FL, 32310*

Mechanochemistry has emerged as a powerful synthetic approach with growing impact across pharmaceuticals, materials science, and sustainable chemistry. Mechanochemical synthesis, which uses mechanical force to drive chemical reactions, can sometimes exploit synthetic pathways that are different from those found in analogous solution-based synthetic techniques. In the realm of active pharmaceutical ingredients (APIs), mechanochemistry provides a greener and more efficient approach for synthesizing conventional solid forms, such as salts and cocrystals, and provides a powerful means for discovery of novel integrative solid forms that combine structural features of multiple simpler classes, including polyheterosalts and ionic solid solutions. Solid form development and screening are critical steps in drug development, as the solid form of an API can dramatically affect its physicochemical properties, such as solubility, thermal stability, and bioavailability, without negatively influencing its pharmacological activity.

In this study, ball milling is used to synthesize salts and integrative solid forms, particularly, ionic solid solutions, of the APIs amlodipine and dapson. These are characterized with powder X-ray diffraction (PXRD) and multinuclear solid-state NMR (SSNMR), focusing on the nuclei ¹³C, ³⁵Cl, and ⁸¹Br. Together, these results demonstrate how comprehensive structural characterization by PXRD and SSNMR provides critical insight into the architectures and compositional flexibility of solid forms of APIs obtained via mechanochemistry.

**Figure 1.** Mechanochemical Synthesis of Pharmaceutical Solid Forms

Structural Characterization of Surface Immobilized Platinum Hydrides by Indirect Detection Solid State NMR Spectroscopy

Authors. Benjamin A. Atterberry,^{1,2,3} Deven P. Estes,⁴ Aaron J. Rossini,^{2,3} Peijie Hu,¹ Keith Searles,¹ and Clifford R. Bowers¹

Author Locations:

¹University of Florida, Department of Chemistry, Gainesville, FL, USA, 32603

²US DOE Ames National Laboratory, Ames, Iowa, USA, 50011

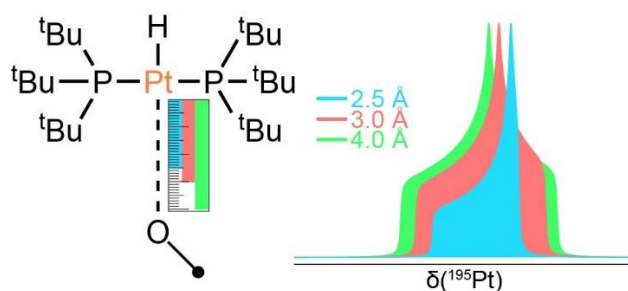
³Iowa State University, Department of Chemistry, Ames, IA, USA, 50011

⁴University of Stuttgart, Department of Chemistry, Stuttgart, Baden-Württemberg, Germany, 70569

Abstract.

Surface-supported Pt compounds and Pt nanoparticles are widely employed in heterogeneous catalysis. Unfortunately, the structure of Pt sites in heterogeneous catalysts are often ill-defined because it is difficult to characterize the Pt electronic and chemical environment. ¹⁹⁵Pt solid-state NMR spectroscopy (SSNMR) can provide essential data about the chemical and electronic environments in Pt catalysts because the chemical shift (CS) tensor is sensitive to the character and symmetry of the neighboring ligands. However, ¹⁹⁵Pt solid-state NMR spectra are often thousands of parts per million wide, and NMR sensitivity is often too low to permit detection of dilute surface Pt sites. Here, we demonstrate methods to enhance ¹⁹⁵Pt NMR sensitivity. We show how fast magic angle spinning (MAS) ¹H- or ³¹P-detected ¹⁹⁵Pt *J*-resolved experiments can be applied to investigate the molecular structure of platinum phosphines and platinum hydride phosphine compounds that find application as catalysts for enyne isomerization. Using ¹H- or ³¹P-detected methods it is possible to record wide-line ¹⁹⁵Pt MAS NMR spectra in a few hours on the pure compounds. We then show how slow MAS cryogenic DNP SENS ³¹P{¹⁹⁵Pt} *J*-resolved experiments can be used to study two low Pt wt% (1.9 and 2 wt%) single-site Pt hydride catalysts. These methods, combined with DFT calculations, offer a picture of the coordination sphere of the surface-supported complexes. Finally, we demonstrate that ³¹P-detected methods enable high-resolution ¹⁰³Rh MAS spectra to be acquired in as little as 30 minutes, and outline plans to integrate ¹H detection with a double-echo RESPDOR sequence to obtain ⁹¹Zr MAS spectra of zirconium hydride catalysts used in hydrogenation and hydrogenolysis reactions.

Graphic:



Structural insight into inhibitor-mediated modulation of Huntingtin Exon 1 aggregation

Greeshma Jain^{1,2*}, Marina Trombetta-Lima^{3,4}, Irina Matlahov¹, Henrique Taborda Ribas^{3,5},
Tingting Chen¹, Amalia M. Dolga³, Patrick C.A. van der Wel¹

¹ Zernike Institute for Advanced Materials, Faculty of Science and Engineering, University of Groningen, Groningen, The Netherlands

² Current: Department of Chemistry, University of Florida, Gainesville, Florida, United States of America

³ Department of Molecular Pharmacology, Faculty of Science and Engineering, Groningen Research Institute of Pharmacy (GRIP), University of Groningen, Groningen, The Netherlands

⁴ Department of Biomedical Sciences of Cells and Systems, Section Molecular Cell Biology, University of Groningen, University Medical Center Groningen, Groningen, The Netherlands

⁵ Graduate Program in Biochemistry Sciences, Department of Biochemistry and Molecular Biology, Federal University of Paraná, Curitiba, PR, Brazil

Huntington's Disease (HD) is a neurodegenerative disease caused by the expansion of the polyglutamine (polyQ) domain in the exon 1 region of the huntingtin (htt) protein. This expansion of the polyQ domain leads to protein misfolding and the formation of β -sheet-rich fibrillar aggregates. The major challenge is to understand the mechanism of amyloid formation and their toxicity. Small molecule inhibitors have been shown beneficial for perturbing the aggregation kinetics, but their molecular modes of action are still not well understood. Here we employ solid-state nuclear magnetic resonance (ssNMR), in combination with electron microscopy (TEM) and kinetic assays, to elucidate the inhibitor's effect on HttEx1 aggregation mechanism. We observe a clear delay of protein aggregation was observed even at sub stoichiometric ratios of inhibitor relative to the protein. Our NMR analysis reveals that inhibitor-bound fibrils adopt a distinct conformation compared to the HttEx1 fibrils. Here, we propose a molecular model for the impact of the inhibitor on the aggregation mechanism, impacting the nucleation process and redirecting it toward a distinct aggregated state with modified toxic properties. Our data lays a foundation of how small molecules reshape the misfolding landscape of HttEx1, highlighting the importance of NMR spectroscopy in characterizing the structure of these aggregates.

References

1. Jain, G., Trombetta-Lima, M., Matlahov, I., Ribas, H. T., Chen, T., Parlato, R., Portale, G., Dolga, A. M., & van der Wel, P. C. A. (2025). Inhibitor-based modulation of huntingtin aggregation mechanisms mitigates fibril-induced cellular stress. *Nature Communications*, *16*(1), 3588.

Gangliosides promote structural heterogeneity in A β 42 aggregates

Jhinuk Saha^{1,2,3*}, Brianna McVay^{1,2}, Riqiang Fu¹, Sungsool Wi¹ and Ayyalusamy Ramamoorthy^{1,2,3}

¹National High Magnetic Field Laboratory, 1800 E. Paul Dirac Drive,
Tallahassee, FL 32310, USA

²Department of Chemical and Biomedical Engineering, FAMU-FSU College of Engineering,
2525 Pottsdamer St., Tallahassee, FL 32310, USA

³Institute of Molecular Biophysics, Florida State University,
91 Chieftan Way, Florida State University, Tallahassee, FL 32306, USA

The deposition of amyloid beta (A β) plaques in the brain is one of the key pathological hallmarks of Alzheimer's Disease (AD). The aggregation of A β into oligomers and fibrils is a complex process influenced by a variety of factors, including cell membrane components, metal ions, salts, and interacting proteins. Among these, gangliosides, sialic acid-containing glycosphingolipids enriched in membrane rafts, have drawn particular interest due to their reported presence within A β plaques, suggesting a direct role in modulating A β aggregation. Previous studies have shown that GM1 ganglioside can bind A β and promote the formation of both toxic oligomeric intermediates and fibrillar aggregates¹⁻³. However, gangliosides are structurally diverse and vary among different cell types, raising the possibility that this diversity may influence the morphology and toxicity of A β aggregates through the formation of structural polymorphs. In this study, we investigated the influence of two structurally different gangliosides, GD3 and GM3, on A β aggregation. Using solid-state NMR spectroscopy and complementary biophysical techniques, we demonstrate that these gangliosides differently modulate the aggregation pathway of A β , leading to the formation of distinct aggregate species that are capable of further seeding and causing cellular toxicity. These findings suggest that different types of gangliosides exhibit distinct impact on conformational landscape and assembly kinetics of A β . Our study provides new insights into how the cellular lipid environment, particularly the diversity of gangliosides, contributes to the complexity of A β aggregation in AD. These findings suggest that the structural features of individual gangliosides can significantly impact the conformational landscape and assembly kinetics of A β , potentially contributing to the heterogeneity observed in A β aggregates in AD.

Keywords: NMR, Amyloid, Aggregation, Gangliosides, cell toxicity

REFERENCES

1. Wakabayashi M, Okada T, Kozutsumi Y, Matsuzaki K. GM1 ganglioside-mediated accumulation of amyloid β -protein on cell membranes. *Biochemical and biophysical research communications*. 2005 Mar 25;328(4):1019-23.
2. Kumar M, Ivanova MI, Ramamoorthy A. Ganglioside GM1 produces stable, short, and cytotoxic A β 40 protofibrils. *Chemical Communications*. 2023;59(46):7040-3.
3. Saha J, Bose P, Dhakal S, Ghosh P, Rangachari V. Ganglioside-enriched phospholipid vesicles induce cooperative A β oligomerization and membrane disruption. *Biochemistry*. 2022 Sep 29;61(20):2206-20.

A Multi-nuclear Volume Coil for H/X Pre-clinical MR at Ultra High Magnetic FieldsDavid Doty^{1*}, G Doty¹, M Skolozub², T Harris², E Montrazi², D Arcos¹, J Doty¹, L Holte¹, and L Frydman²¹Doty Scientific, Columbia, SC, USA, ²Weizmann Institute of Science, Rehovot, Israel

Introduction: There is need for H/X multi-nuclear MRI, but the S/N from low-gamma nuclides is insufficient except at ultra-high fields (UHF). UHF magnets usually have relatively small gradient bores, exacerbating the challenges in H/X volume coil MRI.

Methods: The foil and cross-over patterns in Litz-foil coil designs were optimized using CST and detailed 3D models of the complete module, including both coils, the tune/match networks, the sample, and rf shield (58 mm). The primary objective was a balance between maximizing sensitivity ($B_1/P^{0.5}$) over a large homogeneous volume – enabling for instance pregnant mouse whole body studies – and minimizing the distance from the access end to the region of high B_1 for rat head studies. Additional objectives included clean tuning of the X channel to any frequency of interest from ²³Na to ¹⁴N by simply changing plug-in capacitors. A Symmetric Quarter-Turn (SQT) Litz-Foil coil is used for the outer ¹H-¹⁹F coil, and a Center-Fed 2-turn (CF2b) orthogonal inner Litz-Foil 38-mm coil is used for the multi-X channel.

Results: The simulations (accurately) predicted the following pulse lengths for hard $\pi/2$ nutations with full loads (obese mouse body): 50 μ s at 450 W for ¹H at 650 MHz; 150 μ s at 160 W for ²³Na at 172 MHz; 150 μ s at 210 W for ²H at 99.3 MHz; 200 μ s at 1100 W for ¹⁴N. MRI ¹H and ²H results on a pregnant mouse were recorded in ~2 minute intervals following injection of saline D₂O, providing water transport information across the placentas and into individual fetal organs at a level never before seen. The coronal ¹H and ²H images in Figures 1a and 1b show fetuses and organs in a pregnant mouse 18 minutes after D₂O injection, when D₂O signals in the various regions have reached 70-90% of final values.

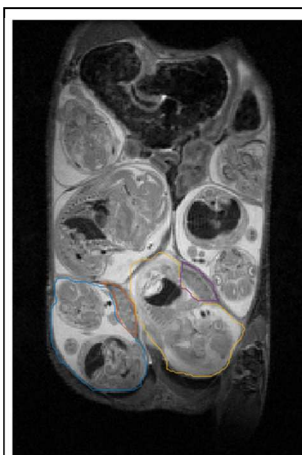


Figure 1a. MRI of the ROI in Figure 5 except ¹H RARE. Matr.: 256x256. Thick: 1 mm.

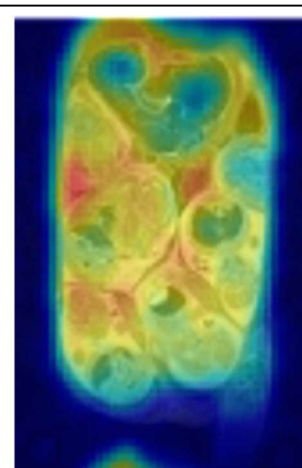


Figure 1b. ²H MRI showing differential uptakes in a pregnant mouse ~18 minutes after D₂O injection. 3D-bSSFP; TR: 2.206 ms; Matr: 32x32x16.

Conclusion: Efficient volume coils make experiments much easier than working with surface coils by capturing large clear slices throughout multiple organs at the same time. Novel H/X rf coils promise to make multi-nuclear pre-clinical MRI more practical.

Reference: FD Doty, G Entzminger, and CD Hauck, Error-Tolerant Litz Coils for NMR/MRI, *J. Magn. Reson.*, 140:17-31 (1999).

Acknowledgements: This work is supported by Doty Scientific and by the Clore Institute for High Magnetic Field Imaging and Spectroscopy, Weizmann Institute.

Abstract title: BOLD Functional Connectivity Correlates of PTSD Severity and Chronicity during Image Viewing

Authors: *Robert D. Claar^{1,2,3,4,5}, Sarah M. Gardy⁶, Andreas Keil⁶, Damon G. Lamb^{1,2,3,4,5}

¹Brain Rehabilitation Research Center, Malcolm Randall VAMC, Gainesville, FL; ²Department of Biomedical Engineering, ³Department of Psychiatry, ⁴Center for OCD and Anxiety-Related Disorders, ⁵McKnight Brain Institute, ⁶Department of Psychology, University of Florida, Gainesville, FL

Background/Introduction

Chronic stress, the sustained exposure to stressors exceeding the body's adaptive capacity, is a hallmark of disorders such as PTSD, anxiety, and depression. Persistent activation of stress-response systems can produce allostatic load, the cumulative physiological burden resulting from prolonged neural and endocrine activation. Models of PTSD implicate not only emotional brain regions (e.g., amygdala, insula, hippocampus) but also sensory-perceptual areas involved in threat discrimination. Growing evidence suggests that the visual cortex contributes to emotional learning and perception and may become dysregulated under chronic stress, leading to altered sensory engagement or blunted differentiation of threat cues.

Methods

We used blood-oxygen-level-dependent (BOLD) functional MRI to examine whole-brain activation and visual cortex functional connectivity in relation to PTSD symptom severity, chronicity, and visual complaints in 109 combat veterans with varying symptoms of emotional dysregulation. During scanning, participants passively viewed emotionally negative, neutral, and positive images.

Results

PTSD severity was positively associated with functional connectivity between visual cortex seeds and clusters in parietal and temporal regions. PTSD chronicity was positively associated with connectivity between the left occipital pole and bilateral frontal poles, but negatively associated with connectivity between the right inferior lateral occipital cortex and bilateral juxtapositional lobule cortex.

Conclusions

These findings highlight altered engagement of visual-limbic and visual-frontal circuits in PTSD, suggesting that chronic stress may disrupt emotion-perception coupling mechanisms within visual pathways.

Abstract title: Calibrated MR-ARFI with a Non-Magnetic Micropositioner

Authors: Ryan Willoughby*, Mark Bolding

Affiliation: Dept. of Radiology, Heersink School of Medicine, The University of Alabama at Birmingham

Background: Magnetic resonance acoustic radiation force imaging (MR-ARFI) is a phase contrast MRI technique that estimates micrometer-scale tissue deformation caused by absorption and scattering of focused ultrasound (FUS).¹ The purpose of this research was to develop a novel automated micropositioner to generate known displacements in the MRI environment that can be used to calibrate MR-ARFI pulse sequences for quantitative measurements.

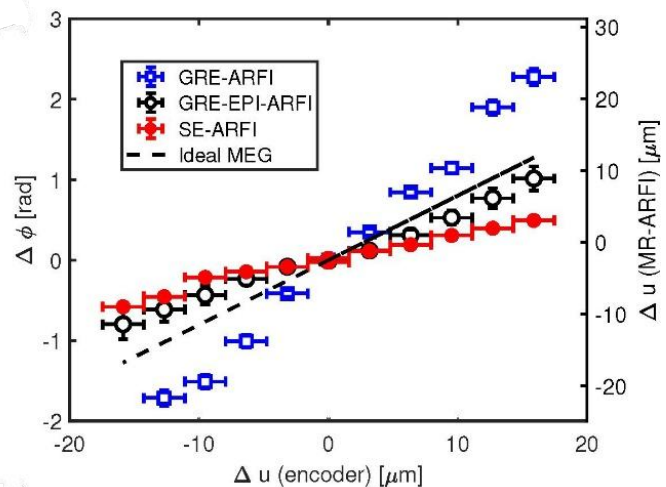
Methods: The micropositioner used a piezoelectric stepper motor and an optical quadrature encoder to move a stage back and forth synchronously with displacement-encoding gradients. A 100-gram agar gel phantom was used in preliminary experiments. Benchtop tests verified the timing and displacement of the phantom. Three different MR-ARFI pulse sequences (spin-echo SE, gradient-recalled echo GRE, and echo planar imaging EPI) were used to map the displacement of the phantom in the MRI scanner (Prisma 3T).

Results: The micropositioner consistently displaced the phantom up to 16 μm from its initial position in 1.6 ± 0.4 ms and returned to initial position in 2.2 ± 0.2 ms. Placement of the device in the field of view resulted in SNR decreases of about 5% for SE and GRE-ARFI and about 10% for EPI-ARFI. MR-ARFI phase differences and estimated displacements were highly correlated to encoder measurements ($R^2 = 0.994, 0.987, \text{ and } 0.982$ for GRE, EPI, and SE respectively), but the slope of each regression was significantly different than theoretical factors ($\alpha = 0.1\%$).

Conclusions: A micropositioner was implemented for 3T MR-ARFI validation. High linearity of MR-ARFI displacements compared to encoder reference and deviations of regression slopes indicate that MR-ARFI calibration is a viable technique with this device. Applications include in situ ultrasound device testing, calibrated MR-guided FUS procedures for safer, more effective treatments, and guiding development of respiratory/motion correction algorithms for MR-ARFI pulse sequences.

References

1. Odéen H, Payne AH, Parker DL. Magnetic Resonance Acoustic Radiation Force Imaging (MR-ARFI). *Journal of Magnetic Resonance Imaging*. 2025;62(1):20-39.



Title: Imaging Neuronal Transmission Using Novel Genetic Encodable MRI Reporters**Authors:** Shuaipeng Ma, Yang Yang, Rui Yang, Ilse Delint Ramirez, Ram Madabhushi, Nan Li*.**Affiliation:** Advanced Imaging Research Center, Department of Neuroscience, Peter O'Donnell Brain Institute, University of Texas Southwestern Medical Center, Dallas, TX

Background/Introduction: The brain operates as a highly interconnected network of neurons communicating via action potentials and synaptic transmission. Understanding how these signals are coordinated remains highly challenging. Calcium indicators combined with optical imaging help visualize neural activity in a limited field of view, while magnetic resonance imaging (MRI) provides non-invasive whole-brain coverage but lacks molecular and cellular specificity. To address this technical gap, we developed novel genetically encodable fMRI reporters, named Axon-terminal-Specific Action-Potential-driven (ASAP), to enable in vivo imaging of synaptic transmission.

Methods: Reporter design - For the first-generation construct, we engineered an ASAP reporter incorporating the neuronal secretory machinery and neurovascular coupling mechanisms. Upon neuronal activation, LDCVs fuse with the presynaptic membrane, releasing vasoactive peptides, producing hemodynamic-based MRI signals, reporting synaptic transmission events. In vitro validation: Functional validation was conducted using a co-culture system comprising mouse neuroblastoma N2a cells expressing ASAP and PAC1R-expressing CHO cells. Vasoactive peptides released from N2a cells upon calcimycin stimulation were quantified by detecting subsequent cAMP signaling in CHO cells. In vivo MRI imaging: N2a cells, with and without ASAP expression, were transplanted into the striatum of anesthetized rats, mounted to the MRI-compatible cradle. All MRI images were obtained in a 7T MRI scanner. T2*-weighted MRI scans were continuously collected for before, during, and after calcium stimulation. High-resolution anatomical MRI images were acquired using a T2-weighted rapid acquisition with refocused echoes (RARE) pulse sequence to localize transplanted cells.

Results: Stimulation of ASAP-expressing N2a cells produced concentration-dependent vasoactive peptides release, quantified by a cAMP assay in CHO reporter cells; no signal was detected from naïve N2A cells. In vivo, transplanted ASAP-N2a cells elicited real-time T2*-weighted MRI signal changes upon calcimycin infusion, whereas control implants of naïve N2a cells showed no significant signal changes. Immunohistochemistry confirmed ASAP expression in the test groups.

Achieving Liquid-State ¹H DNP through Particle-Mediated ¹H–¹H Cross Relaxation.

Authors: Sungsool Wi,^{1*} Angeliki Giannouli,^{2,3} Korin Butbul,² Jenica Lumata,¹ Thierry Dubroca,¹ Faith Scott,¹ Zachary Dowdell,⁴ Robert W. Schurko,^{1,4} Johan Van Tol,¹ and Lucio Frydman^{1,2}

¹ National High Magnetic Field Laboratory, Tallahassee, Florida 32304, USA

² Department of Chemical and Biological Physics, Weizmann Institute of Science, 7610001 Rehovot, Israel

³ Department of Chemistry, University of Crete, Voutes Campus, 70013 Heraklion, Greece

⁴ Department of Chemistry and Biochemistry, Florida State University, Tallahassee, Florida 32306, USA

Abstract

We introduce a potential route for enhancing solution-state ¹H NMR signals via ¹H–¹H cross relaxation in the liquid phase at high magnetic fields for samples on the 100 μL scale, using dynamic nuclear polarization (DNP). The method involves dispersing an inert, proton-rich powder capable of efficient DNP at non-cryogenic temperatures, allowing the DNP-enhanced solid-state ¹H polarization to transfer to the surrounding liquid through spontaneous ¹H–¹H cross-relaxation effects. To this end, BDPA-doped polystyrene (PS) microparticles were suspended in 30 μL of heptane, loaded into 3.2 mm sapphire rotors, and spun at ≈500 Hz in a 14.1 T magnet for sample homogenization. Under irradiation at ≈395 GHz (≈13 W) while maintaining temperatures between 185 K and 220 K, the PS proton polarization was enhanced ≈12-fold within ≈2 s; after ≈6 s of irradiation, this resulted in a threefold enhancement of the heptane proton resonances while preserving their ≤2 Hz linewidths. The dependence of such particle-mediated transfer on sample composition, deuteration, and molecular weight was systematically examined. Optimal results were obtained for a ball-milled powder composed of deuterated-PS/PS/BDPA = 86.4/9.6/4.0 suspended in perdeuterated heptane-d₁₆. Although the solution-state enhancements achieved are still modest, this approach offers a broadly applicable pathway for DNP-enhanced ¹H NMR that preserves large sample volumes, high spectral resolution, and compatibility with multi-scan signal averaging customary in modern liquid-state NMR.

Optical Control of Molecular Qubits

Haochuan Mao

Department of Chemistry and Biochemistry, Florida State University, Tallahassee, USA

In this talk, I will discuss how molecular design and advanced EPR spectroscopy converge to realize spin-based quantum functions. Using transient and pulsed EPR, we probe photogenerated radical pairs and triplet states in tailored donor–acceptor architectures to achieve optical spin initialization, coherent gate operations, and electric-field sensing. By combining pulse-sequence design with pulse-shaping control, we resolve spin dynamics and polarization transfer pathways at the molecular level. These results highlight how EPR can guide the development of molecular qubits based on electron spins.

From light to friction: how metal oxides drive radical formation in lubricants

Julie Matheny, Roshan Rana, Phil Bankaitis, Alex Hamby, and Tatyana I. Smirnova*

North Carolina State University, Raleigh, NC

Nanoparticle (NP) additives have recently attracted considerable attention for their ability to enhance tribological and thermophysical properties of petroleum-based lubricants. However, relatively little research has been done to explore their potential to generate free radicals in oils through photochemical or mechano-activation mechanisms.

In this study, spin-trapping Electron Paramagnetic Resonance (EPR) spectroscopy was employed to quantify and characterize short-lived free radical intermediates formed in light mineral oil (LO) containing nanoparticles. Upon photoactivation with 365 nm UV light, TiO₂, CeO₂, and ZnO₂ nanoparticles significantly increased radical production compared to oil-only controls, particularly when molecular oxygen was present. TiO₂ and CeO₂ primarily promoted the formation of alkoxy radicals, while ZnO₂ supported peroxy radical generation in air-equilibrated samples. In contrast, in the absence of oxygen, the presence of nanoparticles had little to no effect, or even a suppressive effect, on radical formation, primarily by reducing the production of carbon-centered radicals. These results underscore the critical role of molecular oxygen in radical formation initiated by photochemically active nanoparticles.

Mechanoactivation of metal oxide nanoparticles, achieved by milling, led to surface modification of TiO₂ particles, as evidenced by the detection of stable radical species via low-temperature EPR. When added to air-equilibrated LO, mechanoactivated TiO₂ particles induced the formation of both alkoxy and peroxy radicals, with peroxy species being predominant. Extending milling time beyond 30 minutes resulted in a modest increase in radical production. Notably, the mechanoactivated TiO₂ retained approximately 25% of its radical-initiating activity even 24 hours after milling, indicating persistent surface reactivity. The Effects of mechanoactivated ZnO and alumina particles on radical formation in LO are also examined and discussed.

This work was supported by ACS PRF 65503-ND4 grant to TIS.

Intrinsic and Cooperative Dynamics of α -Synuclein Terminal Domains under Controlled Confinement

Katie L. Whitcomb and Kurt Warncke*

Emory University, Department of Physics, Atlanta, GA 30322-2430

The intrinsically disordered protein (IDP), α -synuclein (α S), assumes structurally and dynamically distinct forms in conducting its unknown molecular functions in brain neurotransmission.¹ This plasticity also contributes to dysfunctional aggregation in Parkinson's disease. In α S, the disordered N-terminal domain (NTD, residues 1-60) and C-terminal domain (CTD, 96-140) flank the protein β -structure-forming non-amyloid component (NAC, 61-96). We address the intrinsic structural and dynamical properties of the isolated NTD and CTD protein segments, and their contributions to dynamic allostery in truncated (1-95, 61-140) and full-length (1-140) human α S. Electron paramagnetic resonance spectroscopy of the spin probe, TEMPOL, co-localized with the proteins, and temperature (T)-controlled (200-260 K) ice boundary confinement, characterize the physical and mechanical properties of the proteins and surrounding coupled solvent regions.^{2,3} The observed transformation from fast (disordered region) to slow (hydration region) spin probe motional components with decreasing T (increasing confinement) shows a common compaction 1 (protein collapse and folding), tertiary structure consolidation and stable hydration layer formation, and compaction 2 (collapse and restriction), or C1-SC-C2, sequence for each protein.⁴ Different T ranges and relative amplitudes among the C1-SC-C2 reveal distinct cooperative interactions within the isolated TDs, and among the conjoined domains, that inform proposed molecular mechanisms for in vivo function and pathology. Supported by NIH R01 GM142113.

References

1. Sharma and Burre, *Trends Neurosci.*, 2023, 46, 153.
2. Li et al., *Phys. Chem. Chem. Phys.*, 2022, 24, 23919.
3. Whitcomb and Warncke, *ACS Chem. Neurosci.*, 2023, 14, 3905.
4. Whitcomb and Warncke, *J. Phys. Chem. B.*, 2025, 129, 8351.

Evaluating novel bTurea-based biradicals for MAS-DNP

***Shubha S. Gunaga**¹, Ancy T. Wilson², Frédéric Mentink-Vigier^{1,3}, and Snorri Th. Sigurdsson²

¹ National High Magnetic Field Laboratory, Florida State University, Tallahassee, FL, USA

² University of Iceland, Reykjavík, Iceland

³ Department of Chemistry and Biochemistry, Florida State University, Tallahassee, FL, USA

Dynamic Nuclear Polarization (DNP) enhances the inherently low sensitivity of solid-state NMR by transferring polarization from unpaired electrons to nuclei. The design of efficient, synthetically accessible biradicals remains a central challenge. In this work, we evaluated a new series of bTurea-based bis-nitroxides, bcTCOOKs, to understand how structural modification of the urea bridge influences DNP performance. DNP experiments were performed at 14.1 T (600 MHz ¹H) and 100 K under 8 kHz MAS using a 3.2 mm sapphire rotor setup. Across the bcTCOOK series, increasing N-alkyl substitution enhanced polarization efficiency and shortened the build-up time, consistent with stronger electron–electron coupling and improved relative g-tensor orientation [1]. The best-performing radical, bcTCOOK-M2, achieved an enhancement of ~220 and a T_B of 3.9 s, outperforming bcTol-M [2] and approaching the sensitivity of AsymPol-POK [3] under identical conditions. These results, which correlate with the radicals' EPR and DFT properties, demonstrate that subtle urea-bridge modifications can fine-tune electronic coupling and orientation, yielding a polarizing agent that combines strong performance and synthetic simplicity, even in proton-rich media [4].

References

1. Mentink-Vigier, F.; Dubroca, T.; Van Tol, J.; Sigurdsson, S. T. *J. Magn. Reson.* 2021, 329, 107026.
2. Geiger, M. A. *et al. Chem. Eur. J.* 2018, 24, 13485–13494.
3. Mentink-Vigier, F. *et al. J. Am. Chem. Soc.* 2018, 140, 11013–11019.
4. Sauvé, C. *et al. Angew. Chem. Int. Ed.* 2013, 52, 10858–10861.

Elucidating Electronic Structure and Relaxation Pathways of Transition Metal Complexes via High Power EPR Spectroscopy

Kavipriya Thangavel,^a Dipanti Borah,^b Vignesh Kasi,^b Maheswaran Shanmugam,^b Andreas Pöppel^c, Stephen Hill.^{a,d,e}

(a) *National High Magnetic Field Laboratory, Florida State University, Tallahassee, FL 32310, USA*

(b) *Department of Chemistry, Indian Institute of Technology Bombay, Mumbai 400076, India*

(c) *Felix Bloch Institute of Solid State Physics, University of Leipzig, 04103 Leipzig, Germany*

(d) *Department of Physics, Florida State University, Tallahassee, FL 32306, USA*

(e) *Department of Chemistry and Biochemistry, Florida State University, Tallahassee, FL 32306, USA*

Email: kt24@fsu.edu

Molecular spin qubits, known for their precise control, scalability, tunability, and room temperature capability to sustain multiple quantum states, are poised to impact the field of quantum information science [1]. These qubits combine efficiency and versatility, allowing for large-scale production, precise tuning of spin environments, and arrangement in 2D or 3D lattices. Progress in their design and surface integration is crucial for overcoming challenges related to addressability, coherence, and scalability in future quantum systems. As a result, they represent a highly promising area for ongoing research and development in this cutting-edge field. In addition, the metal–organic framework (MOF) MIL-53, a well-celebrated material known for its breathing nature[3], has begun to attract attention in the field of quantum information science [4].

In this context, we performed high-field continuous-wave (CW) electron paramagnetic resonance (EPR) experiments at frequencies up to 413 GHz on Co(II) based metal complexes and Cr(III)-based MOF to probe their electronic and structural properties. Specifically, we studied two Co(II) low-spin ($S = 1/2$) complexes, both having the molecular formula $[\text{CoCl}(\text{DPPE})_2]\text{SnCl}_3$ but differing in geometry: Co-SP adopts a square pyramidal structure, whereas Co-TBP exhibits a trigonal bipyramidal arrangement. These distinct geometries substantially affect their electronic environments and resultant EPR signatures. Furthermore, high-power W-band EPR spectrometer (HiPER) experiments revealed temperature-dependent relaxation behavior up to 60 K, with both complexes displaying similar characteristics when diluted. At 5 K, the spin-spin relaxation time (T_2) and spin-lattice relaxation time (T_1) for Co-TBP were approximately 5.8 μs and 0.62 ms, respectively, while Co-SP exhibited $T_2 \approx 3.5 \mu\text{s}$ and $T_1 \approx 0.98$ ms. Additionally, we investigated the MOF MIL-53, where the T_2 and T_1 values were found to be 0.96 μs and 50 μs , respectively, at 5 K.

References:

[1] Hill et al., *Nature*. **2016**, 531, 348–351.

[2] Thangavel. K. et al., *RSC Adv.*, **2024**, 14, 4244-4251

[3] Yamachi A. et al., *Nat. Comm.*, **2024**, 15, 7622

Probing the Structures and Dynamics of Cobaltocenium Compounds via Ultra-Wideline ⁵⁹Co Solid-State NMR

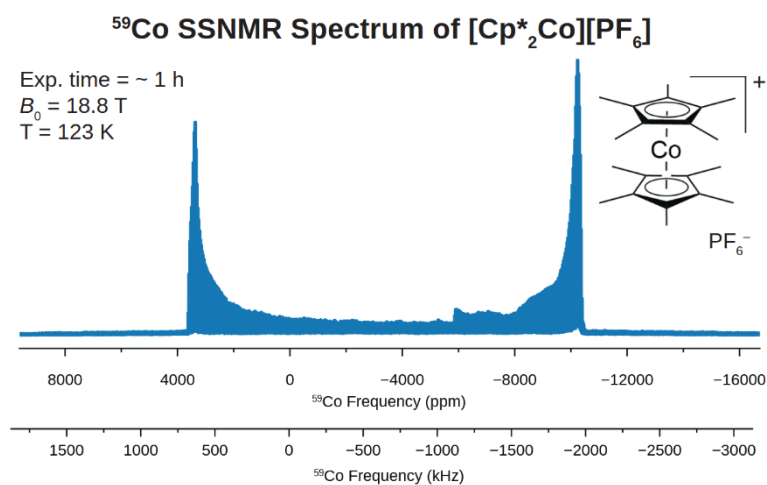
Dominic C. Chantra*^{1,2}, Sara Termos^{1,2}, Sean T. Holmes², Robert W. Schurko^{1,2}

¹*Department of Chemistry & Biochemistry, Florida State University, Tallahassee FL 32306*

²*National High Magnetic Field Laboratory, Tallahassee FL 32310*

Solid-state NMR (SSNMR) is a powerful tool for probing molecular-level structure and dynamics; however, many nuclides remain a challenge due to low receptivity, including unfavorable relaxation characteristics and/or large anisotropic interactions. These difficulties can be mitigated with high magnetic fields, specialized hardware, and advanced pulse sequences. For half-integer quadrupolar nuclei such as ⁵⁹Co ($I = 7/2$), the second-order quadrupolar interaction and chemical shift anisotropy can yield central transition (CT, $+1/2 \leftrightarrow -1/2$) ultra-wideline (UW) powder patterns that may be several MHz in breadth. In such cases, the use of frequency-swept pulses such as *wideband uniform-rate smooth-truncation* (WURST) pulses,¹ in tandem with signal-to-noise enhancing *Carr-Purcell-Meiboom-Gill* (CPMG) sequences,² enable efficient acquisition of uniform CT patterns under static conditions.³

I will discuss the challenges of acquiring ⁵⁹Co UW SSNMR spectra of the cobaltocenium complexes [Cp₂Co][PF₆] and [Cp*₂Co][PF₆] (Cp = C₅H₅; Cp* = C₅Me₅). Spectra were acquired at 18.8 T from 120 to 300 K using the WURST-CPMG sequence and variable-offset cumulative spectroscopy, allowing for detection of these patterns with breadths >2.5 MHz in under one hour. From these data, the chemical shift and electric field gradient tensors were determined and found to be in good agreement with those predicted by DFT calculations. Additionally, temperature-dependent T_2 measurements are used to shed light on the solid-state dynamics in these samples. These new findings, together with previous work on metallocenes,⁴ provide valuable insights into their structure, bonding, and dynamics, which may guide the rational design of new metallocenes with tunable bonding characteristics.



References

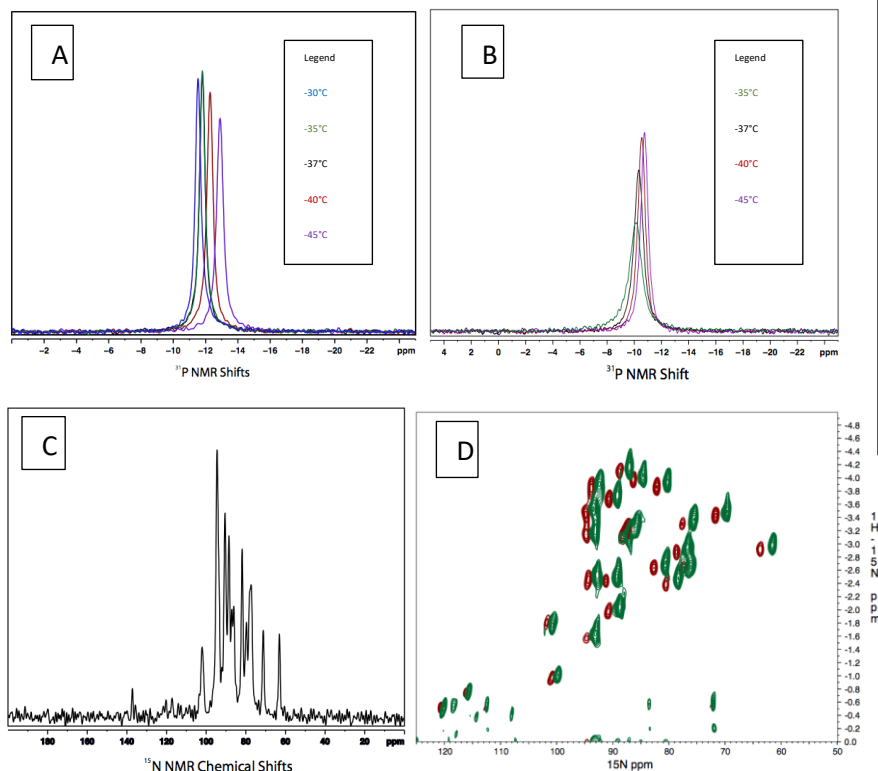
1. O'Dell, L. A. *Solid State NMR*. **2013**, 55-56, 28.
2. Gan, Z.; Hung, I. *J. Magn. Reson.* **2010**, 204, 256.
3. O'Dell, L. A. *et al. Chem. Phys. Lett.* **2009**, 468, 330.
4. Holmes, S. T. *et al. J. Am. Chem. Soc.* **2025**, 147, 20865.

Design and optimization of highly aligned peptoid macrodiscs for solid-state NMR studies of membrane proteins

Adit Shah*, Azamat Galiakhmetov, Alexander Nevzorov

Department of Chemistry, North Carolina State University

Lipid mimetics, such as bicelles and styrene-maleic acid lipid particles (SMALPs), allow one to study membrane in native-like environments where they preserve their structures. However, these lipid mimetics face limitations, such as detergent-like properties and non-uniform disc sizes. Therefore, we have developed a novel lipid mimetic to study membrane proteins by oriented sample solid state NMR using the amphipathic 15mer peptoid consisting of N-phenylethylamine(Npe):N-carboxyethylamine(Nce) at a 2:1 ratio. Peptoids are poly-glycines with side chains attached to the amide nitrogen. They are synthesized through the submonomer solid-phase synthesis method, resulting in highly controllable lengths. With the 15-mer, we obtained uniformly aligned discs oriented perpendicular to the applied magnetic field. This resulted in markedly narrower linewidths in ^{31}P and ^{15}N 1D NMR, and improved resolution for 2D ^{15}N NMR. The discs had a wide range of alignable temperatures from 30 to 45°C. Furthermore, we made lipid macrodiscs with shorter 2:1 Npe:Nce constructs, such as 8-mer and 10-mer. We were also able to obtain uniformly aligned discs and narrower linewidths in ^{31}P and ^{15}N NMR spectra with these shorter peptoid constructs. Macrodiscs based on 8-mer peptoids had narrower linewidths than 15-mer based macrodiscs, while 10-mer based macrodiscs had comparable linewidths in ^{31}P NMR. The 8-mer and 10-mer based macrodiscs retained their alignment from 30-45°C. Based on our results, we have concluded that peptoid-based macrodiscs are superior lipid mimetics to bicelles and SMALPs. Furthermore, we hypothesized that the shorter peptoids most likely align parallel to the lipid bilayer normal rather than laterally.



(A) ^{31}P NMR spectra of 12:1 DMPC:8mer macrodiscs and, (B) 15:1 DMPC:10mer at different temperatures. (C) 1D ^{15}N NMR of 13.6:1 DMPC:10mer with Pf1. (D) Improved resolution in 2D ^{15}N NMR of 13.6:1 DMPC:10-mer with Pf1 coat protein (green) vs 11:1 DMPC:8-mer with Pf1 coat protein (red).

53rd Southeastern Magnetic Resonance Conference

References

- [1] Galiakhmetov, A., Davern, C., Esteves, R., Awosanya, E., Guthrie, Q., Proulx, C. and Nevzorov, A. *Aligned peptoid-based macrodiscs for structural studies of membrane proteins by oriented-sample NMR*. Biophysical Journal. 2022. 121. P.3263-3270.
- [2] Galiakhmetov, A., Shah, A., Lane, A., Davern, C., Proulx, C., Nevzorov, A. *Peptoid-based macrodiscs of variable lipid composition for structural studies of membrane proteins by oriented-sample solid-state NMR*. Journal of Structural Biology. 2024. 9.

Measuring Slow Cerebrospinal Fluid Velocities in Preclinical Models Using Optimized Phase Contrast MRI at 21.1 T

Dayna L. Richter^{1,2*}, Connor Blan^{1,2}, Anamika Roy^{1,2}, Malathy Elumalai^{1,2} and Samuel C. Grant^{1,2}

¹Center for Interdisciplinary Magnetic Resonance, National High Magnetic Field Laboratory

²Chemical & Biomedical Engineering, Florida State University, Tallahassee, FL, USA

Introduction: Cerebrospinal fluid (CSF) is essential for clearing waste products in the brain that contribute to pathologies, such as Alzheimer's disease¹. However, measuring slow CSF flow using MRI is challenging^{2,3}. Williamson *et al.* (2020) provide strategies for optimizing phase contrast with Pulsed Gradient Spin Echo (PGSE) for the measurement of slow flow highlighting the limits of detection⁴. Building on these methods, this study aims to assess CSF velocimetry *in vivo* with an optimized gradient strength. A controlled flow phantom was used to validate sensitivity and optimize gradient strength before translating into *vivo* conditions.

Method: A homebuilt flow phantom was scanned using the 900-MHz vertical scanner at the NHMFL. Average velocities of 100-500 $\mu\text{m/s}$ were tested due to relevance to CSF flow in rodents^{3,5,6}. Five naïve female Sprague Dawley rats (200-250 g) were scanned. A diffusion-weighted EPI sequence with 0.15 mm (phantom) and 0.125 mm (rat) in-plane resolution, TR/TE = 5000/44 ms, and 4 segments. The gradient encoding time was 4 ms, with a gradient spacing of 20 ms between bipolar gradients applied in the positive and negative x-, y- and z-directions. Two-point phase contrast for slow flow has an optimal q-slow, defined as the inverse of the characteristic diffusive length scale. Five gradient strengths, Q₁ - Q₅, were chosen around q-slow.

Result & Conclusion: The phase contrast PGSE EPI method was validated and optimized using the flow phantom. We found that the Q₄ setting was the closest to the theoretical results with the lowest sum of square error. We were able to map the CSF velocity and direction *in vivo* for female Sprague-Dawley rats which aligned well with the expected CSF flow directions⁷. This work shows the feasibility of phase contrast with PGSE to measure CSF dynamics in preclinical MRI. This approach could enable longitudinal, non-invasive CSF assessments in preclinical models of neurological disorders.

References: [1] Iliff JJ, et al. 2012 [2] Mestre H, et al. Nat Commun. 2018 [3] Li J, et al. Magn Reson Med. 2022 [4] Williamson NH, et al. J Magn Reson Open. 2020 [5] Karimy JK, et al. J Neurosci Methods. 2015 [6] Liu G, et al. Cell Rep. 2020 [7] Bito Y, et al. Magn Reson Med. 2021

Acknowledgements: Animal procedures were approved by the Florida State University Animal Care and Use Committee in Tallahassee, FL (PROTO-202100071). Research reported in this abstract was supported by the National Institute of Neurological Disorders and Stroke of the National Institutes of Health (RO1-NS072497). A portion of this work was performed at the National High Magnetic Field Laboratory, which is supported by National Science Foundation Cooperative Agreement No. DMR-2128556* and the State of Florida.

Engineered Iron Oxide Interfaces Enable Reliable MRI Tracking of Therapeutic Extracellular Vesicles

Arshia Arbabian^{*1,2}, Jeff Procida³, Dayna L. Richter^{1,2}, Hedi Mattoussi³, Yan Li²

¹ National High Magnetic Field Laboratory, Florida State University, Tallahassee, Florida, USA

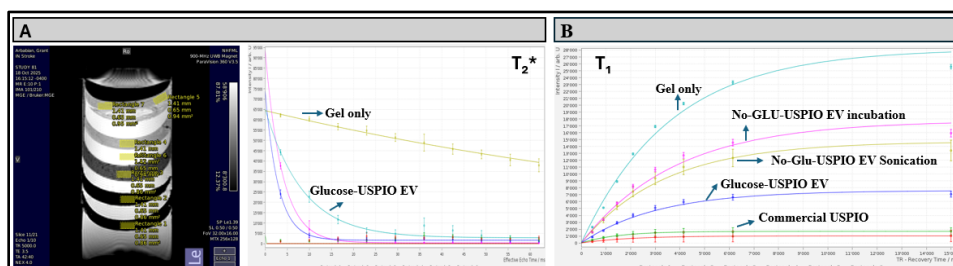
² Department of Chemical & Biomedical Engineering, FAMU-FSU College of Engineering, Florida State University, Tallahassee, Florida, USA

³ Department of Chemistry and Biochemistry, Florida State University, Tallahassee, Florida, USA

Background: Stroke remains a leading cause of long-term neurological disability, driving the need for regenerative, cell-free therapies¹. Mesenchymal stem-cell-derived extracellular vesicles (MSC-EV) have shown strong therapeutic potential in promoting recovery following ischemic injury. However, EV have not yet been reliably visualized in the brain after intranasal (IN) administration, largely due to inefficient labeling and vesicle disruption during conventional magnetic labeling. Prior studies indicate that sonication-based labeling alters miRNA cargo and compromises EV integrity², underscoring the need for improved methods that preserve functionality while enabling MRI-based detection.

Methods: EV were isolated from three-dimensional MSC cultures (passage 6) and labeled using either small core size (~5-6 nm) iron oxide nanoparticles grown using a high temperature decomposition reaction, ligand exchange with a multifunctional polymer and then conjugated with glucose, or commercially available USPIO (Sigma 725358). Labeling was achieved through 24 h glucose incubation or controlled point sonication (three 10 s bursts on ice), followed by re-isolation using the ExtraPEG protocol. Phantoms containing labeled EV in 0.5% agarose gel were imaged on a 21.1 T Bruker system using RAREVTR (T_1 : TE = 6 ms, TR = 450–15000 ms) and MGE (T_2^* : TE = 3.5–62 ms, TR = 5 s, 10 echoes). Relaxation rates (R_1 , R_2^*) were derived from exponential fits ($T_1 = 1/R_1$; $T_2^* = 1/R_2^*$).

Results/Conclusion: Glucose-mediated incubation produced uniform T_2^* shortening and consistent T_1 recovery, confirming controlled iron incorporation. Non-glucose iron oxide showed negligible contrast, suggesting limited uptake, while sonicated and commercial samples displayed strong but artifactual signal loss from iron aggregation and incomplete washing. These findings demonstrate that glucose-assisted labeling preserves EV integrity and enables reproducible MRI contrast, establishing a foundation for quantitative tracking of intranasally delivered EV in stroke models.



References: 1. Martin, S. S. *et al.* 2025 Heart Disease and Stroke Statistics: A Report of US and Global Data From the American Heart

Association. *Circulation* **151**, e41–e660 (2025). 2. Helsper, S. *et al.* Superparamagnetic Iron Oxide Nanoparticle-Labeled Extracellular Vesicles for Magnetic Resonance Imaging of Ischemic Stroke. *ACS Appl. Nano Mater.* **7**, 24160–24171 (2024).

Local Charge Distribution Modulates Hydration Dynamics in the Intrinsically Disordered Protein IA₃Ishani Kumarasinghe^{1*}, Katie M. Dunleavy^{1a}, Tianyan Li¹, Shamon A. Walker², Gail E. Fanucci¹¹ Department of Chemistry, PO BOX 117200, University of Florida, Gainesville, FL 32611-7200^{1a}Smith Hall, 139 Smith Hall, Pleasant St SE, Minneapolis, MN 55455, ²Materials Research Laboratory, University of California, Santa Barbara, CA 93106

IA₃ is a 68-residue intrinsically disordered protein found in yeast of the *Saccharomyces* genus. This inhibitor remains unstructured in solution but adopts an α -helical conformation in its N-terminal domain (NTD) upon binding yeast aspartic proteinase A (YPrA), leaving the C-terminal domain (CTD) unstructured.¹ The two domains differ in charge distribution, with CTD being more charge-segregated than NTD.² Previously, we utilized site-directed spin labeling (SDSL) and low-field Overhauser dynamic nuclear polarization (ODNP) to characterize the local dynamics and measure local water dynamics in the vicinity of 5 -10 Å of a spin-labeled site within each of the two domains of *S. cerevisiae* IA₃.³ ODNP parameters including coupling factor (ξ), cross-relaxation (k_{σ}), self-relaxation (k_{ρ}), and bound-water relaxation (k_{low}) were used to determine hydration diffusivity.⁴ Results revealed markedly different hydration behaviors between domains: NTD sites exhibited surface-like hydration, whereas CTD sites showed unusually high, bulk-like ξ values. Water dynamics on the picosecond scale were similar across both domains and less hindered than those near folded proteins. In contrast, bound-water relaxation, which differed significantly in two domains, indicates that the slower bound water may interact differently with the highly charged CTD environment. Taken together, these results show that IA₃ hydration is governed by sequence-encoded charge distribution.³

Here, we continue this investigation by using the local dynamics and hydration of specific sites in the NTD, CTD, and linker domain across *Saccharomyces* IA₃ sequences. As prior CD studies demonstrate distinct solution conformational ensembles of different disordered characteristics based on sequence variation in the linker domain, we hypothesize that the linker sequence modulates interdomain interactions and conformational preferences. ODNP will be used to evaluate if there is a correlative change in hydration of CTD with ensemble parameters.

References

- (1) Li, M.; Phylip, L. H.; Lees, W. E.; Winther, J. R.; Dunn, B. M.; Wlodawer, A.; Kay, J.; Gustchina, A. *Nat. Struct. Biol.* **2000**, 7 (2), 113–117.
- (2) Holehouse, A. S.; Das, R. K.; Ahad, J. N.; Richardson, M. O. G.; Pappu, R. V. *Biophys. J.* **2017**, 112 (1), 16–21.
- (3) Dunleavy, K. M.; Li, T.; Milshteyn, E.; Jaufer, A. M.; Walker, S. A.; Fanucci, G. E. *J. Phys. Chem. B* **2023**, 127 (45), 9734–9746.
- (4) Barnes, R.; Sun, S.; Fichou, Y.; Dahlquist, F. W.; Heyden, M.; Han, S. *J. Am. Chem. Soc.* **2017**, 139 (49), 17890–17901.

Advancing Liquid-State ¹⁹F DNP: High-Field, Large-Volume Overhauser Polarization at Ambient Temperature.

Authors: Sungsool Wi,^{1*} Jenica Lumata,¹ Thierry Dubroca,¹ Tomas Orlando,¹ and Lucio Frydman^{1,2}

¹ National High Magnetic Field Laboratory, Tallahassee, Florida 32304, USA

² Department of Chemical and Biological Physics, Weizmann Institute of Science, 7610001 Rehovot, Israel

Abstract

We present high-field, large-sample-volume liquid-state ¹⁹F Overhauser dynamic nuclear polarization (DNP) at ambient temperature using 1,3-bis(diphenylene)-2-phenylallyl (BDPA) as the polarizing agent. The achieved ¹⁹F DNP enhancements range from 3 to 37, depending on the molecular system, while maintaining linewidths within a few to a few-tenths of a hertz after microwave irradiation at 14.1 T. These results were obtained using a conventional liquid-state NMR probehead modified to incorporate a waveguide for microwave delivery. All experiments were performed with 50–100 μ L sample volumes, achieving spectral resolution comparable to that of conventional ¹⁹F liquid-state NMR. The study includes applications to several model systems and quantitative determinations of T_{1e} and T_{2e} using pulsed-echo and inversion-recovery measurements on the same samples used for DNP at HiPER. From these measurements, together with leakage factors determined via ¹⁹F's T_1 relaxation experiments with and without radicals, coupling factors were extracted for each system. By addressing all relevant experimental aspects, this work provides a comprehensive framework for conducting large-volume, high-field liquid-state ¹⁹F DNP NMR. The approach demonstrates strong potential to expand the applicability of liquid-state ¹⁹F DNP NMR for small-molecule analysis in analytical and pharmaceutical chemistry, as well as for the detection and characterization of environmentally persistent PFAS compounds.

Investigating the Impact of Charge Distributions on the Unfolded and Folded Conformations of IA3s

Tianyan Li¹, Katie M. Dunleavy^{1a}, Gail E. Fanucci¹

¹ Department of Chemistry, PO BOX 117200, University of Florida, Gainesville FL 32611-7200.

^{1a}Smith Hall, 139 Smith Hall, Pleasant St SE, Minneapolis, MN 55455

The endogenous yeast aspartic proteinase (YprA) inhibitor, IA3 of *Saccharomyces cerevisiae*, is an intrinsically disordered protein (IDP) consisting of 68 amino acid residues that form an alpha-helix when bound to YprA^{1,3}. The helical structure traditionally obtained upon binding to YprA can be mimicked in the presence of the secondary structure stabilizer, 2,2,2-trifluoroethanol^{1,2,3}. Previous studies demonstrated that the alpha-helix of YprA-bound IA3 remains in the N-terminus (2-32) of the protein, leaving the C-terminus (33-68) structurally unresolved, as shown in Fig 1.

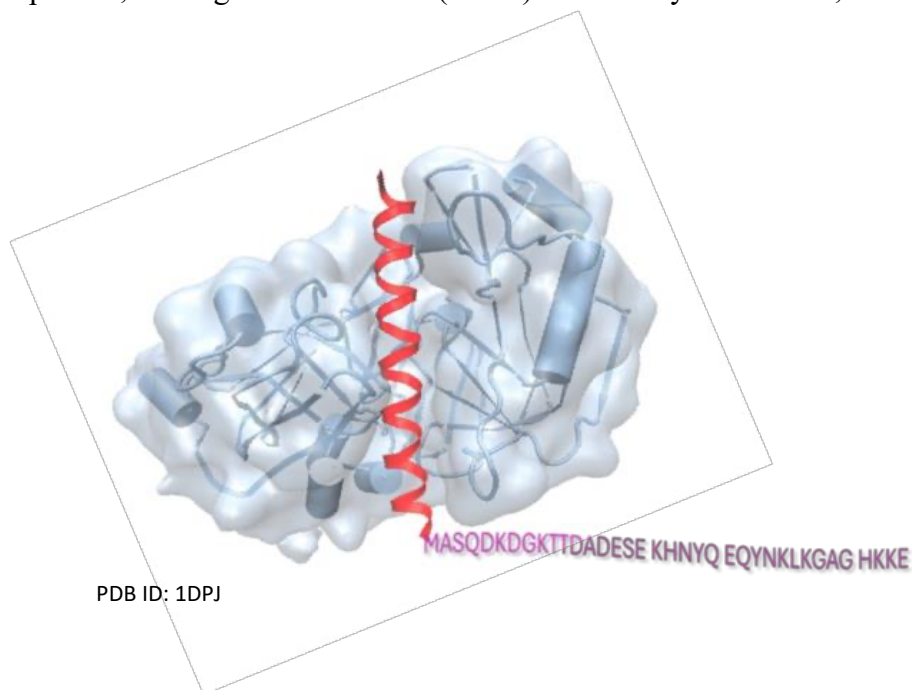


Figure 1. X-ray crystallography resolved crystal structure of IA3 (orange and purple) bound YprA (grey).

Site-directed spin labeling (SDSL) electron paramagnetic resonance (EPR) was used to probe conformational dynamics of IA3. Continuous-wave (CW) X-band EPR spectra were collected for fifteen single-cysteine variants (referred as P1 – IA3), ten located in the N-terminal region and five in the C-terminal region, as a function of increasing concentrations of TFE (v/v). The spectra revealed progressive decreases in probe mobility with higher TFE concentrations, consistent with TFE-induced conformational changes. However, the magnitude and nature of these mobility changes differed across the variants, suggesting that spin labeling perturbs local conformations in a site-specific manner and modulates the apparent helical propensity induced by TFE⁴.

53rd Southeastern Magnetic Resonance Conference

Conformational transitions of P1–IA3 variants were also analyzed by monitoring the CW–EPR mobility parameter $h(+1)/h(0)$ as a function of TFE concentration. In the absence of TFE, all variants exhibited similar spectra, indicating highly mobile, unfolded states. Increasing TFE induced sigmoidal decreases in $h(+1)/h(0)$, consistent with a two-state coil-to-helix transition. N-terminal variants displayed site-specific differences in both transition sharpness and limiting values, whereas C-terminal variants showed more uniform behavior. These results highlight the sensitivity of N-terminal helicity to local environment and residue position within the IA3–YprA interaction surface⁴.

In contrast, C-terminal variants display consistent $h(+1)/h(0)$ transitions that closely resemble wild-type behavior, indicating minimal structural disruption. Consequently, we have turned our attention to the other eight naturally occurring yeast IA3 sequences. While the N-terminal domains (NTDs), which serve as inhibitory sites of the protein, exhibit high sequence conservation across these species, the linker regions and C-terminal domains (CTDs) vary, resulting in distinct charge distributions. As such, we intend to expand our IA3 studies by characterizing how changes in charge patterning structurally and dynamically impact the two domains as ensembles and separate conformational subensembles. To facilitate this investigation, we have conducted a theoretical study using the bioinformatic tool localCIDER9, which provides a series of IDP sequence parameters that depict charge patterning along sequences^{5,6}. Experimentally, we generated wild-type IA3 and spin-labeled variants. The TFE-CD study and spin-labeled magnetic resonance techniques mentioned earlier were applied, along with ¹⁵N HSQC NMR as a complementary approach.

Reference

1. Li, M. et al. The aspartic proteinase from *Saccharomyces cerevisiae* folds its own inhibitor into a helix. *Nat Struct Biol* 7, 113–117 (2000).
2. Dreyer, T., Valler, M. J., Kay, J., Charlton, P. & Dunn, B. M. The selectivity of action of the aspartic-proteinase inhibitor IA3 from yeast (*Saccharomyces cerevisiae*). *Biochem. J.* 231, 777–779 (1985).
3. Phylip, L. H. et al. The Potency and Specificity of the Interaction between the IA3 Inhibitor and Its Target Aspartic Proteinase from *Saccharomyces cerevisiae* *. *J. Biol. Chem.* 276, 2023–2030 (2001).
4. Lotthammer, J. M., Ginell, G. M., Griffith, D., Emenecker, R. J. & Holehouse, A. S. Direct Prediction of Intrinsically Disordered Protein Conformational Properties from Sequence. *bioRxiv* 2023.05.08.539824 (2023) doi:10.1101/2023.05.08.539824.
5. Dunleavy, K. M. et al. Hydrogen Bonding Compensation on the Convex Solvent-Exposed Helical Face of IA3, an Intrinsically Disordered Protein. *Biochemistry* 62, 1716–1724 (2023).
6. Holehouse, A. S., Das, R. K., Ahad, J. N., Richardson, M. O. G. & Pappu, R. V. CIDER: Resources to Analyze Sequence-Ensemble Relationships of Intrinsically Disordered Proteins. *Biophys. J.* 112, 16–21 (2017).

Liquid State ¹³C and ¹⁹F DNP-Enhanced NMR Spectroscopy in One and Two Dimensions

Tomas Orlando,^{1,2*} Maik Reinhard,¹ Marcel Levien,^{1,3} Luming Yang,¹ Alex van der Ham,¹ Igor Tkach,¹ Marina Bennati¹

Max Planck Institute for Multidisciplinary Sciences, Göttingen, Germany
present address: Natl. High Magnetic Field Lab. and Florida State University, Tallahassee, USA
present address: Ecole Polytechnique de Lausanne – EPFL, Lausanne, Switzerland

Liquid-state dynamic nuclear polarization (DNP) is emerging as a practical route to overcome the sensitivity limits of solution NMR for small molecules, drugs, and metabolites. Building on a newly engineered 9.4 T liquid-state DNP platform, we demonstrated robust Overhauser-enhanced 1D and 2D spectroscopy with signal boosts up to two orders of magnitude, enabling acquisition-time gains approaching 10⁴. Importantly, hyperpolarization can be transferred between nuclei, allowing DNP-enhanced two-dimensional ¹³C-¹³C correlation experiments at natural ¹³C abundance, thereby extending multidimensional NMR to samples available only in micro- to millimolar quantities. These advances generalize liquid-state DNP from proof-of-concept experiments to a versatile analytical tool for structural elucidation and metabolite/drug profiling.

Complementing this platform advance, we established ¹⁹F Overhauser DNP at 9.4 T as a powerful nucleus-specific entry point for hyperpolarization. They show steady-state ¹⁹F enhancements (~x20) in solution using organic radicals and, importantly, exploit through-bond polarization transfer (¹⁹F→¹³C INEPT) to amplify adjacent ¹³C signals by up to two orders of magnitude—making otherwise weak or quaternary carbons readily detectable at natural abundance (e.g., in the fluorinated drug flutrimazole). A mechanistic analysis of the ¹⁹F coupling factors rationalizes the efficiency of ¹⁹F OE-DNP and identifies the conditions to maximize ¹⁹F enhancements in aromatic compounds.

This integrated approach broadens liquid-state DNP from specialized demonstrations to a general methodology for small-molecule analytics and drug discovery workflows.

References

- 1 J. Eills, et al., *Chem. Rev.*, **2023**, 123, 1417–1551.
- 2 M. Levien et al., *Nat. Commun.* **2024**, 15, 5904
- 3 M. Reinhard et al., *Angew. Chem.* **2025**, doi: 10.1002/anie.202517498

Phase & Dynamic Behavior in Lyotropic Liquid Crystals for MRI Agent Design and Drug Delivery by Magnetic Resonance Spectroscopy

Mahsa Moshari¹, Mingwei Zhou¹, Gail E. Fanucci¹

Department of Chemistry, University of Florida, Gainesville, FL, USA

Introduction

Biological membranes are heterogeneous; their phase, curvature, and hydration govern function. Linking these mesoscopic phases to molecular-scale dynamics requires practical, quantitative readouts of the local lipid environment. Although monoolein (MO) lyotropic systems have been widely studied, a key challenge has been the absence of a practical method to connect the phase structure (lamellar, hexagonal, sponge, or bicontinuous cubic) to quantitative insights into the microscopic lipid environment and its hydration dynamics.

Methods

Monoolein (MO) was co-formulated with phospholipids (POPC, DOPC, DOPE) to generate lamellar and curvature-rich mesophases (bicontinuous cubic and inverse-hexagonal-like). Nitroxide spin labels—TEMPO-PC, 5-DOXYL-PC, and 10-DOXYL-PC—were incorporated at 0.5 mol% of total lipid as spectroscopic reporters. Mesophase identity and sample integrity were verified by polarized-light microscopy (PLM). Hydrodynamic size and polydispersity of the resulting nanoparticles were quantified by dynamic light scattering (DLS). Electron paramagnetic resonance (CW-EPR) measurements were performed on identically prepared samples to probe local mobility and interfacial water accessibility.

Results

These results reflect the morphology curved networks confine local motion yet create a larger total interface, leading to faster interfacial exchange. EPR line shapes were broader with higher apparent order in curved phases versus α . These trends were expected and mutually consistent across methods, with broader EPR, smaller ΔP , and shorter T_1 co-varying in the curved phases as anticipated from their geometry. Together, the line-shape, power-saturation, and T_1 results provide quantitative, phase-resolved markers that link mesophase to packing and interfacial water dynamics, guiding the design of non-metal MRI scaffolds and drug-delivery carriers. Membrane packing and local dynamics were quantified using nitroxide spin-labeled lipids: CW-EPR line-shape reports rotational mobility/ordering, while power-saturation reports paramagnetic accessibility, reflecting O_2/H_2O collision frequency at the interface. In parallel, benchtop 1H NMR relaxometry provides a direct index of interfacial water mobility through the measurement of the longitudinal relaxation time (T_1) to offer a powerful framework for understanding how different molecular environments influence the performance of non-metallic contrast agents.

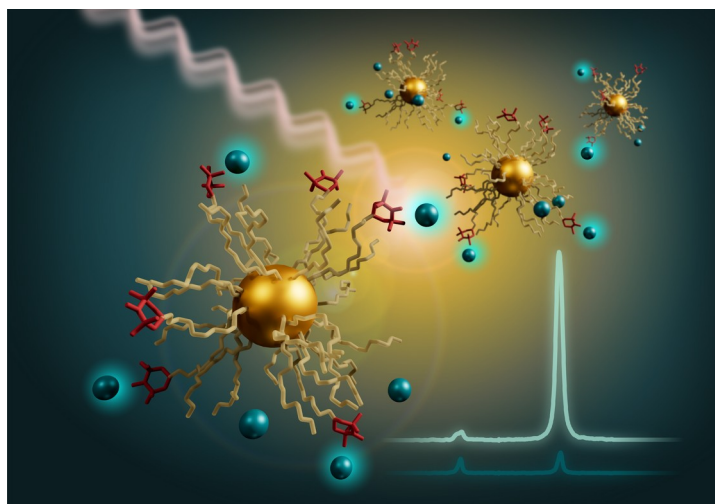
Conclusion

Curved mesophases (cubic/hexagonal-like) exhibit tighter packing and reduced interfacial accessibility, evidenced by broader EPR line shapes, smaller ΔP (air- N_2), and shorter T_1 . These orthogonal readouts—line-shape, power-saturation, and relaxometry—provide quantitative, phase-resolved markers that link morphology to interfacial water dynamics. This framework guides the rational design of non-metal MRI scaffolds and lipid nanocarriers by matching desired dynamics to specific mesophase geometry.

Functionalized Materials as Polarizing Agents for Dynamic Nuclear Polarization in LiquidsKiera Powers,^{1*} Daphne Broerman,¹ Beatrice Mascitti,² Federico Rastrelli,² Tomas Orlando¹National High Magnetic Field Laboratory and Florida State University, Tallahassee, USA
Dept. of Chemical Sciences, University of Padova, Padova, Italy

Nuclear Magnetic Resonance (NMR) spectroscopy provides powerful insights into molecular structure and dynamics but is inherently limited by low sensitivity, often requiring long acquisition times and large sample volumes. Dynamic Nuclear Polarization (DNP) addresses this limitation by transferring electron spin polarization from free radicals to nearby nuclei under microwave irradiation, enhancing NMR signals by up to several hundredfold. While DNP has been successfully demonstrated in solids and liquids, its application to mixed-phase systems—where solid and liquid components coexist—remains largely unexplored.

To tackle this class of materials, we investigated radical-functionalized gold and silica substrates dispersed in liquids as model mixed-phase systems for Overhauser-effect DNP (OE-DNP). Gold nanoparticles (AuNPs) protected by self-assembled monolayers are particularly attractive due to their tunable surface chemistry and ability to mediate selective molecular interactions. By co-functionalizing AuNPs with radical-bearing and recognition thiols, we probe how interfacial dynamics and molecular affinity influence spin polarization transfer in solvent mixtures such as chloroform–methanol. The observed DNP enhancements provide insights into correlation times at the solid–liquid interface and the role of chemical recognition in hyperpolarization efficiency. Finally, we present some preliminary work of silica substrates functionalized with organic radicals and their potential use as polarizing agents in hyperpolarization for applications in high fields.

**References**

- 1 J. Eills, et al., *Chem. Rev.*, **2023**, 123, 1417–1551.
- 2 B. B. Mascitti et al., *Phys. Chem. Chem. Phys.*, **2025**, 22366-22374.

EPR Characterization of a Photo-Responsive Fe³⁺ Spin-Crossover Complex

Brittany Grimm*^{1,2}, Zoi Lada³, Johan Van Tol², Andrew Ozarowski², Grace Morgan³, Stephen Hill^{1,2,4}

1. Florida State University, Physics 2. National High Magnetic Field Laboratory 3. University College Dublin 4. Florida State University, Chemistry

The interconversion between maximally paired (low-spin, LS) and unpaired (high-spin, HS) electronic configurations under certain stimuli (temperature, pressure, magnetic field) make spin-crossover (SCO) materials attractive for use in molecular data storage and processing, display or detection devices.¹⁻² Such systems exhibit a wide variety of thermal spin-switching behaviors, ranging from very sharp and hysteretic transitions, driven by strong spin–lattice coupling that rapidly propagates spin-state changes through the lattice, to more gradual transitions governed by Boltzmann statistics. While thermally induced SCO remains a preferred approach for probing the physical and structural properties of these molecular systems due to its relative experimental simplicity, optical excitation offers a particularly attractive route for spin-state control in practical applications due to its scalability, stability, and ease of implementation. In this work, we investigate the optically induced SCO transitions through light-induced excited spin state trapping (LIESST) in a mononuclear Fe³⁺ complex using electron paramagnetic resonance (EPR) spectroscopy. This approach enables characterization of the electronic configuration and geometric properties of both spin states, as well as examination of the system's behavior under optical irradiation.

References

- [1] Halcrow, M. A. *Spin-Crossover Materials*; John Wiley & Sons, **2013**; pp. 55-72.
- [2] Gülich, P., Goodwin, H. A. Spin Crossover—an Overall Perspective. *Topics in Current Chemistry* **2004**, 233, 1–47.

Effects of Anomeric Linkage of α - and β -Cerebrosides on Biophysical Properties of the Lipid Membrane

Authors: Shayak Biswas*, Sayan Kundu, Mingwei Zhou, Rajendra Rohokale, Shamiul Islam, Gail E. Fanucci, Zhongwu Guo

Affiliation: University of Florida

Glycosphingolipids (GSLs), including galactosylceramide (GalCer) and glucosylceramide (GlcCer), show subtle yet important differences in membrane organization and function due to variations in glycosidic linkage. In this study, α - and β -anomeric derivatives of GalCer and GlcCer, each spin-labeled at the 6-position of the sugar, were used to examine how glycan structure and anomeric configuration affect lipid bilayer organization. Using continuous-wave electron paramagnetic resonance (EPR) spectroscopy alongside dynamic light scattering (DLS), we explored the rotational dynamics, packing, and membrane interactions of these cerebrosides within lamellar lipid environments. Although they share an identical ceramide backbone, the α - and β -anomers showed different motional and environmental profiles, indicating that even small differences in configuration at the glycosidic linkage can cause significant changes in membrane incorporation and lipid domain behavior. Our results reveal that the orientation of the glycosidic bond is crucial in determining GSL arrangement in membranes, providing molecular insights into how carbohydrate stereochemistry influences membrane biophysics and may contribute to the functional diversity of glycosphingolipids in biological systems.

Field homogeneity Improvement and Dead-Time Reduction for an Integrated EPR and DNP Spectrometer

Korrigan Amadi*, Ilya Litvak, Thierry Dubroca

National High Magnetic Field Laboratory at Florida State University, Tallahassee, FL 32310

Dynamic nuclear polarization (DNP) and electron paramagnetic resonance (EPR) experiments share stringent requirements for magnetic field homogeneity and precise timing control. Achieving both high-resolution NMR and low-dead-time EPR on the same sample, under identical temperature and field conditions, is essential for studying DNP mechanisms and developing new DNP methods, particularly at high magnetic fields. Two complementary hardware developments were implemented within a W-band spectrometer. First, a set of ferroschims was designed and fabricated to significantly improve field homogeneity, thus improving the sensitivity of DNP experiments. Using field mapping techniques to optimize ferroschims, the field homogeneity was improved by almost a factor 10 from 60 ppm (Figure 1a). Figure 1b shows a narrower and higher NMR resonance peak demonstrating this improvement, but the sensitivity gain is not as large as expected from the field map results, suggesting a less-than-ideal sample positioning relative to the magnet field center. Independently, a microwave switch triggered by a laser was fabricated and integrated into the microwave bridge; the new laser switch provides 11 dB of attenuation when actuated with a switching speed under 5 ns, reducing the dead time multiple-fold from 300 ns and increasing EPR detection sensitivity to allow short electron spin relaxation studies. Together, these developments establish a unified magnetic resonance platform capable of conducting EPR, NMR, and DNP studies on the same sample under identical field and temperature, enabling systematic investigation of DNP mechanisms.

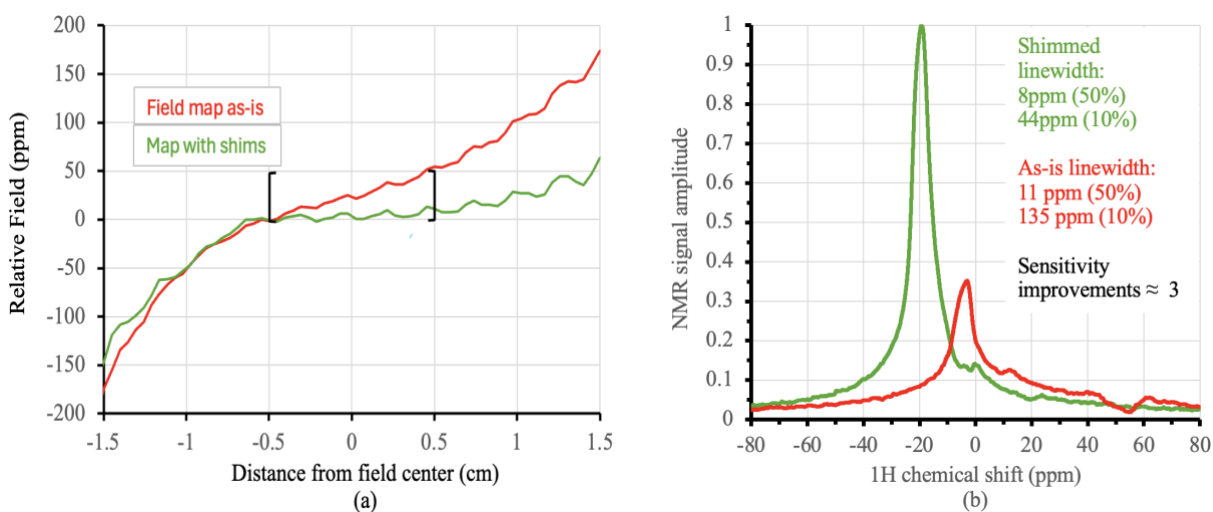


Figure 1: (a) Field Maps at 3.35 T collected by ¹H NMR (143 MHz). (b) ¹H NMR signal of water at 300K as labeled.

Acknowledgment: This work was funded by the National Science Foundation (DMR-2128556) and the State of Florida. We also acknowledge the advice and technical detail discussion from the Group of Graham Smith at the University of St. Andrews.

Dual EPR spin probe and label approach resolves origins of robust protein and coupled solvent dynamics in fibrillar amyloid- β (1-42)

Hana Alsheikh*, Katie L. Whitcomb, and Kurt Warncke

Emory University, Department of Physics, Atlanta, GA 30322-2430

Monomeric amyloid- β (A β) is an intrinsically disordered protein (IDP), with common lengths of 38-42 residues. A β forms fibrils with the characteristic amyloid cross- β sheet structure with a mobile N-terminus (residues 1-17).¹ To gain insight into molecular mechanisms of A β function and dysfunction, the protein-coupled solvent dynamical properties of fibrils of A β 42 are addressed by using electron paramagnetic resonance (EPR) spectroscopy in a low-temperature, frozen solution system,^{2,3} that affords controlled confinement and co-localization of the spin-probe, TEMPOL, in the solvent around the protein. The temperature-dependence (220-265 K) of the rotational mobility of the spin probe resolves two distinct correlation times, denoted "fast" (dynamically disordered region) and "slow" (hydration region), with corresponding normalized weights, W_f and W_s . The overall decrease in W_f with descending T (increasing confinement) proceeds in three stages: compaction 1 (C1) - structure consolidation (SC) - compaction 2 (C2). This behaviour is also characterized in the IDP, α -synuclein,⁴ and differs widely from that of globular proteins.⁵ Spin-labelling of A β 42 fibrils with Cu²⁺ was used to address the origin of the confinement-resistant dynamics. The Cu²⁺ ligands with histidine residues (His 6, 13, 14) in the N-terminal region of the peptide.⁶ The EPR spectrum of A β 42-bound Cu²⁺ itself displayed decreasing mobility during C1. Cu²⁺ binding decreased the TEMPOL-detected C1 amplitude and increased W_f during C2. These results are consistent with Cu²⁺ pre-organization of N-terminus structure during C1, which enhances stable structure formation at the SC event. The three-stage compaction, and terminal domain origin and persistence of protein-coupled solvent dynamics, under physiological degrees of confinement provide properties for quantitative assessment of molecular mechanisms of A β 42–drug interactions. Supported by NIH R01 GM142113.

1. Lee, PNAS, 2023, 120.
2. Nforneh and Warncke, J. Phys. Chem. B, 2019, 123, 5395.
3. Li et al., Methods Enzymol., 2022, 666, 25.
4. Whitcomb and Warncke, ACS Chem. Neurosci., 2023, 14, 3905.
5. Li et al., Phys. Chem. Chem. Phys., 2022, 24, 23919.
6. Abelein et al., JACS Au 2022, 2, 11, 2571.

A 263 GHz Pulsed EPR Spectrometer with AWG Capabilities

Johan van Tol*, Tomas Orlando

National High Magnetic Field Laboratory, Florida State University, Tallahassee, FL32310

There is a need for high-frequency pulsed EPR for the study of transition metal ion systems and lanthanide systems at high magnetic fields and higher frequencies. Also the characterization of the properties of the relaxation properties of electron spins used for DNP at the magnetic fields of the DNP/NMR experiments. At the NHMFL we have capabilities for pulsed EPR at various frequencies. AT 95 GHz the HIPER spectrometer, which is a high power system with full phase control, ELDOR (electron-electron double resonance) and pulse shaping capabilities is a very capable spectrometer available for external users. At various higher frequencies (120-395 GHz) a different quasi-optical superheterodyne spectrometer also has pulsed capabilities at higher fields and frequencies.[1,2] However, the available power is limited to about 40 mW, which limits time-resolution and sensitivity, while also phase control of the pulses and multifrequency (ELDOR) capabilities are lacking. Therefore, taking advantage of new microwave technology, we are currently constructing a 257-268 GHz spectrometer, which uses an AWG (Arbitrary Waveform Generator) and has about 300 mW of power. We present the layout and initial results obtained on this spectrometer, which we estimate will be available for use to external researchers in the maglab user facility starting in the Spring of 2026.

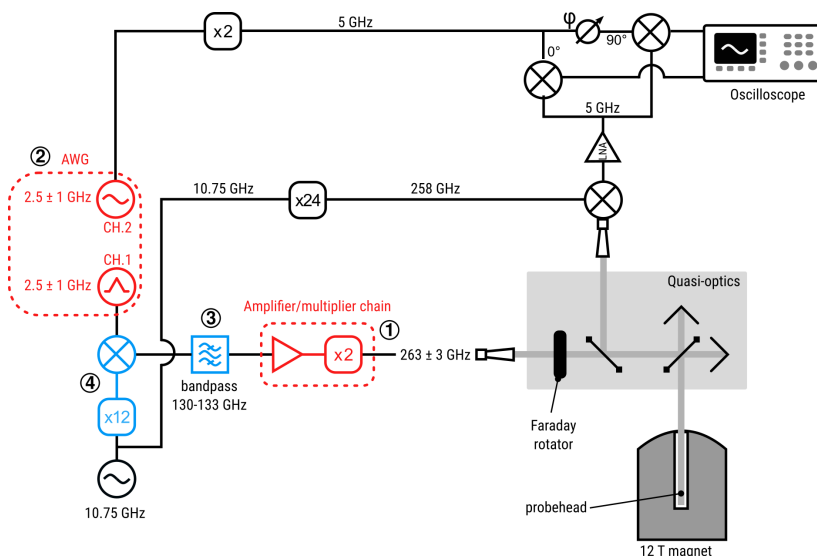


Figure 1. Block diagram of the quasi-optical heterodyne system equipped with a 300mW multiplier-amplifier chain (1) and an AWG (2).

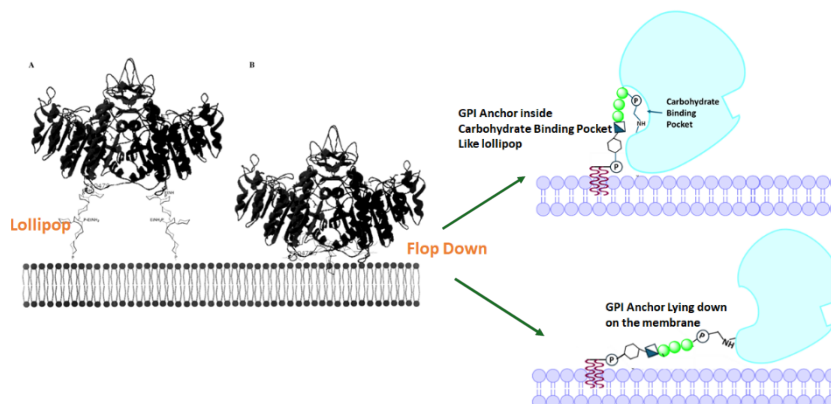
References

1. Morley, G. W., Brunel, L. C. & Van Tol, J. A multifrequency high-field pulsed electron paramagnetic resonance/electron-nuclear double resonance spectrometer. *Review of Scientific Instruments* 79, (2008).
2. Van Tol, J., Brunel, L. C. & Wylde, R. J. A quasi-optical transient electron spin resonance spectrometer operating at 120 and 240 GHz. *Review of Scientific Instruments* 76, (2005).

Biophysical Characterization of GPI Anchor Conformation Using a Synthetic Bifunctional Probe

*Md.Shamiul Islam¹, Sayan Kundu¹, Xin Yan¹, Gail E Fanucci¹, Zhongwu Guo¹

1. Department of Chemistry,
University of Florida,
Gainesville, FL 32611, USA



Background/Introduction

Glycosylphosphatidylinositol (GPI) anchors are complex glycolipids that tether proteins to the outer leaflet of the plasma membrane. GPI-anchored proteins play vital roles in numerous cellular processes, including signaling, immune response, and the organization of the membrane. Proximity studies of GPI-anchored proteins have shown that the protein portion remains close to the membrane surface; however, the structural behavior of the GPI anchor itself at the membrane interface remains poorly understood. The anchor may either support the protein by lying along the membrane surface or adopt a “lollipop-like” conformation in which the glycan chain extends outward and fits into the carbohydrate-binding pocket of the protein. To investigate this spatial organization, we designed a synthetic bifunctional GPI probe containing an azide group at the first mannose and a biotin group at the phosphoethanolamine linker of the third mannose.

Methods

The probe was incorporated into DPPC liposomes and analyzed using Förster resonance energy transfer (FRET) and continuous-wave electron paramagnetic resonance (CW-EPR) spectroscopy. The azide handle was labeled with DBCO–Cy3.5 (donor) while PE–Cy5.5 in the bilayer served as acceptor. Distance measurements were derived from FRET efficiency. Spin labeling at the azide site followed by power saturation analysis with O₂, NiEDDA, and DOGS–NTA–Ni provided depth and accessibility information.

Results

FRET revealed an average azide-to-liposome surface distance of ~ 39 Å, consistent with a lollipop-like conformation rather than a collapsed structure. EPR data showed minimal collision with lipid-bound DOGS–NTA–Ni, indicating that the glycan moiety resides above the bilayer in the aqueous phase.

Conclusions

The synthetic bifunctional GPI probe adopts an extended, upright “lollipop-like” conformation on the membrane surface. This orientation suggests that the GPI glycan extends into the carbohydrate-binding pocket of the protein, allowing for both flexibility and stable attachment. The system provides a robust model for investigating the spatial organization and dynamics of GPI-anchored proteins using combined FRET and EPR spectroscopy.

Coupling of protein backbone and solvent dynamics in α -synuclein revealed by using controlled confinement and multi-probe EPR spectroscopy

Shady Fouad and Kurt Warncke

Emory University, Department of Physics, Atlanta, GA, 30322-2430

α -Synuclein (α -syn) is an intrinsically disordered protein (IDP) involved in neural transmission.¹ α -Syn possesses context-sensitive structural plasticity that results in domain-specific, heterogeneous dynamics that connect structural disorder to function. These features also contribute to dysfunctional aggregation in Parkinson's disease. Understanding the dynamical coupling between protein (backbone and surface) and surrounding solvent, and its sensitivity to confinement, is essential for describing α -syn function and dysfunction. Toward this, we use continuous-wave EPR spectroscopy and three nitroxide reporters: the free spin probe, TEMPOL, which senses protein-coupled solvent dynamics, and two site-directed spin labels, 4-maleimido-TEMPO (4MT) and dithione-based MTSL, covalently attached to Cys9 in the S9C mutant of human α -syn. Temperature is varied to control ice-boundary confinement (200–265 K). Earlier TEMPOL tracking of protein hydration and dynamically disordered solvent components revealed a three-stage, compaction 1 (C1), structure consolidation (SC), compaction 2 (C2) response of α -syn to increasing confinement.² 4MT-S9C mobility is reduced overall, but consistent with this sequence, and additionally resolves pre-organization of the N-terminal domain under low confinement. MTSL-S9C exhibits overall higher mobility, resolving tethered spin label motion from the backbone dynamics that dominate 4MT-S9C motion. The dual spin probe and label approach resolves coupled protein-solvent responses to confinement, revealing how dynamic allostery among central and flanking domains shapes α -syn conformational behavior, and establishes a platform for quantitative evaluation of drug interactions. Supported by NIH R01 GM142113.

1. Sharma and Burre, *Trends Neurosci.* 2023, 46, 153.

2. Whitcomb and Warncke, *J. Phys. Chem. B.*, 2025, 129, 8351.

Elucidating Electronic Structure and Relaxation Pathways of Transition Metal Complexes via High Power EPR Spectroscopy

Kavipriya Thangavel,^a Dipanti Borah,^b Vignesh Kasi,^b Maheswaran Shanmugam,^b Andreas Pöppel^c, Stephen Hill.^{a,d,e}

(a) *National High Magnetic Field Laboratory, Florida State University, Tallahassee, FL 32310, USA*

(b) *Department of Chemistry, Indian Institute of Technology Bombay, Mumbai 400076, India*

(c) *Felix Bloch Institute of Solid State Physics, University of Leipzig, 04103 Leipzig, Germany*

(d) *Department of Physics, Florida State University, Tallahassee, FL 32306, USA*

(e) *Department of Chemistry and Biochemistry, Florida State University, Tallahassee, FL 32306, USA*

Email: kt24@fsu.edu

Molecular spin qubits, known for their precise control, scalability, tunability, and room temperature capability to sustain multiple quantum states, are poised to impact the field of quantum information science [1]. These qubits combine efficiency and versatility, allowing for large-scale production, precise tuning of spin environments, and arrangement in 2D or 3D lattices. Progress in their design and surface integration is crucial for overcoming challenges related to addressability, coherence, and scalability in future quantum systems. As a result, they represent a highly promising area for ongoing research and development in this cutting-edge field. In addition, the metal–organic framework (MOF) MIL-53, a well-celebrated material known for its breathing nature[3], has begun to attract attention in the field of quantum information science [4].

In this context, we performed high-field continuous-wave (CW) electron paramagnetic resonance (EPR) experiments at frequencies up to 413 GHz on Co(II) based metal complexes and Cr(III)-based MOF to probe their electronic and structural properties. Specifically, we studied two Co(II) low-spin ($S = 1/2$) complexes, both having the molecular formula $[\text{CoCl}(\text{DPPE})_2]\text{SnCl}_3$ but differing in geometry: Co-SP adopts a square pyramidal structure, whereas Co-TBP exhibits a trigonal bipyramidal arrangement. These distinct geometries substantially affect their electronic environments and resultant EPR signatures. Furthermore, high-power W-band EPR spectrometer (HiPER) experiments revealed temperature-dependent relaxation behavior up to 60 K, with both complexes displaying similar characteristics when diluted. At 5 K, the spin-spin relaxation time (T_2) and spin-lattice relaxation time (T_1) for Co-TBP were approximately 5.8 μs and 0.62 ms, respectively, while Co-SP exhibited $T_2 \approx 3.5 \mu\text{s}$ and $T_1 \approx 0.98$ ms. Additionally, we investigated the MOF MIL-53, where the T_2 and T_1 values were found to be 0.96 μs and 50 μs , respectively, at 5 K.

References:

[1] Hill et al., *Nature*. **2016**, 531, 348–351.

[2] Thangavel. K. et al., *RSC Adv.*, **2024**, 14, 4244-4251

[3] Yamachi A. et al., *Nat. Comm.*, **2024**, 15, 7622

Engineering Surface Lysines and Hydrophobic Clusters to Modulate Hydration, Stability, and Bioconjugation in *Bacillus subtilis* Lipase A

Ritu Kaushik^{a,*}, Afnan M. Jaufer^{a,b}, Adam Bouhadana^a, Amir Kharrazizadeh^a, Mingwei Zhou^a, Coray M. Colina^{a,b,c}, Gail E. Fanucci^{a,b}

a Department of Chemistry, University of Florida, PO BOX 117200, Gainesville, FL 32611, USA

b George and Josephine Butler Polymer Research Laboratory, University of Florida, Gainesville, FL 32611, USA

c Department of Materials Science and Engineering, University of Florida, PO BOX 117200, Gainesville, FL 32611, USA

Lipases enable fat hydrolysis and hold key roles in biomedical, environmental, and industrial applications. *Bacillus subtilis* Lipase A (BSLA), known for its minimal α/β hydrolase fold and surface-accessible catalytic triad, is an ideal template to investigate and engineer enzyme structure for greater stability and catalytic efficiency. The surface hydration landscape of BSLA, a significant factor in flexibility and thermal resilience, remains understudied compared to its well-known catalytic and structural features. Our research employs spin labeling, ODNP-NMR, and molecular dynamics to build a comprehensive hydration map, with computational filtering used to pinpoint eight solvent-accessible positions for labeling and subsequent modification, excluding regions required for catalysis, substrate recognition, and stable packing as well as lysine residues for polymer conjugation. Data revealed a heterogeneous hydration landscape, dominated by two principal hydrophobic clusters that slow water diffusion and closely tie local mobility to enzyme dynamics. Building on these insights, we analyzed how lysine positioning and hydrophobic clusters influence BSLA performance and surface modification potential. We will systematically engineer the BSLA surface to refine hydration-driven flexibility, stability, and conjugation. Polymer-conjugated variants will be prepared through site-selective PEGylation at solvent-accessible lysines, with resulting changes in enzyme hydration, mobility, and function measured using integrated spectroscopic and biochemical assays. In parallel, targeted lysine mutations in salt bridges and hydrophobic clusters will dissect their individual and combined roles in hydration shell dynamics, thermostability, and modification uniformity. These strategies will extend to thermostable BSLA variants, combining structure-guided engineering with comprehensive functional evaluation to generate robust, homogeneous enzyme constructs suitable for demanding industrial and biomedical applications. This integrated experimental approach enables precise control over enzyme surface chemistry and supports the rational design of next-generation biocatalysts.

References:

1. Jaufer AM, Bouhadana A, Kharrazizadeh A, Zhou M, Colina CM, Fanucci GE. Designing surface exposed sites on *Bacillus subtilis* lipase A for spin-labeling and hydration studies. *Biophys Chem*. 2024 May; 308:107203. DOI: 10.1016/j.bpc.2024.107203.
2. Jaufer AM, Bouhadana A, Fanucci GE. Hydrophobic Clusters Regulate Surface Hydration Dynamics of *Bacillus subtilis* Lipase A. *J Phys Chem B*. 2024 Apr 25;128(16):3919-3928. DOI: 10.1021/acs.jpcc.4c00405.
3. Guangli Hu, Shuqi Xing, Wei Xie, Jia Long, Laping He, Cuiqin Li, Xiao Wang, Xuefeng Zeng, Effect of m-PEG modification on the properties and structure of recombinant lipase from *Aspergillus niger* GZUF36, *Food Bioscience*, Volume 59,2024,104258, ISSN 2212-4292, DOI: 10.1016/j.fbio.2024.104258.
4. Yun HS, Park HJ, Joo JC, Yoo YJ. Thermostabilization of *Bacillus subtilis* lipase A by minimizing the structural deformation caused by packing enhancement. *J Ind Microbiol Biotechnol*. 2013 Nov;40(11):1223-9. DOI: 10.1007/s10295-013-1330-2.

Abstract title: CW and Pulsed EPR Investigation of HoW₁₀ Crystals as Potential Spin Qubit MaterialsAuthors: S. Ivan Weaver^{*1,2}, Eugenio Coronado³, Stephen Hill^{1,2,4}Affiliation: ¹National High Magnetic Field Laboratory, Tallahassee, FL 32310, USA; ²Department of Chemistry and Biochemistry, Florida State University, Tallahassee, FL 32306, USA.; ³University of Valencia, Valencia, Spain; ⁴Department of Physics, Florida State University, Tallahassee, FL 32306, USA

Molecular qubits are emerging as promising candidates for scalable quantum information systems due to their chemical tunability and potential for coherent spin control. Lanthanide-based polyoxometalates (POMs) offer a particularly attractive platform, as their rigid, oxide-based frameworks stabilize isolated magnetic centers while minimizing vibrational decoherence. Among these, HoW₁₀ clusters provide a model system for exploring single-ion magnetic anisotropy and spin relaxation dynamics relevant to qubit implementation.

Continuous-wave (CW) and pulsed electron paramagnetic resonance (EPR) techniques were employed to characterize the magnetic and dynamic properties of single-crystalline HoW₁₀. Multi-frequency CW-EPR spectra were recorded to resolve fine structure associated with the Ho³⁺ 4f⁰ electronic configuration. Spectral simulations based on an effective spin Hamiltonian were used to extract anisotropic g-values and zero-field splitting parameters, providing insight into the ligand field environment and energy level structure. Complementary pulsed EPR experiments, including spin echo and inversion recovery measurements, were performed to probe coherence and relaxation behavior across variable temperatures.

CW-EPR results reveal well-defined resonance features consistent with strong crystal-field-induced magnetic anisotropy. Simulations indicate a highly anisotropic ground state dominated by low-lying m_J sublevels. Pulsed EPR measurements show measurable spin echo signals at low temperatures, with phase memory (T₂) and spin-lattice (T₁) relaxation times reflecting a competition between spin-phonon coupling and hyperfine interactions. The long T₁ values and detectable coherence confirm that HoW₁₀ clusters can host addressable spin states under appropriate conditions. These findings establish HoW₁₀ as a promising molecular platform for understanding and optimizing lanthanide-based qubit behavior.

References

1. Shiddiq, M.; Komijani, D.; Duan, Y.; Gaita-Ariño, A.; Coronado, E.; Hill, S. Enhancing Coherence in Molecular Spin Qubits via Atomic Clock Transitions. *Nature* **2016**, *531* (7594), 348–351. <https://doi.org/10.1038/nature16984>.
2. Ghosh, S.; Datta, S.; Friend, L.; Cardona Serra, S.; Gaita-Ariño, A.; Coronado, E.; Hill, S. Multifrequency EPR Studies of a Mononuclear Holmium Single-molecule Magnet Based on the Polyoxometalate [HoIII(W₅O₁₈)₂]⁹⁻. *Dalton Trans.* **2012**, *41* (44), 13697–13704. <https://doi.org/10.1039/C2DT31674A>.
3. Caliskan, B.; Caliskan, A. Dipolar Interactions: Hyperfine Structure Interaction and Fine Structure Interactions; 2020. <https://doi.org/10.5772/intechopen.91791>.

Region-specific GNAL Knockout Reveals Differential Network Dysfunction in a Mouse Model of Dystonia

Barbara Balsamo^{1,2*}, Mark Moehle¹, Bradley Wilkes³,

¹Department of Pharmacology and Therapeutics, University of Florida, Gainesville, FL

²Department of Neuroscience, University of Florida, Gainesville, FL

³Department of Applied Physiology and Kinesiology, University of Florida, Gainesville, FL

Background

Dystonia is a neurological movement disorder characterized by involuntary, sustained muscle contractions that lead to abnormal postures or repetitive movements. There are limited treatment options, and current therapeutics are only symptomatic. Identifying the circuit dysfunction causative for dystonia is crucial for developing targeted interventions. Genetic mutations have been linked to familial forms of dystonia, including *GNAL*, which encodes an α -subunit of a heterotrimeric G protein that regulates circuits linked to dystonia. In mice, striatal *GNAL* loss reproduces dystonia-like motor symptoms. Evidence suggests that the cerebellum also plays a role in dystonia, though its role remains unclear. We hypothesize that striatal *GNAL* loss would produce more substantial motor-network disruptions than cerebellar *GNAL* loss. Examining these networks will help develop targeted interventions for patients with dystonia.

Methods

Using *GNAL* flox/flox mice, we injected a Cre-expressing virus into the striatum or cerebellum to produce region-specific *GNAL* knockout. We performed sensory-evoked fMRI using a heat stimulus on the hind paw to measure BOLD activation patterns and functional connectivity. Voxel-wise statistics were computed using a 2x2 design (factors: site and virus) in AFNI.

Results

In mice with striatal *GNAL* knockout, voxel-wise analysis revealed a significant difference in BOLD responses within the striatum and cerebellum ($p < 0.05$). We show post-hoc comparisons across injection site (striatum vs cerebellum) and virus (active vs control) in voxels that showed a significant effect in the full model.

Conclusion

GNAL loss produces different sensorimotor dysfunction patterns depending on knockout location, with the strongest interaction effects in the cerebellum. Thus, striatal and cerebellar *GNAL* systems influence each other rather than functioning independently. These findings suggest network-level disruptions in dystonia, guiding future circuit-based therapies.

53rd Southeastern Magnetic Resonance Conference

References

- Bostan, Andreea C., and Peter L. Strick. “The Basal Ganglia and the Cerebellum: Nodes in an Integrated Network.” *Nature Reviews Neuroscience*, vol. 19, no. 6, 11 Apr. 2018, pp. 338–350, www.ncbi.nlm.nih.gov/pmc/articles/PMC6503669/, <https://doi.org/10.1038/s41583-018-0002-7>.
- Breakefield, Xandra O., et al. “The Pathophysiological Basis of Dystonias.” *Nature Reviews Neuroscience*, vol. 9, no. 3, Mar. 2008, pp. 222–234, <https://doi.org/10.1038/nrn2337>. Accessed 16 Nov. 2020.
- Chambers, N. E., Hall, D., Barsoum, S., Miller, E., Curry, T., Kaplan, M., Garan, S., Gallardo, I., Staab, R., Nabert, D., Hutchinson, K., Millett, M., & Moehle, M. S. (2024). Conditional Knockout of Striatal Gnal Produces Dystonia-like Motor Phenotypes. *bioRxiv: the preprint server for biology*, 2024.08.26.609754. <https://doi.org/10.1101/2024.08.26.609754>
- Shakkottai, Vikram G, et al. “Current Opinions and Areas of Consensus on the Role of the Cerebellum in Dystonia.” *The Cerebellum*, vol. 16, no. 2, 1 Apr. 2017, pp. 577–594, <https://doi.org/10.1007/s12311-016-0825-6>. Accessed 24 Apr. 2023.
- Wilkes, B.J, et al. “Cell-Specific Effects of Dyt1 Knock-out on Sensory Processing, Network-Level Connectivity, and Motor Deficits.” *Experimental Neurology*, vol. 343, 1 Sept. 2021, pp. 113783–113783, <https://doi.org/10.1016/j.expneurol.2021.113783>. Accessed 26 Apr. 2024.
- Wilkes, B.J., et al. “Cell-Specific Dyt1 Δ GAG Knock-in to Basal Ganglia and Cerebellum Reveal Differential Effects on Motor Behavior and Sensorimotor Network Function.” *Experimental Neurology*, vol. 367, Sept. 2023, p. 114471, <https://doi.org/10.1016/j.expneurol.2023.114471>. Accessed 22 Oct. 2025.

In vivo Hyperpolarized ¹³C MRI Detects Abnormal Mitochondrial Metabolism in CDAA-induced Hepatic Steatosis

Nesmine Maptue¹, Qingyang Shen^{1,2}, Chalermchai Khemtong^{1,2}

¹Department of Medicine, Division of Endocrinology, Diabetes & Metabolism, ²Department of Biochemistry and Molecular Biology, University of Florida

Introduction: Metabolic dysfunction–associated steatosis liver disease (MASLD) is a major health burden worldwide. Assessments of MASLD progression are challenging. Changes in liver metabolism occur in the early onset of MASLD and therefore are excellent biomarkers for characterizing this disease. In this study, we employed hyperpolarized (HP) ¹³C MRI to detect metabolic alterations in the liver of a choline-deficient, amino acid defined (CDAA)-induced MASLD mouse model.

Method: MASLD was induced by feeding C57BL/6 mice with a CDAA diet for 10 weeks. [1-¹³C]Pyruvic acid was polarized in a HyperSense polarizer. HP ¹³C MRI was carried out in an 11T Bruker Avance III HD scanner. ¹H MRI was acquired using an 85-mm quad volume coil while a home-built surface linear coil was used to acquire ¹³C MR. HP [1-¹³C]pyruvate was injected into the animals via a tail vein catheter over ~ 5 second. Simultaneously, a series of ¹³C NMR spectra were acquired every 2 s with 20-deg flip angles.

Results: Soon after the HP [1-¹³C]pyruvate injection, signals of HP ¹³C metabolites were readily observed in both groups of animals. Major metabolites of HP [1-¹³C]pyruvate, i.e. bicarbonate (Bic), alanine (Ala), and lactate (Lac), were clearly detectable in both groups of livers. Production of [1-¹³C]lactate was comparable between the two groups of animals (Lac/tC = 39.7±7.9% for ND and 38.0±4.6% for CDAA). Production of [1-¹³C]alanine trended higher in the ND group (Ala/tC = 26.1±5.5%) compared to the CDAA livers (Ala/tC = 19.7±9.3%). However, the difference is not statistically significant (*P* > 0.05). ND livers produced much higher production of ¹³C-bicarbonate (Bic/tC = 1.7±0.4%) than the liver of the CDAA mice (Bic/tC = 0.3±0.05%). Our results suggest that the metabolism of HP [1-¹³C]pyruvate to [1-¹³C]lactate and [1-¹³C]alanine by lactate dehydrogenase (LDH) and alanine transaminase (ALT), respectively, was not severely affected by MASLD progression. However, pyruvate oxidation by hepatic pyruvate dehydrogenase (PDH) was greatly suppressed in CDAA-induced MAASLD mice. Isotopomer analyses of liver metabolism on the same animals using non-HP [U-¹³C]pyruvate agreed well with the HP ¹³C MRI results.

Conclusions: We have demonstrated that altered liver metabolism induced by MASLD can be detected in vivo using HP ¹³C MRI. The results suggest that HP ¹³C MRI could be a potential valuable imaging tool for the treatments and management of fatty liver diseases.

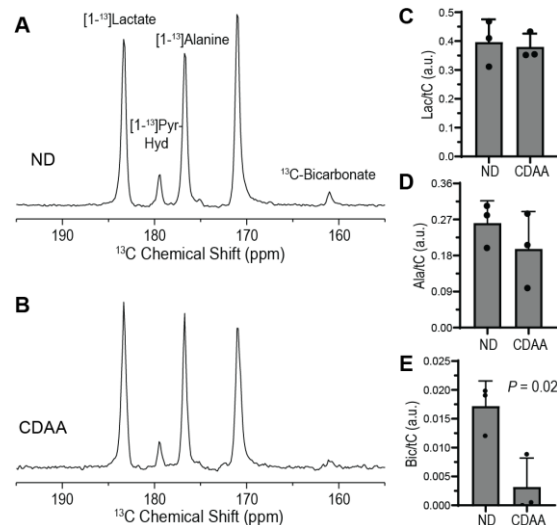


Fig. 1. (A-B) Summed ¹³C spectrum of a healthy and MASLD liver, showing downstream metabolites of HP [1-¹³C]pyruvate. (C-E) Normalized [1-¹³C]lactate, [1-¹³C]alanine, and ¹³C-bicarbonate signals.

Measuring Slow Cerebrospinal Fluid Velocities in Preclinical Models Using Optimized Phase Contrast MRI at 21.1 T

Dayna L. Richter^{1,2*}, Connor Blan^{1,2}, Anamika Roy^{1,2}, Malathy Elumalai^{1,2} and Samuel C. Grant^{1,2}

¹Center for Interdisciplinary Magnetic Resonance, National High Magnetic Field Laboratory

²Chemical & Biomedical Engineering, Florida State University, Tallahassee, FL, USA

Introduction: Cerebrospinal fluid (CSF) is essential for clearing waste products in the brain that contribute to pathologies, such as Alzheimer's disease¹. However, measuring slow CSF flow using MRI is challenging^{2,3}. Williamson *et al.* (2020) provide strategies for optimizing phase contrast with Pulsed Gradient Spin Echo (PGSE) for the measurement of slow flow highlighting the limits of detection⁴. Building on these methods, this study aims to assess CSF velocimetry *in vivo* with an optimized gradient strength. A controlled flow phantom was used to validate sensitivity and optimize gradient strength before translating into *vivo* conditions.

Method: A homebuilt flow phantom was scanned using the 900-MHz vertical scanner at the NHMFL. Average velocities of 100-500 $\mu\text{m/s}$ were tested due to relevance to CSF flow in rodents^{3,5,6}. Five naïve female Sprague Dawley rats (200-250 g) were scanned. A diffusion-weighted EPI sequence with 0.15 mm (phantom) and 0.125 mm (rat) in-plane resolution, TR/TE = 5000/44 ms, and 4 segments. The gradient encoding time was 4 ms, with a gradient spacing of 20 ms between bipolar gradients applied in the positive and negative x-, y- and z-directions. Two-point phase contrast for slow flow has an optimal q-slow, defined as the inverse of the characteristic diffusive length scale. Five gradient strengths, Q₁ - Q₅, were chosen around q-slow.

Result & Conclusion: The phase contrast PGSE EPI method was validated and optimized using the flow phantom. We found that the Q₄ setting was the closest to the theoretical results with the lowest sum of square error. We were able to map the CSF velocity and direction *in vivo* for female Sprague-Dawley rats which aligned well with the expected CSF flow directions⁷. This work shows the feasibility of phase contrast with PGSE to measure CSF dynamics in preclinical MRI. This approach could enable longitudinal, non-invasive CSF assessments in preclinical models of neurological disorders.

References: [1] Iliff JJ, et al. 2012 [2] Mestre H, et al. Nat Commun. 2018 [3] Li J, et al. Magn Reson Med. 2022 [4] Williamson NH, et al. J Magn Reson Open. 2020 [5] Karimy JK, et al. J Neurosci Methods. 2015 [6] Liu G, et al. Cell Rep. 2020 [7] Bito Y, et al. Magn Reson Med. 2021

Acknowledgements: Animal procedures were approved by the Florida State University Animal Care and Use Committee in Tallahassee, FL (PROTO-202100071). Research reported in this abstract was supported by the National Institute of Neurological Disorders and Stroke of the National Institutes of Health (RO1-NS072497). A portion of this work was performed at the National High Magnetic Field Laboratory, which is supported by National Science Foundation Cooperative Agreement No. DMR-2128556* and the State of Florida.

Engineered Iron Oxide Interfaces Enable Reliable MRI Tracking of Therapeutic Extracellular Vesicles

Arshia Arbabian^{*1,2}, Jeff Procida³, Dayna L. Richter^{1,2}, Hedi Mattoussi³, Yan Li²

¹ National High Magnetic Field Laboratory, Florida State University, Tallahassee, Florida, USA

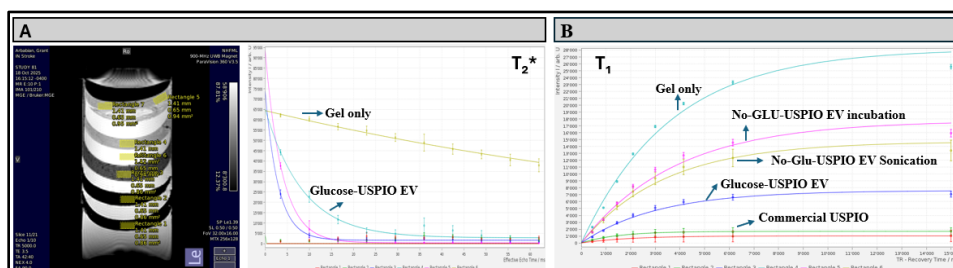
² Department of Chemical & Biomedical Engineering, FAMU-FSU College of Engineering, Florida State University, Tallahassee, Florida, USA

³ Department of Chemistry and Biochemistry, Florida State University, Tallahassee, Florida, USA

Background: Stroke remains a leading cause of long-term neurological disability, driving the need for regenerative, cell-free therapies¹. Mesenchymal stem-cell-derived extracellular vesicles (MSC-EV) have shown strong therapeutic potential in promoting recovery following ischemic injury. However, EV have not yet been reliably visualized in the brain after intranasal (IN) administration, largely due to inefficient labeling and vesicle disruption during conventional magnetic labeling. Prior studies indicate that sonication-based labeling alters miRNA cargo and compromises EV integrity², underscoring the need for improved methods that preserve functionality while enabling MRI-based detection.

Methods: EV were isolated from three-dimensional MSC cultures (passage 6) and labeled using either small core size (~5-6 nm) iron oxide nanoparticles grown using a high temperature decomposition reaction, ligand exchange with a multifunctional polymer and then conjugated with glucose, or commercially available USPIO (Sigma 725358). Labeling was achieved through 24 h glucose incubation or controlled point sonication (three 10 s bursts on ice), followed by re-isolation using the ExtraPEG protocol. Phantoms containing labeled EV in 0.5% agarose gel were imaged on a 21.1 T Bruker system using RAREVTR (T_1 : TE = 6 ms, TR = 450–15000 ms) and MGE (T_2^* : TE = 3.5–62 ms, TR = 5 s, 10 echoes). Relaxation rates (R_1 , R_2^*) were derived from exponential fits ($T_1 = 1/R_1$; $T_2^* = 1/R_2^*$).

Results/Conclusion: Glucose-mediated incubation produced uniform T_2^* shortening and consistent T_1 recovery, confirming controlled iron incorporation. Non-glucose iron oxide showed negligible contrast, suggesting limited uptake, while sonicated and commercial samples displayed strong but artifactual signal loss from iron aggregation and incomplete washing. These findings demonstrate that glucose-assisted labeling preserves EV integrity and enables reproducible MRI contrast, establishing a foundation for quantitative tracking of intranasally delivered EV in stroke models.



References: 1. Martin, S. S. *et al.* 2025 Heart Disease and Stroke Statistics: A Report of US and Global Data From the American Heart

Association. *Circulation* **151**, e41–e660 (2025). 2. Helsper, S. *et al.* Superparamagnetic Iron Oxide Nanoparticle-Labeled Extracellular Vesicles for Magnetic Resonance Imaging of Ischemic Stroke. *ACS Appl. Nano Mater.* **7**, 24160–24171 (2024).

Accelerating jHSQC Acquisition through Non-Uniform sampling: Achieving Uniform-quality Spectra in Half the time

Gaurav Sharma*, Victor de Paula, Matthew E Merritt

Department of Biochemistry and Molecular Biology, University of Florida, USA, 32610

Background: Non-uniform sampling (NUS) has drawn significant attention from researchers in recent decades. It cuts the experimental time drastically while maintaining spectral fidelity. ^{13}C isotopomer analysis provides direct information about isotopomer pools. However, acquisition of $\{^1\text{H}\}^{13}\text{C}$ -Carbon spectra is often limited by sensitivity. In the past, Merritt *et al.* developed the adiabatic jHSQC experiment, which takes 3 to 5-fold less time than $\{^1\text{H}\}^{13}\text{C}$ direct detection and offers the same ^{13}C isotopomer information for metabolic studies.¹ However, full sampling in the indirect dimension remains time-intensive for routine metabolic experiments. Here, we extend this adiabatic j-HSQC framework by implementing NUS strategies to achieve faster data acquisition without losing resolution and quantitative accuracy.

Methods: All the NMR experiments were acquired using a 600 MHz Avance Neo spectrometer (Bruker Bio-Spin) equipped with a cryo 1.7 mm probe. Topspin 4.0.5 was used to post-process the NMR data. For reconstructing the NUS-jHSQC spectra, the IST method available in TopSpin was used. A concentrated standard mixture ($[2-^{13}\text{C}]$ acetate, $[1,2-^{13}\text{C}_2]$ acetate, $[U-^{13}\text{C}]$ glutamine, and $[U-^{13}\text{C}]$ Alanine) was used to optimize different NUS schemes to get high spectral fidelity. To demonstrate the robustness of the optimized NUS-jHSQC sequence, a glioblastoma (GBM) cell line treated with $[U-^{13}\text{C}]$ glucose was used.

Results: Among the various tested NUS schemes, Poisson-gap sampling 50% coverage, weight 3 (PG_50_3), and 30% coverage, weight 2.5 (PG_30_2.5) reconstructed qualitatively comparable spectra. However, when enrichment of any isotopomer is less than 5%, PG_30_2.5 fails to provide accurate quantitative results, whereas PG_50_3 provided the best results within 5% error for all metabolites compared to uniformly sampled jHSQC in standard mixture as well as GBM cell samples.

Conclusions: Incorporation of NUS in jHSQC reduces the experimental time significantly and may fit this experiment into the routine metabolomics pipeline.

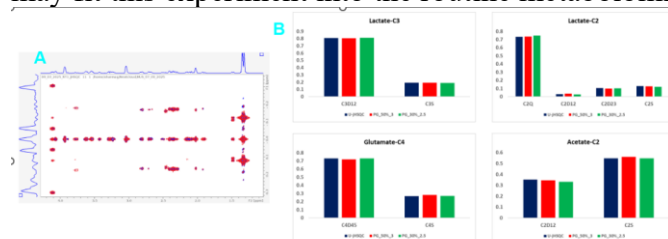


Figure A. Overlay of uniformly sampled (blue) and NUS (red, PG_50_3) jHSQC spectra showing comparable spectral quality.
B. Quantitative comparison of ^{13}C isotopomer enrichment derived from uniform and NUS-jHSQC experiments confirms reproducible enrichment estimates.

Reference:

1. Merritt, M.E., Burgess, S.C., and Spitzer, T.D. (2006), Adiabatic JHSQC for ^{13}C isotopomer analysis. *Magn. Reson. Chem.*, 44: 463-466.

Abstract title:**Characterization of lipid based Lyotropic Liquid Crystals Phase Behavior and Their Potential as MRI Contrast Agents and therapeutic Applications**Authors: **Diba Allameh Zadeh, Gail E. Fanucci***

Department of Chemistry, University of Florida, Gainesville, FL 32611, USA

Abstract

Incorporating chelating lipids into lipid matrices provides a promising route toward the design of multifunctional molecular assemblies with biomedical imaging applications, particularly as Magnetic Resonance Imaging (MRI) contrast agents. In this study, we investigated the integration of diethylenetriaminepentaacetic acid (DTPA) chelates, with and without gadolinium (Gd^{3+}), into lipid mixtures composed of glyceryl monooleate (MO) and 1,2-dioleoyl-sn-glycero-3-phosphocholine (DOPC). The effects of chelating lipids on phase behavior, molecular dynamics, and water proton relaxation were systematically examined to assess their suitability as T_1 MRI contrast agents. Nanoassemblies were characterized using Polarized Light Microscopy (PLM) for phase identification, Dynamic Light Scattering (DLS) for size distribution, and Nuclear Magnetic Resonance (NMR) relaxometry at 1.4 T to probe bulk water relaxation and lipid molecular dynamics. Complementary 1D NMR studies provided molecular-level insight into hydration and lipid organization. A notable outcome was the formation of highly stable dispersions without the need for external polymeric stabilizers (e.g., Pluronic F127), a major advantage for biomedical use as it reduces the risk of additional toxicity or undesired interactions. In parallel, coordination of Eu^{3+} with DTPA-lipids was evaluated in MO/DOPC/PE-DTPA systems prepared with two distinct chelating lipid contents (10% and 12%). The resulting Eu -DTPA nanoassemblies displayed strong luminescence, with excitation at ~ 320 nm yielding characteristic Eu^{3+} emission bands. In particular, a distinct emission observed at 645–650 nm was assigned to the ${}^5D_0 \rightarrow {}^7F_3$ transition, confirming the successful coordination of Eu^{3+} within the lipid matrix. Fluorescence intensity was quantified using a fluorescence spectrophotometer, underscoring the potential of these systems as dual MRI-fluorescence probes. Ongoing work will focus on altering the internal nanostructure of these lipid assemblies to optimize water accessibility and exchange, thereby enhancing T_1 relaxation efficiency. By systematically varying lipid composition, metal loading, and internal phase geometry, these systems may be rationally tuned into a versatile platform of stable, self-assembled, and biocompatible nanoprobes for multimodal imaging applications.

References

- Dydak, Karolina, et al. "Nanoassemblies with Gd-chelating lipids (GMO@ DTPA-BSA-Gd) as a potential new type of high molecular weight contrast agents." *Journal of Materials Chemistry B* 12.46 (2024): 12017-12029.
- Van Dalsen, L.; Weichert, D.; Caffrey, M. In *Meso Crystallogeneses Glyco-Diosgenin*. J. Appl. Crystallogr. 2020, 53 (2), 530–535.
- S.L. Yap et al. *Journal of Colloid And Interface Science* 656 (2024) 409–42

Title: Phase Dispersion in Multiband Imaging

Authors: Warren Boschen^{1*}, Guita Banan^{2,3}, Rosalind Sadleir⁴, Thomas H. Mareci^{2,5}.

1: Department of Biomedical Engineering, Vanderbilt University, 2: Department of Physics, University of Florida, 3: Department of Science and Technology Studies, York University, 4: School of Biological and Health Systems Engineering, Arizona State University 5: Department of Biochemistry and Molecular Biology, University of Florida

Introduction: Phase-sensitive measurements such as magnetic resonance electrical impedance tomography (MREIT) [1] can be affected by various sources of phase dispersion, including drift in the main magnetic field (B_0), physiological effects, and pulse sequence timing. Here, we investigate how the number of averages N_A and the time between averages may alter phase measurements.

Methods: Multiband MREIT data of a phantom were acquired on a Siemens 3.0 T Prisma with ten gradient echoes ($TE_1 = 7$ ms, $\Delta TE = 3$ ms), and all combinations of $TR = 50, 150$ ms, $N_A = 2, 6$. Phase maps were produced by complex dividing paired averages and compared to simulation. Additionally, MREIT data of a phantom were acquired with similar TR/TE and $N_A = 100$. Short-term averaging (acquiring all averages for one line of k-space) and long-term averaging (acquiring all lines of k-space for one average) were performed to mitigate the effects of B_0 drift. Phase maps were produced as before.

Results: Both simulation and phantom measurements showed a large phase dispersion is observed with $TR = 50$ ms and $N_A = 6$, which is reduced by extending TR or decreasing N_A (see Figure 1). Short-term averaging yielded minimal phase shift compared to long-term averaging.

Conclusions: The phase patterns from increasing the number of averages suggests the build-up of steady state transverse magnetization, notably as $TR < T_2$. We recommend extending the TR or using RF spoiling [2]. Furthermore, short-term averaging minimizes the effects of B_0 drift by placing the phase shift into the spatial domain, causing minimal offset.

References:

- [1] R. Sadleir and A. S. Minhas, Eds., *Electrical properties of tissues: quantitative magnetic resonance mapping*. in *Advances in experimental medicine and biology*, no. 1380. Cham: Springer, 2022.
- [2] Y. Zur, M. L. Wood, and L. J. Neuringer, "Spoiling of transverse magnetization in steady-state sequences," *Magn. Reson. Med.*, vol. 21, no. 2, pp. 251–263, Oct. 1991, doi: 10.1002/mrm.1910210210.

Characters: 1984

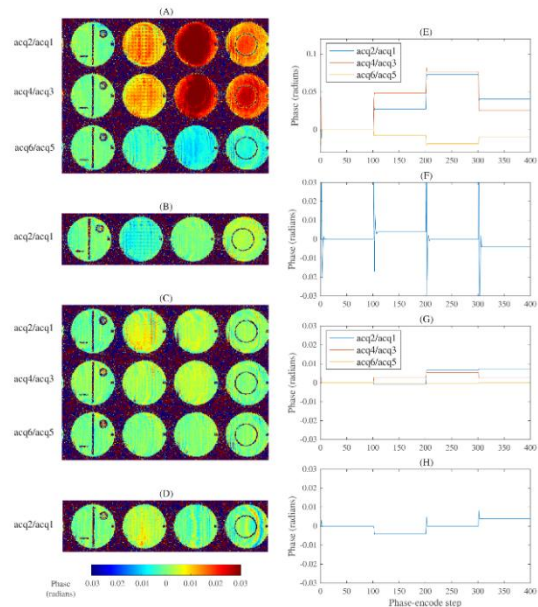


Figure 1: ACR phantom (A-D) and simulation (E-H) results. Parts (A) and (E): $TR = 50$ ms, $N_A = 6$, Parts (B) and (F): $TR = 50$ ms, $N_A = 2$, Parts (C) and (G): $TR = 150$ ms, $N_A = 6$, and Parts (D) and (H): $TR = 150$ ms, $N_A = 2$.

An Educational Approach to Connecting Chemistry and Healthcare Using Magnetic Resonance Imaging

Emily G. Cushman*, Leah B. Casabianca

Department of Chemistry, Clemson University, Clemson, SC

For many high school students, it can be hard to decide what to major in during undergraduate studies to prepare themselves for a healthcare career^{1,2}. While chemistry is not the most popular degree for a career in the medical field, a degree in chemistry may prepare students for a healthcare career^{1,2}. Magnetic Resonance Imaging (MRI) was developed by chemists and physicists, and is an integral part of the healthcare system for diagnostic imaging^{3,5}. It is hypothesized that MRI is an ideal tool for demonstrations and experiments to teach students about the connection between chemistry and healthcare. To test this hypothesis, a presentation was created to educate students on the specific chemical physics of MRI as it relates to how the MRI goes from a pulse sequence and radiofrequency waves to an image^{4,5}.

A sample of water and oil was created to demonstrate the contrast of fat and water in the human body. Using this water and oil sample, T₁ and T₂ weighted images were demonstrated using different default benchtop MRI pulse sequences^{4,5}. These sequences showed a clear image of either the oil, water, or both. Concepts like spin, T₁ and T₂ relaxation, and echo time were explained at the level of high school students with no prior knowledge of this subject^{4,5}. Students put their own samples into the benchtop MRI, and were challenged to figure out the contents of a final sample. Students learned how chemistry can help them pursue a career in the healthcare field through the application of MRI. When experimenting with their samples, students practice critical thinking and decision-making skills crucial for higher education and the healthcare field. Future work includes presenting to more students and collecting data through surveys on how ideal the demonstration and experiment is at explaining the scientific process, and how thinking like a chemist connects to healthcare.

References

- ¹Barr, D.A., Matsui, J., Wanat, S.F. *et al.* Chemistry courses as the turning point for premedical students. *Adv in Health Sci Educ.* 2010, 15, 45-54.
- ²Malvitz, M.; Khan, N.; Morgenstern, L. B.; College preparation for a medical career in the United States. *PLoS ONE.* 2024.
- ³National Historic Chemical Landmarks program of the ACS. *NMR and MRI: Applications in Chemistry and Medicine*, online ed.; Ginsberg, J.; American Chemical Society, 2011.
- ⁴Britton, M.M. Magnetic resonance imaging of chemistry. *Chemical Society Reviews.* 2010, 39, 4036-4043.
- ⁵Plewes, D.B.; Kucharczyk, W. Physics of MRI: A primer. *Journal of Magnetic Resonance Imaging.* 2012, 35(5), 1038-1054

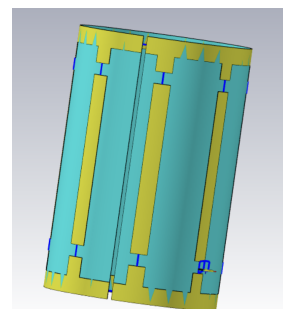
Methodologies for analyzing RF shield efficiency at 21.1T MRI

Julia Martin*(1, 2), Dayna Ritcher (1, 2), Taylor Vanderlinden (1, 2) Malathy Elumalai (1)

(1) FAMU-FSU College of Engineering, Department of Chemical & Biomedical Engineering Tallahassee, FL (2) National High Magnetic Field Laboratory (NHMFL), Tallahassee, FL

Introduction: The 21.1T ultra-high field magnet at NHMFL enables high resolution pre-clinical imaging. RF shielding prevents eddy currents generated by the gradients from coupling into the RF circuit and compromising SNR. This project evaluates RF shields made from copper-clad laminate joined with different conductive materials- silver epoxy, solder, gold, capacitors, and no sealant - against a reference electroplated shield. Testing was done to evaluate S21, Q-factor using VNA on bench, Echo Planar Imaging (EPI)/QA_SNR sequence in a 21.1T magnet, and S11 simulations using CST EM software.

Methods: CST EM Simulation: 3D Electromagnetic simulations were performed in CST Microwave Studio to measure S11 at 900 MHz and visualize the B1 field generated by a ¹H low pass birdcage volume coil (fig 1) with various shield configurations. **Bench Testing:** Shield performance was measured by placing each prototype between two pickup loops and measuring S21, treating the shield as the device under test. Pickup loops were normalized over 200 MHz span, with one at coil center (B1) and another above shield to assess signal coupling. RF coil efficiency was measured by Q(-3 dB)/tuning range under loaded (tissue-equivalent phantom)/unloaded conditions. **Magnet Evaluation:** RF shields were tested in a 21.1T magnet using a rapid gradient switching EPI sequence to induce strong eddy currents and assess shielding effectiveness. Imaging data were analyzed for Nyquist ghosting, reference power, and echo time. Normalized SNR was measured using the QA_SNR sequence, and B1 homogeneity maps were generated.



Results: RF shield built with 3525 copper clad laminate joined by silver conductive epoxy performed best across the tuning range of 809-921 MHz, with loaded/unloaded Q (77.24/112.42). Magnet tests showed normalized SNR-1633 and a uniform B1 field map. The EPI sequence, matched in resolution to the reference, required less power (0.543 W) to produce high-resolution images in both Le-Rt and V-D directions.

Acknowledgements:

A portion of this work was performed at the NHMFL, which is supported by National Science Foundation Cooperative Agreement Nos.DMR-1644779 and DMR-2128556 and the State of Florida.

53rd Southeastern Magnetic Resonance Conference

References:

1. Copper Mountain Technologies. (n.d.). *What are S-parameters?* Retrieved July 25, 2025
2. Bart de Vos, Rob Remis, Andrew Webb, Segmented RF shield design to minimize eddy currents for low-field Halbach MRI systems, *Journal of Magnetic Resonance*, Volume 362,2024, 107669,ISSN 1090-7807
3. Insulectro (Indianapolis, IN). Provided *copper-clad laminates*.
<https://insulectro.com/offerings/laminates/>
4. B. L. Beck, K. A. Jenkins, J. R. Rocca, and J. R. Fitzsimmons, "Tissue-equivalent phantoms for high frequencies," *Concepts in Magnetic Resonance Part B: Magnetic Resonance Engineering*, vol. 20B, no. 1, pp. 30-33, Feb. 2004. doi: 10.1002/cmr.b.20002
5. A. M. Nagel, R. Umathum, M. B. Rösler, M. E. Ladd, I. Litvak, P. L. Gor'kov, W. W. Brey, and V. D. Schepkin, "³⁹K and ²³Na relaxation times and MRI of rat head at 21.1 T," *NMR Biomed.*, vol. 29, no. 6, pp. 759–766, Jun. 2016, doi: 10.1002/nbm.3528

Sustainability: Assessing ways to reduce energy consumption in NMR/MRI systems

- (1) Florida State University, College of Arts and Sciences, Department of Computer Science
- (2) FAMU-FSU College of Engineering (3) National High Magnetic Field Laboratory (NHMFL)

Authors: **Kate Payen (1,2)**, Marshall Wood (3), Julia Martin (2,3), Ashley Blue (3), Malathy Elumalai (3)

Abstract: NHMFL, home to the world’s strongest MRI scanner and leading magnet technologies, is committed to sustainability. Its helium recycling program recovers 85–90% of helium, cutting costs and waste. Beyond helium, energy use is another focus. The custom-built 900 MHz magnet supports NMR, MRI, and micro-imaging, depending on the connected equipment. While only one application runs at a time, auxiliary components like RF amplifiers/chillers may remain active unnecessarily [2]. Automating their shutdown during idle periods can reduce energy waste. My project aims to (1) Evaluate energy consumption across all applications (2) Promote circular economy practices by creating a website to track scientific instrument reuse at NHMFL.

Methods: To achieve Aim 1, we are logging power consumption of all test equipment's during ON, OFF and Idle state. We have documented the electrical specs of each instrument to select appropriate power loggers. The 230V, single phase, 2-wire system makes the market availability minimum and involves direct wiring to the sub-panel. We chose the Spartan Power SP-PM120 for monitors, EKM metering EKM-25XDSE for Bruker 2-bay console [4] and Murata Power Solutions’ ACM20-4-C1-R-F-C [3] housed in a custom 3D-printed box for individual RF amplifiers. Average kWh consumption will be estimated to calculate potential energy cost savings and assess the financial impact of powering down equipment during non-operational periods.

Results:

	Host CPU	Left monitor #1	Right Monitor #2	ECG CPU	ECG Monitor	Console
During Experiment	56.13	20.79	25.4	21	13.845	1210
No Experiment	52.645	19.387	23.41	22.48	13.86	Not yet collected
IDLE State	Not yet collected	0	1.407	Not yet collected	0	Not yet collected

Preliminary results show that turning OFF the monitors/host CPUs for a 12-hour period will save 241 kWh. Console during active experiment shows 1210 kWh consumption. Our previous study showed that an RF amplifier uses 19W during IDLE state and 90W during active state. Our console has five RF amplifiers and placing the four unused RF amplifiers in IDLE state will save 280W per experiment. Future studies will focus on automating the software to place the unused equipment in IDLE state based on usage patterns.

53rd Southeastern Magnetic Resonance Conference

Acknowledgements

A portion of this work was performed at the National High Magnetic Field Laboratory, which is supported by the National Science Foundation Cooperative Agreement Nos.DMR-1644779 and DMR-2128556* and the State of Florida.

References

- [1] National High Magnetic Field Laboratory. (n.d.). *Helium recovery Bags - MagLab*.
<https://maglabweb.magnet.fsu.edu/about-the-maglab/around-the-lab/what-is-that/helium-recoverybag/#:~:text=The%20helium%20recovery%20bags%20are%20basically%20hightech%20recycling,liquid%2C%20making%20about%2026%20gallons%20of%20liquid%20helium.>
- [2] Karliner JSS, Boyd R, Ashby B, et al. Healthcare's climate footprint: how the health sector contributes to the global climate crisis and opportunities for action.
https://noharm-global.org/sites/default/files/documents-files/5961/HealthCaresClimateFootprint_092319.pdf.
- [3] Murata Power Solutions. (n.d.). *ACM20 series: Four-function AC power meters* [Datasheet]. Murata Manufacturing Co., Ltd.
<https://www.murata.com/-/media/webrenewal/products/power/datasheet/acm20.pdf>
- [4] *NMR Consoles | AVANCE NEO*. (n.d.). Bruker.
<https://www.bruker.com/en/products-and-solutions/mr/nmr/avance-neo-consoles.html>

Structural insight into inhibitor-mediated modulation of Huntingtin Exon 1 aggregation

Greeshma Jain^{1,2*}, Marina Trombetta-Lima^{3,4}, Irina Matlahov¹, Henrique Taborda Ribas^{3,5},
Tingting Chen¹, Amalia M. Dolga³, Patrick C.A. van der Wel¹

¹ Zernike Institute for Advanced Materials, Faculty of Science and Engineering, University of Groningen, Groningen, The Netherlands

² Current: Department of Chemistry, University of Florida, Gainesville, Florida, United States of America

³ Department of Molecular Pharmacology, Faculty of Science and Engineering, Groningen Research Institute of Pharmacy (GRIP), University of Groningen, Groningen, The Netherlands

⁴ Department of Biomedical Sciences of Cells and Systems, Section Molecular Cell Biology, University of Groningen, University Medical Center Groningen, Groningen, The Netherlands

⁵ Graduate Program in Biochemistry Sciences, Department of Biochemistry and Molecular Biology, Federal University of Paraná, Curitiba, PR, Brazil

Huntington's Disease (HD) is a neurodegenerative disease caused by the expansion of the polyglutamine (polyQ) domain in the exon 1 region of the huntingtin (htt) protein. This expansion of the polyQ domain leads to protein misfolding and the formation of β -sheet-rich fibrillar aggregates. The major challenge is to understand the mechanism of amyloid formation and their toxicity. Small molecule inhibitors have been shown beneficial for perturbing the aggregation kinetics, but their molecular modes of action are still not well understood. Here we employ solid-state nuclear magnetic resonance (ssNMR), in combination with electron microscopy (TEM) and kinetic assays, to elucidate the inhibitor's effect on HttEx1 aggregation mechanism. We observe a clear delay of protein aggregation was observed even at sub stoichiometric ratios of inhibitor relative to the protein. Our NMR analysis reveals that inhibitor-bound fibrils adopt a distinct conformation compared to the HttEx1 fibrils. Here, we propose a molecular model for the impact of the inhibitor on the aggregation mechanism, impacting the nucleation process and redirecting it toward a distinct aggregated state with modified toxic properties. Our data lays a foundation of how small molecules reshape the misfolding landscape of HttEx1, highlighting the importance of NMR spectroscopy in characterizing the structure of these aggregates.

References

1. Jain, G., Trombetta-Lima, M., Matlahov, I., Ribas, H. T., Chen, T., Parlato, R., Portale, G., Dolga, A. M., & van der Wel, P. C. A. (2025). Inhibitor-based modulation of huntingtin aggregation mechanisms mitigates fibril-induced cellular stress. *Nature Communications*, *16*(1), 3588.

The Conformational Equilibria of a Human GPCR Compared between Lipid Vesicles and Aqueous Solutions by Integrative ¹⁹F-NMRBeining Jin^{1*†}, Arka Prabha Ray^{1†} and Matthew T. Eddy¹¹Department of Chemistry, University of Florida, Gainesville, FL 32611, USA

†Indicates authors with equal contribution

G protein-coupled receptors (GPCRs) are the largest family of integral membrane proteins and top drug targets in academic and industrial labs. Phospholipids, as an essential component of biological membrane, sensory integral membrane proteins for most physiological processes and modulate receptor's activity in a manner highly dependent on the membrane environment. To date, NMR studies have provided a vast majority of GPCR structural plasticity and dynamic information, utilizing the preparations of GPCRs in aqueous solutions containing membrane mimetics including detergent micelles or lipid nanodiscs.¹ While helpful, these membrane mimetics differ from membrane systems such as lipid vesicles, which can better represent conditions in the cellular membrane environment, for example, their bulk physical properties.

Here we present an optimized protocol for preparing samples of the human A_{2A} adenosine receptor (A_{2A}AR), a representative class A GPCR, in unilamellar vesicles for ¹⁹F magic angle spinning (MAS) solid-state NMR spectroscopy. Utilizing multiple functional and biophysical assays, we confirmed that vesicles containing ¹⁹F-labeled A_{2A}AR bound ligands with native affinities, and we quantified the density and relative orientation of receptors in lipid vesicles. By optimizing spectral dispersion and resolution as a function of MAS frequency and ¹H decoupling strength, we obtained ¹⁹F MAS SSNMR data of similar spectral resolution and dispersion as preparations with lipid nanodiscs in aqueous solution. The similar resolution and dispersion facilitated direct comparisons of the conformational equilibria of A_{2A}AR between lipid nanodiscs and unilamellar vesicles. This provided new insights into the potential role of bulk membrane properties, such as lipid curvature, on modulating the conformational landscape of A_{2A}AR.

References

[1] Shimada I., Ueda T., Kofuku Y., Eddy M.T., Wüthrich K. *Nature Reviews Drug Discovery* 18, 59-82 (2019)

¹⁹F-NMR quantification of drug efficacy exemplified with the human A_{2A} adenosine receptor**Nessa Pesaran Afsharian¹, Beining Jin¹, Bahareh Tavasoli¹, Antara Banerji¹, Kenneth Jacobson², Jens Carlsson³, Sunny Kim⁴, Zhan-Guo Gao², Matthew Eddy¹**

1. Department of Chemistry, University of Florida, Gainesville, FL 32611, USA
2. Laboratory of Bioorganic Chemistry, National Institute of Diabetes and Digestive and Kidney Diseases, National Institutes of Health, Bethesda, MD 20892, USA
3. Department of Cell and Molecular Biology, Science for Life Laboratory, Uppsala University, Uppsala, Sweden
4. National Institute on Drug Abuse, National Institutes of Health, Bethesda, MD 20892-1013, USA

G protein-coupled receptors (GPCRs) are membrane sensory proteins and targets for more than one-third of all FDA-approved drugs. The magnitude of GPCR signaling is determined by the efficacy of bound ligands and spans a wide range, from inverse agonists, which completely inhibit activity, to full agonists, which induce maximum signaling output. Current efficacy measurements rely on cell-based assays, which are limited by variability in transfection efficiency, differences among cell lines, and indirect readouts that depend on downstream secondary messengers rather than direct receptor activation. Our recent fundamental studies elucidating how the cellular environment influences GPCR signaling have led to the development of a novel *in vitro* methodology that overcomes these limitations. Using ¹⁹F-nuclear magnetic resonance (NMR) spectroscopy, we can directly observe and quantitatively define ligand efficacy in GPCRs. This approach not only correlates with results from cell-based assays but also surpasses them by providing a direct, biophysical measurement of receptor activation. We demonstrate the application of this approach with a small library of compounds that bind to the human A_{2A} adenosine receptor (A_{2A}AR) and are predicted to elicit a range of signaling outputs. Our study includes several FDA-approved drugs, including Istradefylline, a Parkinson's treatment, and ligands currently in clinical trials for cancer and Parkinson's disease. We find that our ¹⁹F-NMR measurements quantitatively correlate with efficacies determined in cell-based assays. Interestingly, however, for several compounds currently in clinical trials, we find that their NMR-determined efficacies differ from that reported in cell-based assays. These findings underscore the power of ¹⁹F NMR as a high-resolution analytical tool for GPCR pharmacology, enabling precise assessment of ligand efficacy beyond the capabilities of conventional cell-based assays. This approach not only complements traditional functional assays, but also offers new opportunities to refine GPCR drug design and deepen our understanding of how therapeutics modulate receptor activity.

References:

N. Thakur, A. P. Ray, B. Kim, N.P. Afsharian, E. Lyman, Z.-G. Gao, K. A. Jacobson, and M. T. Eddy, "Membrane Mimetic-Dependence of GPCR Energy Landscapes," *Structure* (2024).

Investigating lipid organization and GPCR-lipid interactions in membrane mimetics with NMR spectroscopy and molecular dynamic simulations

Anuradha Viraj Wijesekara, Naveen Thakur, Arka P. Ray, Niloofar Gopal Pour, Bar Elmaleh, Keen Zang, Jingjing Ji, Ed Lyman, Matthew T. Eddy

University of Florida, Department of Chemistry

Phospholipid nanodiscs are among the most widely used *in vitro* systems to study integral membrane and membrane-associated proteins. Compared to detergents, nanodiscs are thought to provide a more native-like environment, consisting of a phospholipid bilayer encircled by membrane scaffold proteins (MSPs). Recent literature suggests that MSPs themselves may influence the structure and function of membrane proteins reconstituted into lipid nanodiscs, but a structural basis for these observations is not yet known. In earlier work, our group utilized lipid nanodiscs to investigate how anionic phospholipids affected drug-stimulated activation of the A_{2A} adenosine receptor (A_{2A}AR), a representative class A G protein-coupled receptor (GPCR). Rather than using nanodiscs to investigate mechanisms of A_{2A}AR activation, here we use A_{2A}AR activation as a readout to investigate how MSPs influence GPCR structure and function inside lipid nanodiscs. We found that both the amount of anionic phospholipids, type of anionic lipids, and the size of the membrane scaffold protein had pronounced effects on the activity and conformational ensemble of A_{2A}AR. Further, we observed a clear, quantifiable dependence of A_{2A}AR activation on the proportion of anionic lipids. This was complemented by experiments that varied the size of the lipid nanodisc, which supported the idea that MSPs influenced the organization of lipids within nanodiscs. NMR-based analyses of the A_{2A}AR conformational ensemble across nanodiscs of varying sizes were complemented by functional assays that measured the impact of lipid composition and MSP size on nucleotide exchange, confirming that the ratio of nanodisc size to anionic lipid content regulated receptor activity. In addition, in 2D ¹⁵N-¹³C Solid-State NMR (SSNMR) experiments recorded with isotopically enriched lipid nanodiscs showed changes in lysine side chain residues with the introduction of anionic lipids, consistent with interactions between anionic lipids and positively charged residues within the disc. Molecular dynamic simulations of lipid nanodiscs with scaffold proteins of variable size revealed interactions of anionic lipids with the belt protein. Together, these data demonstrate that MSPs influence the spatial organization of phospholipids within nanodiscs in a manner that influences the conformational equilibria and function of embedded membrane proteins. As MSPs are derived from apolipoprotein A, the main protein component of high-density lipoprotein (HDL) particles, we discuss a potential greater context for understanding protein-lipid interactions in lipid transport.

A ¹⁷O Solid-State NMR Relaxation Approach for Probing Water on Membrane Surfaces

Rongfu Zhang ^{*,1,2}, Riqiang Fu ², Tim Cross ^{1,2,3}, Yan-Yan Hu ^{1,2,3}

1. Department of Chemistry and Biochemistry, Florida State University, Tallahassee, FL 32306
2. National High Magnetic Field Laboratory, Tallahassee, FL 32310
3. Institute of Molecular Biophysics, Florida State University, Tallahassee, FL 32306

Nuclear Magnetic Resonance (NMR) relaxation time measurements are powerful tools for elucidating the molecular dynamics of biological systems such as proteins. Here, we focus on the relaxation properties of water, which play an essential role in nearly all biological processes. In particular, the relaxation properties of the ¹⁷O nucleus in water provide unique and sensitive insights into the interactions between water molecules and their surrounding environments. We present a unique approach for disentangling distinct relaxation components and quantifying their relative contributions. This methodology enables a more precise characterization of water dynamics in heterogeneous environments, such as membrane proteins and cell membranes. By applying ¹⁷O NMR relaxation analyses, we reveal the complex interplay between water states associated with protein channels and membrane surfaces, each exhibiting distinct relaxation times. Our results directly probe different classes of water in relation to lipids and protein channels. These findings underscore the potential of ¹⁷O NMR relaxation as a versatile probe for studying water behavior in biological systems, including proteins and membranes.

Gangliosides GM3 And GD3 Modulate Insulin Aggregation Pathways and Reduce Cytotoxicity Through Structural Remodeling

Nazifa Tasnim Ahmad^{1,2}, Jhinuk Saha^{1,2}, Yimin Mao², Robert Silvers³, Zaid Abulaban², Joshua Mysona², Ayyalusamy Ramamoorthy^{1,2,4}

¹National High Magnetic Field Laboratory, 1800 E. Paul Dirac Drive, Tallahassee, FL 32310, United States

²Department of Chemical and Biomedical Engineering, FAMU-FSU College of Engineering, 2525 Pottsdamer St., Tallahassee, FL 32310, United States

³Department of Chemistry and Biochemistry, Florida State University, Tallahassee, FL, USA

⁴Institute of Molecular Biophysics, Florida State University, Tallahassee, FL 32304, United States

Background: Insulin aggregation is a major pathological and pharmaceutical concern in Type 2 Diabetes (T2D), where amyloid deposition can reduce therapeutic efficacy and trigger β -cell death, leading to local tissue damage¹⁻³. Anionic lipids are known to modulate the amyloidogenic pathway of insulin⁴. Although gangliosides, glycosphingolipids containing sialic acid residues, are also known to modulate amyloid formation in neurodegenerative diseases^{5,6}, their influence on insulin aggregation remains largely unknown.

Methods: We investigated the effects of gangliosides GM3 and GD3 on insulin aggregation using Thioflavin-T (ThT) fluorescence kinetics, Fourier Transform Infrared (FTIR) spectroscopy, Circular Dichroism (CD), Small-Angle X-ray Scattering (SAXS), Nuclear Magnetic Resonance (NMR) spectroscopy, and Transmission Electron Microscopy (TEM) and cytotoxicity assays.

Results: Results show that both GM3 and GD3 accelerated insulin aggregation in a concentration-dependent manner but diverted it from classical fibrillation, yielding short, beaded structures rather than extended fibrils. FTIR and CD analyses revealed distinct non-fibrillar intermediates: β -sheet-rich globular clusters for GD3 and α -helical intermediates for GM3. NMR experiments under low-salt conditions showed rapid insulin precipitation upon exposure to GM3, accompanied by ~30% loss in ¹H NMR signal intensity, indicating strong electrostatic interactions between positively charged insulin and negatively charged GM3 micelles. Higher lipid concentrations led to complete signal loss, whereas added salt (100 mM NaCl) reduced precipitation and signal attenuation (~17%). No GM3 resonances were detected, consistent with the formation of large micelles or coprecipitates. Cytotoxicity assays demonstrated that ganglioside-induced aggregates are markedly less toxic than insulin-only fibrils, yet these species retain seeding capacity.

Conclusion: Gangliosides modulate insulin amyloid polymorphism through charged, lipid-mediated interactions that favor off-pathway aggregation and reduce toxicity. These findings highlight ganglioside-specific molecular mechanisms revealed by NMR and provide new insights into lipid-regulated amyloidogenesis relevant to T2D pathology and therapeutic formulation design.

Abstract title: Title: Magnetic Alignment of Saponin-based Lipid Nanodiscs.

Authors: Cletus Obi*^{1,2}, Sam McCalpin^{1,2}, Ayyalusamy Ramamoorthy^{1,2}.

**¹Department of Biomedical Engineering, FAMU-FSU College of Engineering,
Tallahassee, Florida.**

**²National High Magnetic Field Laboratory, Florida State University, Tallahassee,
Florida, 32310.**

Abstract

Background/Introduction

Saponins are plant-derived amphiphilic glycosides known to interact with lipid membranes and form magnetically alignable bicelles/nanodiscs that are suitable for NMR-based studies of lipid membranes.^{1,2} While most prior studies have focused on zwitterionic lipids such as DMPC, biological membranes contain substantial fractions of anionic lipids that influence bilayer properties.^{1,3} Understanding how saponins interact with anionic systems is essential for developing biologically relevant, detergent-free membrane mimetics.

Methods

Binary and ternary mixtures of saponins; glycyrrhizic acid (GA), hederacoside C (HC), and Crude *Quillaja* saponin (CQS) with 1,2-dimyristoyl-sn-glycero-3-phosphocholine (DMPC) and the anionic lipid 1,2-dimyristoyl-sn-glycero-3-phospho-(1'-rac-glycerol) (DMPG) were characterized using optical transmittance assays and temperature-dependent ³¹P solid-state NMR spectroscopy. The effects of lanthanide ions (Tm³⁺) and divalent ions (Ca²⁺, Mg²⁺) on the magnetic-alignment properties were also examined.

Results

Transmittance assays confirmed that all three saponins solubilized DMPG, though with distinct efficiency. ³¹P NMR spectra revealed that pure DMPG inhibited magnetic alignment, but bicelle formation persisted in DMPC-DMPG mixtures containing ≤10% anionic lipid for GA and up to 55% for HC. The addition of Tm³⁺ ions to DMPC-HC nanodiscs caused a 90° reorientation of the bicelle bilayer normal, confirming the tunable magnetic susceptibility of the system. Within the temperature range of 295-320 K, Ca²⁺ enhanced magnetic alignment and lowered the transition temperature, whereas Mg²⁺ induced reduction of peak intensity and partially disrupted alignment in DMPC-HC nanodiscs.

Conclusion

Overall, saponin-based nanodiscs tolerated limited incorporation of anionic lipids; however, while DMPC-HC nanodiscs alone remained stable in the presence of Ca²⁺, they exhibited reduced stability when exposed to Mg²⁺ under the same temperature conditions. These findings expand the utility of natural saponins as biocompatible alternatives to synthetic polymers for constructing stable, magnetically alignable membrane mimetics for NMR applications, membrane protein studies, and drug delivery.

53rd Southeastern Magnetic Resonance Conference

References:

1. McCalpin, S. D., Kassinger, K., Gilmore, M. & Ramamoorthy, A. Characterization of lipid solubilization, bicelle formation, and magnetic-alignment induced by saponins. *J Colloid Interface Sci* **702**, 139008 (2025).
2. Geisler, R. *et al.* Aescin - a natural soap for the formation of lipid nanodiscs with tunable size. *Soft Matter* **17**, 1888–1900 (2021).
3. McCalpin, S. D., Ravula, T. & Ramamoorthy, A. Saponins Form Nonionic Lipid Nanodiscs for Protein Structural Studies by Nuclear Magnetic Resonance Spectroscopy. *J Phys Chem Lett* **13**, 1705–1712 (2022).

Nutation-Induced Distortions in Solid-State NMR Spectra of High-Spin Quadrupolar Nuclei

Sara Termos^{1,2*}, James J. Kimball^{1,2}, Mia J. Cohen^{1,2}, and Robert W. Schurko^{1,2}1. *Department of Chemistry and Biochemistry, Florida State University, Tallahassee, FL 32306*2. *National High Magnetic Field Laboratory, Tallahassee, FL 32310*

Solid-state NMR (SSNMR) provides deep insights into structure, bonding, and dynamics; however, its application to quadrupolar nuclei, which account for about 73% of the NMR-active nuclides in the periodic table, remains challenging. In static NMR spectra of half-integer quadrupolar nuclei (HIQN), spectral distortions arise from orientation-dependent nutation frequencies and overlap between central- and satellite-transition patterns.^{1,2} These effects become increasingly prominent as the nuclear spin quantum number increases, complicating spectral analysis and hindering the accurate extraction of electric field gradient (EFG) tensor and chemical shift tensor parameters.

In this work, we examine the origin of these distortions, discuss the acquisition of distortion-free SSNMR spectra of HIQN, and provide practical pathways for the acquisition of uniform powder patterns. First, it is shown that these distortions, which are referred to as *magic-angle dips* (MADs), arise from the different nutation behaviors of the isochromats of the EFG tensors with their largest components, V_{33} , oriented at $\theta \approx 54.74^\circ$ with respect to \mathbf{B}_0 . Numerical simulations with SIMPSON³ are used to systematically illustrate this phenomenon, showcasing examples for HIQN with varying EFG tensor parameters and spin quantum numbers (*e.g.*, ^{35}Cl ($I = 3/2$), ^{55}Mn ($I = 5/2$), ^{59}Co ($I = 7/2$)). Second, the effects of MADs on experimental ^{55}Mn and ^{59}Co spectra are demonstrated. Finally, simple pathways are explored to decrease the effects of MADs and increase pattern uniformity, using rectangular and WURST^{4,5} pulses in CPMG-type⁶ sequences to improve pattern homogeneity.

References

- (1) Medek, A.; Frydman, V.; Frydman, L. *J. Phys. Chem. A* **1999**, *103*, 4830.
- (2) Bodart, P. R. *et al. Mol. Phys.* **2000**, *98*, 1545.
- (3) Bak, M. *et al. J. Magn. Reson.* **2000**, *147*, 296.
- (4) Kupce, E.; Freeman, R. *J. Magn. Reson. Ser. A* **1995**, *115*, 273.
- (5) O'Dell, L. A. *Solid State Nucl. Magn. Reson.* **2013**, *55–56*, 28.
- (6) Hung, I.; Gan, Z. *J. Magn. Reson.* **2010**, *204*, 256.

Understanding Self-Association of Fluorinated Phenylalanine through NMR Spectroscopy and Quantum Chemistry

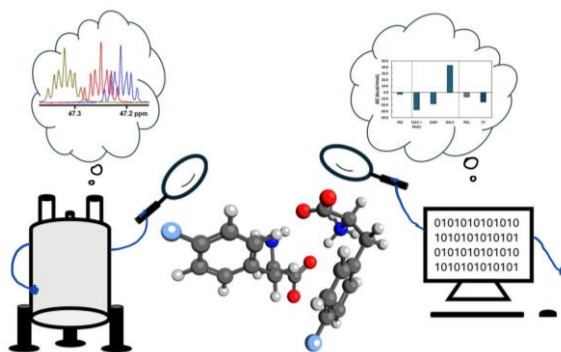
Rajan Rai*, Justin Talbot, and Leah Casabianca

Department of Chemistry, Clemson University, Clemson, SC

Aromatic amino acids, such as phenylalanine, play a vital role in the self-assembly of peptides and the formation and stability of amyloid fibrils.¹ Understanding how they self-aggregate can provide insights into protein folding and functions, which are fundamental to several biological phenomena.² This can help in understanding the underlying mechanisms of the diseases caused by protein misfolding or aggregation. Furthermore, the understanding also aids in designing targeted drugs and in synthesizing biological molecules with desired properties.³

In this study, we use NMR chemical shift perturbation (CSP) analysis to investigate the self-association behavior of fluorophenylalanine, attempting to obtain detailed information about the local chemical environment and binding sites, and a quantitative estimation of binding affinities.⁴ This is made possible by the high NMR sensitivity, 100% natural abundance, broad chemical shift range, and clean spectra of the ¹⁹F nucleus. Additionally, a fluorine incorporation at the ring position of the aromatic side chain does not significantly disrupt the structure or function of a protein.⁵

To complement the experimental findings, density functional theory (DFT) calculations were performed on the model systems. The calculated NMR chemical shifts and binding energies were compared with the experimentally obtained values to validate the computational model. Additionally, an absolutely localized molecular orbital energy decomposition analysis (ALMO-EDA) was carried out to provide a clear, physically meaningful breakdown of the intermolecular interactions.⁶ This comprehensive approach offers a solid framework for characterizing weak molecular interactions and highlights the usefulness of fluorine as a probe nucleus in molecular recognition studies, thereby contributing to the fields of biochemistry and molecular biology.



References

1. I. M. Stanković, S. Niu, M. B. Hall, S. D. Zarić, *Int. J. Biol. Macromol.* **2020**, 156, 949.
2. C. M. Dobson, *Nature* **2003**, 426, 884.
3. K. K. Sharma, K. Sharma, K. Rao, A. Sharma, G. K. Rathod, S. Aaghaz, N. Sehra, R. Parmar, B. VanVeller, R. Jain, *J. Med. Chem.* **2024**, 67, 19932.
4. M. P. Willaimson, *Prog. Nucl. Magn. Reson. Spectrosc.* **2013**, 73, 1.
5. M. A. Danielson, J. J. Falke, *Annu. Rev. Biophys. Biomol. Struct.* **1996**, 25, 163.
6. R. Z. Khaliullin, E. A. Cobar, R. C. Lochan, A. T. Bell, M. Head-Gordon, *J. Phys. Chem. A* **2007**, 111, 8753.

Mechanochemical Synthesis and Multinuclear Solid-State NMR Characterization of Amoxicillin Hydrochloride Salts

Alexander M. Perez*^{1,2}, Peyton G. Osborn^{1,2}, Sean T. Holmes^{1,2}, Robert W. Schurko^{1,2}

¹*Department of Chemistry & Biochemistry, Florida State University, Tallahassee, FL 32306*

²*National High Magnetic Field Laboratory, Tallahassee, FL 32310*

Hydrochloride (HCl) salts are the most widely used solid forms of active pharmaceutical ingredients (APIs), constituting *ca.* 50% of drugs on the market.¹ Understanding their solid-state structures is essential for interpreting key physicochemical properties, such as stability, solubility, and bioavailability. While methods for solution-state recrystallizations of HCl salts are well established, they tend to consume a lot of energy, generate solvent waste, and may limit access to undiscovered solid forms. Mechanochemistry is a green and efficient alternative, yielding novel materials in quantitative yields that are otherwise unobtainable.^{2,3}

In this work, we investigate the ball milling and multinuclear solid-state NMR (SSNMR) characterization of HCl salts of the API amoxicillin trihydrate (Amox·3H₂O). Three reactions of 1:1, 1:2, and 1:3 Amox·3H₂O:HCl were carried out, with products analyzed by powder X-ray diffraction (PXRD) and ¹⁵N, ¹³C, and ³⁵Cl SSNMR. PXRD and ³⁵Cl SSNMR were used to confirm differences between the starting reagents and products: (i) the 1:1 product appears to form a new crystalline Amox:HCl salt; (ii) the 1:2 product is a crystalline material with disordered Cl⁻ sites; and (iii) the 1:3 product appears to be amorphous amoxicillinoic acid. ¹⁵N SSNMR spectra reveal chemical shift differences relative to Amox·3H₂O consistent with amide-site protonation for both the 1:1 and 1:2 products, whereas for the 1:3 product, they are consistent with β-lactam nitrogen shifts, indicating acid hydrolysis.

Collectively, these results demonstrate that mechanochemical reactivity in HCl salts of antibiotics can generate unexpected protonation and chloride disorder motifs, providing new insights into salt formation, solid-state acid-base chemistry, and solid-form diversity in pharmaceuticals.

References

- (1) Paulekuhn, G. S. *et al. J Med Chem* **2007**, *50*, 6665.
- (2) Andersen, J. M. *et al. Chem. Sci.* **2017**, *8*, 5447.
- (3) Ross, S. A. *et al. Chem. Commun.* **2016**, *52*, 8772.

Structurally characterizing FtsL101-146 in lipid bilayers

Authors: Jiaying Fan^{1,2*}, Rongfu Zhang^{1,2}, Ramesh Prasad^{3,4}, Timothy A. Cross^{1,2}, Huan-Xiang Zhou^{3,4}, Yan-Yan Hu^{1,2}

¹Department of Chemistry and Biochemistry, Florida State University, Tallahassee, FL, 32306, USA

²National High Magnetic Field Laboratory, Tallahassee, FL, 32310, USA

³Department of Chemistry, University of Illinois Chicago, Chicago, IL, 60607, USA

⁴Department of Physics, University of Illinois Chicago, Chicago, IL, 60607, USA

Mycobacterium tuberculosis (Mtb), the causative agent of tuberculosis (TB), causes millions of deaths annually, and its drug resistance further complicates TB treatment¹. The latent phase, during which Mtb stays inactive, plays an important role in its drug resistance². To explore the role of divisome proteins in Mtb latency, this study focuses on the structure of one of the core Mtb divisome components, FtsL. FtsL is an integral membrane protein (IMP). IMPs account for a quarter of all protein-coding genes and are associated with various essential cellular functions³. However, only a tiny proportion of structures deposited in the Protein

Data Bank are from IMPs, suggesting the experimental challenges in structural characterizations of IMPs⁴. To determine the structure of the FtsL transmembrane (TM) domain. An FtsL truncation, FtsL101-146, containing the entire TM domain and part of the cytoplasmic region, was expressed and investigated in a native-like environment using oriented sample solid-state NMR (OS ssNMR). The tilt and orientation angles of the FtsL TM domain were determined. Complemented with circular dichroism (CD) and molecular dynamics (MD), the cytoplasmic domain of FtsL is shown to adopt an α -helix structure. Overall, this study highlights the potential importance of FtsL in the cooperative interactions of Mtb divisome proteins.

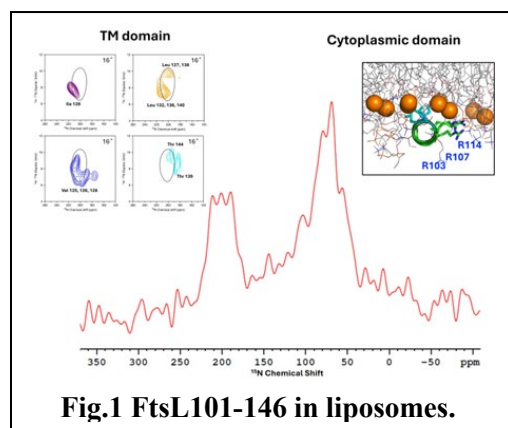


Fig.1 FtsL101-146 in liposomes.

References:

- (1) Khawbung, J. L.; Nath, D.; Chakraborty, S. Drug Resistant Tuberculosis: A Review. *Comp. Immunol. Microbiol. Infect. Dis.* **2021**, *74*, 101574. <https://doi.org/10.1016/j.cimid.2020.101574>.
- (2) Colangeli, R.; Gupta, A.; Vinhas, S. A.; Chippada Venkata, U. D.; Kim, S.; Grady, C.; Jones-López, E. C.; Soteropoulos, P.; Palaci, M.; Marques-Rodrigues, P.; Salgame, P.; Ellner, J. J.; Dietze, R.; Alland, D. Mycobacterium Tuberculosis Progresses through Two Phases of Latent Infection in Humans. *Nat. Commun.* **2020**, *11* (1), 4870. <https://doi.org/10.1038/s41467-020-18699-9>.
- (3) Hegde, R. S.; Keenan, R. J. The Mechanisms of Integral Membrane Protein Biogenesis. *Nat. Rev. Mol. Cell Biol.* **2022**, *23* (2), 107–124. <https://doi.org/10.1038/s41580-021-00413-2>.
- (4) Lee, H. J.; Lee, H. S.; Youn, T.; Byrne, B.; Chae, P. S. Impact of Novel Detergents on Membrane Protein Studies. *Chem* **2022**, *8* (4), 980–1013. <https://doi.org/10.1016/j.chempr.2022.02.007>.

**An experimental proof of the applicability of cryogen-free technology
for high resolution solid state and liquid state NMR**

Eugeny Kryukov¹, Alexander Karabanov¹, Denis Langlais¹, Shashwata Moitra*², Jeremy Good¹

¹Cryogenic Ltd, London, UK ²Cryogenic US LLC, USA

A 9.4 T cryogen-free system developed by Cryogenic Limited has been used for the high resolution solid-state magic angle spinning (MAS) and liquid state NMR experiments. The temporal magnetic field distortion due to the cold head operation was 2 Hz peak-to-peak on the resonance frequency 400 MHz [1]. This distortion occurred at the frequency of 1.7 Hz in our experimental setup.

In solid-state NMR measurements, the distortion appears as additional line broadening that is too small to be visible in ordinary MAS experiment. To see the effect, the amplitude of the distortion was enhanced by a factor of 40 above its natural value. Notably, if the NMR signal only lasts a small fraction of the cold head period, for instance 100 ms, the effect of the cold head can be fully removed by synchronizing the signal acquisition with the cold head operation. In this case the distortion amplified by 400 times remained invisible. This approach was successfully demonstrated through our experiments in recording the solid state multi-quantum 2D spectra of ⁸⁷Rb in RbNO₃. The spinning speed was 11 kHz.

In liquid-state NMR measurements, however, the signal acquisition time normally covers several cold head periods. In this case the additional peaks separated by the cold head frequency appear in the NMR spectra. The sweep coil of the room-temperature (RT) shim set was used for the correction (or amplification as above) of the cold head distortion. Our experimental observations showed that the amplitude of the distortion needs to be reduced by a factor of 10 to stop be important in liquid state NMR.

In addition, we have demonstrated that applying reference deconvolution post-acquisition software processing [2] helps remove the field instability artifacts from NMR data, in both 1D and 2D NMR. We have also developed a method to stabilize the magnetic field in a short period of time following a field ramp [3], enabling high resolution measurements at different fields every day. We have measured four double quantum (DQ) filtered COSY spectra in ethyl acetate at 50, 100, 155 and 400 MHz. These spectra were measured at different fields in four consecutive days [4].

Currently, we are developing a dedicated liquid state NMR system based on a cryogen-free magnet with an improved design. This next-generation system aims to eliminate the need for field corrections or post-acquisition processing, thereby improving both measurement accuracy and operational efficiency.

References

1. E. Kryukov et al, SS NMR, 113(2021)101732
2. A. Karabanov et al, JMR, 353(2023)107494
3. E. Kryukov et al, SS NMR, 109(2020)101684
4. E. Kryukov et al, JMR, 381(2025)107985

Pushing the Limits of NMR Crystallography: A Study on Three Forms of Glycylglycine

Sean T. Holmes,^{1,2*} Aaron Viggiano,³ Christine Plavchak,³ Haylee Holman,³ Megan Joyce,³
Cameron S. Vojvodin,^{1,2} Xinsong Lin,² Robbie J. Iulucci,^{3,*} Robert W. Schurko^{1,2,*}

¹ National High Magnetic Field Laboratory, Tallahassee, FL 32310

² Department of Chemistry & Biochemistry, Florida State University, Tallahassee, FL 32306

³ Department of Chemistry, Washington and Jefferson College, Washington, PA 15301

NMR crystallography (NMRX), which integrates solid-state NMR (SSNMR) spectroscopy, X-ray diffraction (XRD), and density functional theory (DFT) calculations, provides deeper insight into crystal structures than any of these methods individually. NMRX is especially powerful for characterizing many atomic sites within the solid, particularly through multinuclear SSNMR methods. With the goal of pushing the limits of NMRX, we have characterized three solid phases of the dipeptide glycylglycine, including a free base, a hydrochloride salt, and a hemihydrochloride salt — the latter form is synthesized and characterized by single-crystal XRD here for the first time. SSNMR data include 2D ¹H–¹H DQ–SQ BABA spectra that are used to measure ¹H chemical shifts and provide assignments through homonuclear dipolar correlations, slow-spinning ¹H–¹³C and ¹H–¹⁵N CP/MAS spectra to determine the ¹³C and ¹⁵N chemical shift tensors, ultra-wideline ¹⁴N WURST-CPMG spectra to measure the ¹⁴N electric field gradient (EFG) tensors, various 1D ³⁵Cl spectra to determine the ³⁵Cl EFG and chemical shift tensors, and 2D ³⁵Cl→¹H D-RINEPT spectra to determine heteronuclear dipolar correlations between the chloride ions and nearby protons. Together with state-of-the-art DFT calculations, these parameters are related directly to molecular- and crystal-level structure and intermolecular hydrogen bonding. Modern DFT approaches using double-hybrid functionals are critical for predicting subtle differences in ¹³C and ¹⁵N chemical shift tensors between the three solid phases. It is hoped that these results highlight the current capabilities of NMRX, and open new avenues for the exploration of a plethora of materials and biosolids.

Understanding Interactions between Micro and Nano Plastics with Metabolites at the Molecular Level

Sekinah O. Dauda* and Leah B. Casabianca

Department of Chemistry, Clemson University, Clemson, SC

The application of plastics for commercial and personal purposes is constantly on the increase. When plastics break down in the environment they lead to micro and nano plastics. The accumulation of micro and nanoplastics has severe implications in areas concerning food, health and environmental pollution. Upon breakdown, these plastics acquire altered¹ and larger surface area thus increasing their capability to adsorb other environmental contaminants². Accumulated micro and nanoplastics from drinking water, food and air have been found in the human body³.

Metabolites are small biological molecules present in the body. Once nanoplastics enter the body, small molecules like metabolites, nucleic acids and proteins can be adsorbed on nanoplastics surfaces forming a biomolecular corona³. Typically, in biomedical analysis, blood chemistry tests are used in clinical laboratories to measure chemical enzymes, hormones and other metabolites. The interaction between metabolites and nanoplastics can influence the result from a blood chemistry analysis which could lead to incorrect analysis of metabolites present. Metabolites serve as biomarkers to detect dysfunction which is a hallmark of diseased state⁴.

In this study, quantitative and qualitative NMR techniques were employed to study the interaction between surface modified nanoscale plastics and different metabolites used in biomedical analysis. Water-Ligand Observed via Gradient Spectroscopy⁵ (waterLOGSY) and Saturation Transfer Difference^{6,7} (STD) NMR techniques were used to identify nanoplastics binders, while competition STD NMR was used identify cases of competition for binding sites on the nanoparticle surface.

This study aims to develop robust techniques for screening and characterizing interaction between small metabolites and nanoscale plastic. This is an important step towards understanding how competition may affect the final result of blood chemistry analysis and potentially strategies for more accurate analysis.

References

1. Peller, J. R.; Mezyk, S. P.; Shidler, S.; Castleman, J.; Kaiser, S.; Horne, G. P. *Water* **2021**, *13*, 3120.
2. Huffer, T.; Metzelder, F.; Sigmund, G.; Slawek, S.; Schmidt, T.; Hofmann, T. *Sci. Total Environ.*, **2019**, *657*, 242-247.
3. Pitek, A. S.; O'Connell, D.; Mahon, E.; Monopoli, M. P.; Baldelli Bombelli, F.; Dawson, K. A. *PLOS One*, **2012**, *7*, e40685.
4. Qiu, S.; Cai, Y.; Yao, H.; Lin, C.; Xie, Y.; Tang, S.; Zhang, A. *Nature Signal Transduction and Targeted Therapy*, **2023**, *8*, 132.
5. Dalvit, C.; Pevarello, P.; Tatò, M.; Veronesi, M.; Vulpetti, A.; Sundström, M. *J. Biomol. NMR*, **2000**, *18*, 65– 68.
6. Mayer, M.; Meyer, B. *J. Am. Chem. Soc.* **2001**, *123*, 6108– 6117.
7. Mayer, M.; Meyer, B. *Angew. Chem., Int. Ed.* **1999**, *38*, 1784– 1788.

Developing a Tool to Understand the Structure of Hydrogens on Nanoplastics Surface

Jordan Sanders* and Leah B. Casabianca

Department of Chemistry, Clemson University, Clemson, SC

Polystyrene is a polymer of styrene that is used to make Styrofoam products. Polypropylene is a thermoplastic that is used in multiple plastics products, such as packaging. Since these products are non-biodegradable, they ultimately go through various degradation processes in the environment and are broken down into micro- and nanoplastics, which present numerous health concerns¹. Nanoplastics pose a major threat due to their small size, as they can penetrate various organs and biological systems, such as the blood brain barrier². Additionally, due to their large surface area, they can bind to other molecules, including biological molecules, pollutants, and more, compounding the threat they present. In this work, we examine whether nuclear Overhauser effect spectroscopy (NOESY)-Nuclear Magnetic Resonance (NMR) can be used to study the binding interactions of nanoplastics.

This study was done with nanoplastics bound to the molecule 4-Bromo-2,3-difluorophenol (BDF). The fluorine and hydrogen NOESY build-up curves exhibit a difference. We hypothesize that this difference is due to the influence of spin diffusion on the hydrogen NOESY curve. To test this hypothesis, we used the full relaxation matrix model to predict the NOESY build up curves for fluorine and hydrogen. For hydrogen, we modeled hydrogens on the nanoparticles surface with a hemispherical arrangement of different numbers of hydrogens at different radii, as shown in Figure 1. This model can be modified to understand the nature of hydrogens on the nanoparticles surface.

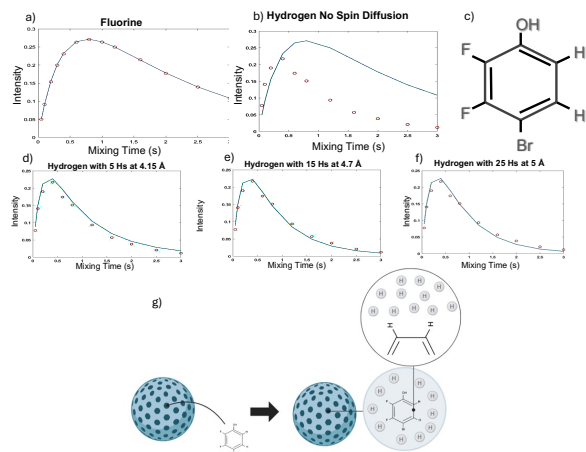


Figure 1. a-b: Fluorine and hydrogen build up curves of polystyrene nanoplastics (PSNP) bound to BDF modeled^{3,4} with the same rotational correlation constant (τ_c) and leakage relaxation constant, showing the need to account for spin diffusion to accurately model the hydrogen build up curve. c: The structure of BDF. d-f: Hydrogen build up curves with varying number of hydrogens at varying radii on the nanoplastics surface. g: Illustration of our model showing the justification for the hemispherical model of hydrogens representing the inside of the pore of PSNP⁵.

References

1. Winiarska, et al., The potential impact of nano- and microplastics on human health: Understanding human health risks., *Environmental Research*, 251, 118535 (2024)
2. Mattsson, et al. Brain damage and behavioral disorders in fish induced by plastic nanoparticles delivered through the food chain. *Sci Rep*, 7, 11452 (2017)
3. Campbell and Sykes. Theoretical Evaluation of the Two-Dimensional Transferred Nuclear Overhauser Effect. *Journal of Magnetic Resonance*, 93, 77-92 (1991)
4. Strotz, et al., *Journal of Chemical Theory and Computation*, 13, 4336-4346 (2017)
5. Created using BioRender

Investigating the Relationship Between Carbon Quantum Dots and Nuclear Spin RelaxationMakaylab Grandal^{1*}, Cody Soper¹, Nicholas Whiting^{1,2}¹Department of Physics & Astronomy, Rowan University. Glassboro, NJ 08028 USA²Department of Biological & Biomedical Sciences, Rowan University. Glassboro, NJ 08028 USA

*Undergraduate Researcher

Carbon-based quantum dots (CQDs) are nanocrystals (<10 nm diameter) composed primarily of carbon that exhibit remarkable optoelectronic properties. Unlike traditional metallic quantum dots, CQDs are both biocompatible and possess a magnetic resonance (MR) signature due to their carbon-based composition. CQDs are synthesized via hydrothermal solvation and can be isotopically enriched in ¹³C using labelled precursors. While fluorescent properties of CQDs have been reported, there remains a lack of magnetic resonance characterization for these nanoparticles. Here, we investigate the relationship between CQDs and nuclear spin relaxation—specifically, how precursor choice may extend the ¹³C T_1 of CQDs for future hyperpolarization experiments and how the presence of CQDs can affect ¹H T_1 & T_2 values in water.

To investigate how precursor choice may affect ¹³C T_1 within CQDs, we used o-xylene as the precursor and optimized the synthesis conditions to facilitate the production of CQDs between 5-9 nm that fluoresced strongly at 410 nm with a quantum yield of 7%. Xylene was chosen due to its low cost of deuteration and lack of quadrupolar ¹⁴N nuclei; the next steps include synthesizing deuterated CQDs using deuterated xylene and performing comparative studies on the effects of ¹³C T_1 .

Additionally, benchtop NMR was used to monitor the changes to ¹H T_1 and T_2 values of water in solutions of CQDs. Briefly, CQDs were suspended in DI water (1-22 mg/mL); ¹H T_1 and T_2 were measured using inversion recovery and spin echo sequences. While ¹H T_2 steadily decreased with CQD concentration, ¹H T_1 initially decreased before rebounding to levels approaching that of the control. Ongoing experiments look to replicate this effect at 9.4 T.

Extending ¹³C T_1 values and investigating how CQDs affect the nuclear spin relaxation of water aligns with our aim of CQDs serving as next-generation MRI contrast agents and contributes to the body of knowledge on the MR properties of carbon dots.

References: [1] Kopf, *et. al. Chem. Rev.* (2022); [2] Ji, *et. al. ACS Appl. Nano Mater.* (2021); [3] Liu, *et. al. ACS Cent. Sci.* (2020); [4] Long, *et. al. J Magn. Reson.* (2019).

Abstract Title: Design and NMR Investigation of Ni²⁺-Chelated Monoolein Nanoparticles: A Path to Stabilizer-Free Lipid Carriers

Authors: Kattayani Sarkar*, Gail Fanucci, University of Florida

Background:

Lipidic cubic mesophases formed by Monoolein (MO) are highly adaptable nanostructures capable of encapsulating hydrophilic, hydrophobic, and amphiphilic molecules. Despite their promise in biomedical delivery, these systems often rely on surfactants such as Pluronic F127 or Tween 80 for stability, which often compromises biocompatibility. Reducing or eliminating the need for such stabilizers could improve their suitability for therapeutic use. In this work, we investigate the development of stabilizer-free lipid nanoparticles (LNPs) by incorporating a Ni²⁺-chelating lipid, DGS-NTA(Ni), along with a phospholipid, DOPC, into Monoolein-based matrices to create stable, functional nanostructures capable of pH-responsive protein delivery.

Methods:

Ternary mixtures of MO, DOPC, and DGS-NTA(Ni) were prepared via the Bottom Up Thin-Film Hydration method with varying chelating lipid contents (2.5–12.5 mol%). Samples were characterized using Polarized Light Microscopy (PLM) for mesophase identification, Dynamic Light Scattering (DLS) and zeta potential for stability, ¹H NMR and T₁ relaxometry for molecular dynamics, and Negative Stain TEM for structural analysis.

Results:

Lipidic sample formulations having 7.5–12.5 mol% DGS-NTA(Ni) yielded stable nanoparticles (<500 nm) without external stabilizers. Zeta potential values of samples became increasingly negative with higher Ni²⁺ incorporation, indicating enhanced colloidal stability. NMR spectra demonstrated signal broadening and shortened T₁ relaxation times due to paramagnetic Ni²⁺ effects. TEM imaging revealed bicontinuous nanostructures resembling the *sponge* (L₃) phase, indicating a transitional cubic topology that is capable of encapsulating biomolecules.

Conclusions:

Chelated lipids effectively stabilize Monoolein-based nanoparticles while enabling site-specific protein binding via His-tag coordination and pH-triggered release. These findings show a new class of *biocompatible, stabilizer-free LNPs* for protein and drug delivery, advancing the design of smart lipid nanocarriers for biomedical applications.

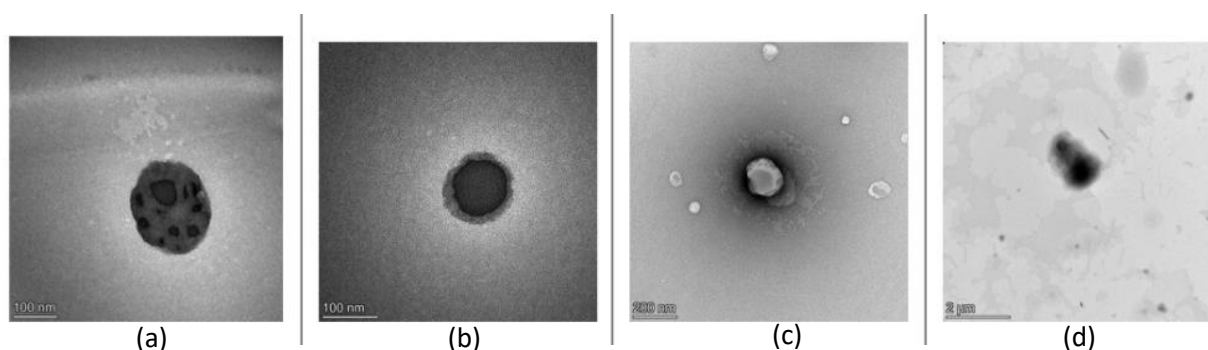


Figure 1: Negative stain TEM images of (a) MO 100mol%, (b) MO/DOPC (85 mol% MO and 15 mol% DOPC), (c) MO/DOPC/DGS NTA (12.5 mol% DGS NTA), and (d) MO/DOPC/DGS NTA Ni (12.5 mol% DGS NTA Ni).

53rd Southeastern Magnetic Resonance Conference

References:

- (1) Barriga, H. M. G. *et al.*, *Angew. Chem. Int. Ed.*, 2019, 58, 2958–2978.
- (2) Zabara, M. *et al.*, *Adv. Funct. Mater.*, 2019, 29, 1904007.
- (3) Zheng, Y. *et al.*, *ACS Chem. Biol.*, 2023, 18, 1435–1443.
- (4) Gowda, B. H. J *et al.*, *Environmental Research* 2023, 237, 116894.
- (5) Rajput, S. *et al.*, *Biophys Rev* 2022, 14 (1), 67–74.
- (6) Yaghmur, A. *et al.*, *Acta Pharm Sin B* 2021, 11 (4), 871–885.
- (7) Meikle, T. G. *et al.*, *Langmuir* 2020, 36 (22), 6254–6260.
- (8) Pramanik, S. *et al.*, *Soft Matter* 2022, 18 (34), 6372–6383.

Peptide nanostructures can be pathological or therapeutic: how solid-state NMR guides control assembly pathways to produce desired molecular structures

Tzu-Ying Chiu* and Anant K. Paravastu
School of Chemical and Biomedical Engineering
Georgia Institute of Technology
Atlanta, GA 30332

The Paravastu group studies nanoscale assemblies of peptides (small proteins) and proteins, including naturally occurring and human-designed molecules. I will present structural studies of both naturally occurring and human-designed amino acid sequences, primarily using solid-state nuclear magnetic resonance (NMR) and cryo-electron microscopy (cryo-EM). I will also discuss analyses of cellular and tissue responses in pathological and therapeutic contexts.

I will discuss a variety of self-assembled peptide and protein nanostructures. These nanostructures can be pathological (e.g., neurotoxic oligomers), serve as therapeutic materials (e.g., wound-healing hydrogels), or act as technological platforms (e.g., photoconductive fiber matrices). We do not fully understand the relationships between structure and function, but we know that function is sensitive to structure. For example, the Alzheimer's amyloid- β can form oligomers or fibrils, depending on assembly conditions. Cellular responses (e.g., inflammation) vary significantly between oligomers and fibrils. Other proteins can induce liquid-liquid phase separation, creating intracellular "stress granules" and "membraneless organelles."

I will also share our efforts to control assembly pathways by introducing mutations or designing entire amino acid sequences. I will show: 1) that single amino acid mutations of amyloid- β can either promote or deter oligomer formation; 2) how to rationally control the assembly of parallel versus antiparallel β -sheets; 3) that α -helical assembly can mediate β -sheet formation; 4) how to place cell-stimulating domains within β -sheet assemblies; and 5) how to control phase diagrams related to liquid-liquid phase separation. These results demonstrate a degree of rational control over amyloid assembly but also highlight gaps in our mechanistic understanding.

Unveiling Catalytic Intermediates on Metal Nanoparticle Surfaces via Parahydrogen-Enhanced NMR

*Rasaq Ayinde Adams, University of Florida

Abstract

In nuclear magnetic resonance (NMR), magnetic equivalence refers to a group of two or more spins that are (1) chemically equivalent and (2) have identical couplings to all other nucleons in the molecule. Representatives include the proton pairs in dihydrogen and acetylene, or the four protons in ethene. Magnetic equivalence in H₂ accounts for the para spin isomer (para-H₂), which exists in a singlet state, in accordance with the Pauli Principle. Para-H₂, which is easily prepared to 99% purity by simply cooling normal H₂ gas to 20 K in the presence of a catalyst, provides a convenient source of pure spin order that can be transformed into hyperpolarized magnetization by introducing interactions that break the magnetic equivalence of the proton pair. While hydrogenation of propyne to propene achieves the requisite symmetry breaking, hydrogenation of ethyne to ethene does not, as the four protons of the adduct remain magnetically equivalent. In the present work, we exploited this symmetry property for the indirect detection of a catalytic intermediate wherein magnetic equivalence is temporarily lifted during its lifetime on the surface of TiO₂-supported Rh or Ir nanoparticles. Hence, we observed hyperpolarized ethene upon hydrogenation of ethyne, which is unexpected for the net reaction. Based on prior experimental and computational studies, we hypothesize that a likely candidate is a metal-ethylidene species. As the reaction occurs on a solid surface, singlet-triplet mixing is mediated by dipolar proton-proton coupling on time scales comparable to the lifetime of the intermediate, thereby providing a new means of interrogating the reaction kinetics and mechanism of the surface reaction. Plans for testing this hypothesis will be discussed.

Microwave Fixation Prevents Post-Mortem Metabolism for NMR Spectroscopy Metabolomics

Authors: Neel Shah^{1*}, Megan Jewell¹, Ryan Smith¹, Nehal Dwaram¹, James Collins¹, Joanna Long¹

¹*Department of Biochemistry and Molecular Biology, University of Florida, Gainesville, FL*

Background: Postmortem enzymatic activity rapidly alters tissue metabolite concentrations, compromising metabolomic analyses. Conventional euthanasia methods, such as cervical dislocation, allow for anaerobic respiration leading to major shifts in metabolite concentrations. Here we test if focused microwave irradiation provides rapid enzyme inactivation, preserving native metabolite levels.

Methods: Adult female mice (n=6) were divided between microwave fixation (5 kW, 0.60 s) and cervical dislocation controls. Brain, liver, heart, and muscle tissues were collected and analyzed using solution-state nuclear magnetic resonance (NMR) spectroscopy. Extractions were prepared using methanol/chloroform/water, lyophilized, and analyzed on 800 and 600 MHz spectrometers. ¹H and ³¹P spectra were collected on all polar and nonpolar phases.

Results: NMR spectra of the microwaved tissues showed a decrease in lactate and an increase in glucose levels relative to the control tissues. We also observed an increase in ATP, ADP, NADH, and phosphocreatine levels, indicating microwave irradiation effectively halted post-mortem metabolite breakdown. Interestingly, fumarate levels were observed to increase in the microwaved heart tissue, despite all the other intermediates of the TCA cycle decreasing relative to the controls.

Conclusions: This study shows the promise of microwave fixation as an effective method for euthanasia that minimizes post-mortem enzyme activity, producing metabolite concentration profiles that more closely reflect in-vivo states and preserving energy-related metabolites. Replication with an expanded sample size and comparison to other methods of euthanasia for individual tissue types will confirm whether microwave fixation should replace traditional forms of euthanasia for metabolism research.